Faculty of Medicine
and Health Sciences
School of Life Sciences

The University of Nottingham
UNITED KINGDOM · CHINA · MALAYSIA

Mechanism of Action of Somatostatin in Pancreatic β-Cells: Oxidative Metabolism, Glycolysis Pathway and Role of Extracellular Calcium Influx

By

JALA A S ALAHMED

BVMS (Hons) MSc Pharm

Thesis submitted to the University of Nottingham in fulfillment of the requirements for the Degree of Doctor of Philosophy
In Molecular Pharmacology

April 2019

Abstract

The mechanism of action of somatostatin (SRIF) has been extensively studied during the last five decades since the discovery of the peptide in 1974. However, there are many concealed actions of the peptide to control insulin secretion from pancreatic β–cells. This can contribute to resolving the dilemmas of cancer and diabetes mellitus. To achieve this goal, the MIN6 cell line was used as a model of insulin secreting pancreatic β-cells. Polarographic oxygen and enzymatic lactate electrodes were used to measure oxygen consumption rate (OCR) and lactate production rate, respectively. Imaging techniques were used to measure the mitochondrial membrane potential ($\Delta\Psi_{mit}$) using Rhodamine 123 (Rh123) dye and Ca^{2+} influx using Fluo-4 probe. Glucose uptake and ATP production were measured by Promega® plate-based assays, the Glucose Uptake-Glo™ Assay, and CellTiter-Glo® 2.0 Assay, respectively.

100 nM SRIF significantly and equally inhibited OCR stimulated by both 10 mM glucose and 10 mM α-ketoisocaproate (KIC); this effect was not seen in the absence of substrates. 10 mM glucose significantly decreased basal Rh123 fluorescence, the effect was reversed by 100 nM SRIF. In Ca^{2+} free condition, 100 nM SRIF did not affect $\Delta\Psi_{mit}$ while it depolarized $\Delta\Psi_{mit}$ in the presence of nifedipine. The peptide had no effect on ATP production either in the presence or in the absence of each mitochondrial fuels. It neither affected the glucose uptake nor the glucokinase activity in MIN6 cells. The peptide also inhibited lactate production in the absence and presence of 1 μM cyclosporine A (CSA) but not in the presence of each 100 nM okadaic acid (OKA) or ethanol. SRIF decreased the basal and substrate-induced Ca^{2+} influx into MIN6, the effect was abolished by pre-incubation of the cells with pertussis toxin (PTX). 1 μM dibutyryl cAMP significantly decreased the inhibitory action of SRIF.

In conclusion, SRIF inhibited glycolysis and mitochondrial metabolism but not glucose uptake nor ATP production. This indicates that the inhibitory effect of the peptide on plasma membrane electrical activity was not due to inhibition of metabolism. It is also concluded that SRIF effectively inhibited Ca^{2+} influx into MIN6 cells directly via blocking VGCCs and indirectly by activation of K^+ channels conductance. The inhibitory action of the peptide is achieved via a PTX sensitive pathway, and it is a cAMP independent mechanism.

Acknowledgments

I would like to express my sincere gratitude to my supervisors Dr. Paul A. Smith and Dr. Sue L. F. Chan for their continuous support during my Ph.D. study. Their patience, motivation, and guidance are so much appreciated. I also would like to thank my thesis committee Dr. Steve P. H. Alexander and Dr. Astrid C. Hauge-Evans for their valuable comments and discussions during the viva voce.

I am so grateful to my family: mother, brothers and sister with a special mention to my wife and the four kids for spiritual and emotional support. Thanks for providing lots of hope to achieve my goal successfully.

A very special gratitude goes out to my sponsor The Iraqi Ministry of Higher Education and Scientific Research for funding this project and financial support.

Thanks to all of my friends and colleagues in the faculty of medicine and health sciences school of life sciences and in the CELE at the University of Nottingham; especially those in the Pharmacology and Neuroscience research group and the cell culture team in the E floor medical school at the Queens Medical Centre.

Publications, conferences and posters

1. An oral presentation in the Neuroscience and Pharmacology at the school of life sciences UoN (January 2015): "The inhibitory effects of somatostatin on B-cells: oxidative respiration and cAMP pathways".
2. Poster presented in the PGR symposium at the school of life sciences UoN (July 2016): "Mitochondria and glycolysis as potential targets for somatostatin action in pancreatic β-cells".
3. Poster presented in the Pharmacology 2016 of the British pharmacological society London (December 2016): Conference abstract "An early metabolic target for somatostatin in pancreatic β-cells".
4. An oral presentation in the PGR symposium at the school of life sciences UoN (July 2017): "Effects of Somatostatin on Mitochondrial Function and Intracellular Calcium Levels in MIN6 Pancreatic β Cells".
5. Co-author of the journal article "The Glycolytic Pathway is the Predominate Path for Glucose Utilization in Human Pancreatic Beta Cells (1.1B4)". European Scientific Journal February 2018 edition Vol.14, No.6 ISSN: 1857 – 7881 (Print) e - ISSN 1857-7431. URL:http://dx.doi.org/10.19044/esj.2018.v14n6p41.
6. Co-Author of the journal article "Simvastatin Inhibits L-Type Ca^{2+}-Channel Activity Through Impairment of Mitochondrial Function". Toxicological Sciences, March 2019. URL: https://doi.org/10.1093/toxsci/kfz068.

List of abbreviations

2DG	2-deoxyglucose
2DG6P	2-deoxyglucose-6-phosphate
AC	Adenylyl cyclase
Ag/AgCl	silver – silver chloride
AM	Acetoxymethyl ester
ATP	Adenosine triphosphate
BSA	Bovine serum albumin
Ca^{2+}	Calcium ions
cAMP	Cyclic adenosine monophosphate
CICR	Calcium-induced calcium release
CSA	Cyclosporine A
dbcAMP	N^6,2'-O-dibutyryladenosine 3':5' cyclic monophosphate
DMSO	Dimethyl sulfoxide
EDTA	Ethylene diamine tetra acetic acid
ER	Endoplasmic reticulum
ETC	Electron transport chain
FBS	fetal bovine serum
FCCP	Carbonyl cyanide-4-(trifluoromethoxy) phenylhydrazone
GLUT	Glucose transporter
GPCR	G protein-coupled receptor
KIC	α-Ketoisocaproic acid
Ø	diameter
OCR	oxygen consumption rate
OKA	Okadaic acid
PBS	phosphate buffered saline
PDH	Pyruvate dehydrogenase
PK	Pyruvate Kinase
PLC	phospholipase C
PTX	Pertussis toxin
Rh123	Rhodamine 123

RPMI medium	Roswell Park Memorial Institute medium
RT	Room temperature
SRIF-14	Somatostatin 14
SSTs	Somatostatin receptors
SV	Slop values
TC	Tissue culture
TCA	Tricarboxylic acid cycle
VGCCs	Voltage-gated calcium channels
ΔpH_{mit}	Mitochondrial pH gradient
$\Delta\Psi_{mit}$	Mitochondrial membrane potential

Table of Contents

Table of Figures

Chapter One:
General Introduction

1.1 Introduction

Insulin secretion from pancreatic β-cells is one of the most crucial processes to control glucose homeostasis; therefore, understanding the intracellular mechanisms by which insulin is secreted will provide further knowledge in the treatment of metabolic disorders such as diabetes mellitus. The hormone somatostatin is considered to be a significant factor in the regulation of blood insulin levels. It regulates insulin secretion mainly via a systemic effect and to a lesser extent by a paracrine effect (Barrett et al., 2012).

1.2 Physiology of the Pancreas

The pancreas is a glandular organ composed of two types of secretory glands, the exocrine and the endocrine glands. The exocrine glands are composed of ducts and cells called the acini which secrete digestive enzymes such as proteases, lipase, and amylase. While the endocrine glands are represented by the islets of Langerhans which secrete hormones and polypeptides. The islet consists of four main types of cells, first alpha cells (α-cells) secrete glucagon and constitute 35-40% in human and 15-20% in rodents of the total islet cells. Second, beta cells (β-cells) secrete insulin and amylin and occupy ~60% of cells in human islets and ~70% in the rodents. Third, delta cells (δ-cells) secrete somatostatin and comprise 10-15% in human and around 5% in the rodents. Fourth, F cells, sometimes called PP cells, which secrete pancreatic polypeptides, total less than 5% of islet cells (Brissova et al., 2005, Cabrera et al., 2006). There is a reciprocal, paracrine action among islet cells hormones, e.g. α-cells secretes glucagon which stimulates the secretion of insulin and somatostatin, while δ-cells secretes somatostatin which inhibits the secretion of all other peptides (Barrett et al., 2012).

1.3 Classical mechanism of insulin secretion

The gene of insulin encodes mRNA to produce a large peptide (preprohormone) called preproinsulin which enters the rough endoplasmic reticulum of the β-cells and is converted to proinsulin by the formation of disulfide bonds. The proinsulin is transported to the Golgi apparatus where it is packaged into secretory granules that move near the plasma membrane to be ready for exocytosis (Chan et al., 1976). Figure 1.1 illustrates the steps of glucose stimulated insulin secretion in pancreatic β-cells.

1.3.1 Glucose uptake and glycolysis

Food intake leads to increased plasma levels of glucose, amino acids, and free fatty acids. These are sensed by pancreatic β-cells and subsequently lead to the release of insulin. The main function of insulin is to act on its target tissues such as liver, muscle and adipose tissue to store glucose and other circulating nutrients of the plasma (Jitrapakdee et al., 2010, Rorsman, 1997). Glucose enters the β-cells via glucose transporters, GLUT1, and GLUT2, in human and rodents, respectively, by means of facilitated diffusion as a result of an elevation in plasma glucose levels (Tal et al., 1992, De Vos et al., 1995). GLUTs are protein molecules expressed in the β-cells and stored in vesicles in the cytoplasm. Although, it has a low affinity for glucose with a high Km 42mM (Marshall et al., 1993). GLUT2 transporters translocate to the cell membrane in response to high plasma glucose levels, the resultant increase in the number of glucose transporters allows more glucose to diffuse into the cells (Thorens et al., 1988, Thorens, 2015). Consequently, this process is not rate limiting for glucose entry into the β-cell even when the glucose plasma concentration is between 12-20 mM after a meal, in comparison with normal physiological glucose concentrations (4-8 mM) (Matschinsky, 1990, Barrett et al., 2012).

Glucokinase (GK) then phosphorylates glucose into glucose-6-phosphate by a rate limiting process. However, GK has a high K_m (5-10 mM) for glucose relative to other hexokinases. In fact, Matschinsky et al., (1993) suggested that GK plays a vital role as a "glucose sensor" in β-cells to maintain glucose homeostasis. Moreover, the activation of this enzyme by exogenous glucokinase activators (GKAs) such as piragliatin (Sarabu et al., 2012) and MK0941 (Eiki et al., 2011) lead to a significant improvement in insulin secretion, thus GK acts as a promising new target for treating type II diabetes mellitus. However, the use of GKAs was limited because the drug lost efficacy within several months of the phase II trial; in addition, some patients developed hyperlipidaemia and vascular hypertension (Matschinsky, 2013).

The deficiency or mutation of GK leads to permanent neonatal and type 1B diabetes which is due to inhibition of glucose metabolism and insulin release (Lin et al., 2019, Njølstad et al., 2001). On the other hand, others suggested that GK deficiency is not a common cause of neonatal diabetes (Gloyn et al., 2002).

Glycolysis is the process by which glucose-6-phosphate is broken down to produce pyruvate, lactate or both in order to finally provide energy as ATP. There are two types of glycolysis. First, aerobic glycolysis in which the existence of oxygen is essential and the pyruvate produced enters the tricarboxylic acid cycle (TCA) in the mitochondria. Then pyruvate metabolism occurs through a respiratory enzyme pathway to produce carbon dioxide and water. This process leads to the conversion of ADP into ATP, providing 38 molecules of ATP (Barrett et al., 2012). Second, anaerobic glycolysis happens in the absence of oxygen when pyruvate was converted to lactate instead of entering the mitochondria. This process produces only two molecules of ATP (Barrett et al., 2012).

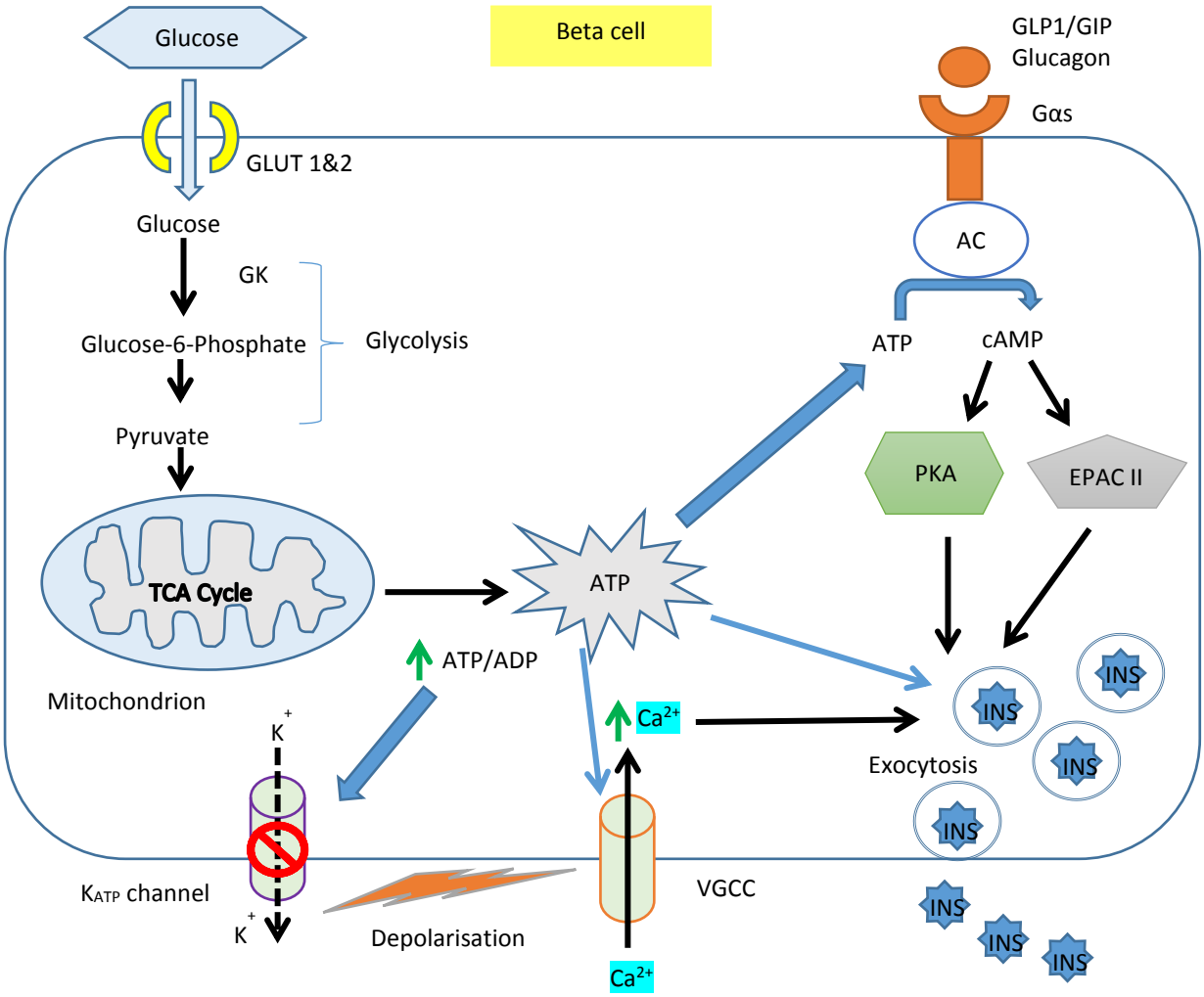

Figure 1.1: A simple diagram illustrates the mechanism of glucose stimulated insulin secretion. Food intake leads to increase plasma glucose concentration which is sensed by pancreatic β-cells. Glucose uptake occurs via glucose transporters (GLUTs) and glucose rapidly phosphorylated by glucokinase (GK) to glucose-6-phosphate as a first step of glycolysis. Pyruvate is the last product of glycolysis which enters the mitochondria and produce energy as ATP. Increase ATP/ADP ratio blocks K_{ATP} channels, depolarizing the plasma membrane and activate Voltage-gated calcium channels (VGCC) allowing the influx of Ca^{2+} from the extracellular fluids. ATP converts to cAMP by the action of adenylyl cyclase (AC) which activates both protein kinase A (PKA) and EPAC II to stimulate insulin (INS) exocytosis. ATP and Ca^{2+} play role in potentiation of exocytosis.

1.3.2 Mitochondrial metabolism

The mitochondrion consists of matrix surrounded by two membranes, inner and outer, with intermembrane space in between. The TCA cycle happens in the matrix while oxidative phosphorylation occurs in the inner membrane (Figure 1.2). In the oxidative phosphorylation process, electrons are transferred from electron donors (NADH and $FADH_2$) produced by the TCA cycle to electron acceptors (oxygen) in redox reactions. These redox reactions are achieved with the electron transport chain via five protein complexes (I-V). This process starts when NADH reacts with NADH dehydrogenase, complex I, to donate two electrons (see figure 1.2). As a result of passing of those electrons through complex I, four protons (H^+) are transported from the matrix to the intermembrane space and coenzyme Q10 or ubiquinone (Q) is reduced to ubiquinol (QH_2) (Hirst, 2010). The second step in the electron transport chain occurs at complex II or succinate dehydrogenase, which oxidizes succinate to fumarate and transfers the electrons via the reduction of flavin adenine dinucleotide (FAD) to $FADH_2$. This step reduces ubiquinone to ubiquinol as well. Since the oxidation of succinate in complex II produces less energy than that of NADH in complex I, complex II does not transport H^+ through the membrane and it is considered the only complex that transport electrons without pumping H^+ to the intermembrane space. However, it is believed that complex II plays an important role in reactive oxygen species (ROS) formation. Complex II is a unique enzyme because it participates in both the TCA cycle in the matrix, in addition to electron transport chain in the inner membrane (Yankovskaya et al., 2003, Horsefield et al., 2004, Chaban et al., 2014). Complex III (cytochrome c reductase) consists of two protein subunits, it oxidises ubiquinone to ubiquinol, releasing two H^+ to the intermembrane space and the electrons are passed through the cytochrome units of the complex (Chaban et al., 2014). The final enzyme of the mitochondrial electron transport chain is cytochrome c oxidase or complex IV. It receives electrons from complex III and to reduce molecular oxygen which is the final acceptor for electrons in the chain. During this process, four H^+ are pumped to the intermembrane space (Chaban et al., 2014, Calhoun et al., 1994). Finally, ATP synthase (complex V) performs the last step in the oxidative phosphorylation pathway by phosphorylation of ADP to ATP. Energy is obtained from the H^+ gradient transported from

intermembrane space. The mitochondria of β-cells have a crucial role in the process of insulin secretion not only by producing ATP but also by creating active metabolites such as NADH, GTP, glutamate, and acyl-CoA, which act inside and outside the mitochondria to stimulate insulin secretion (Jitrapakdee et al., 2010). The elevation of ATP concentration or the increase in ATP/ADP ratio has many signaling roles that finally potentiate insulin secretion.

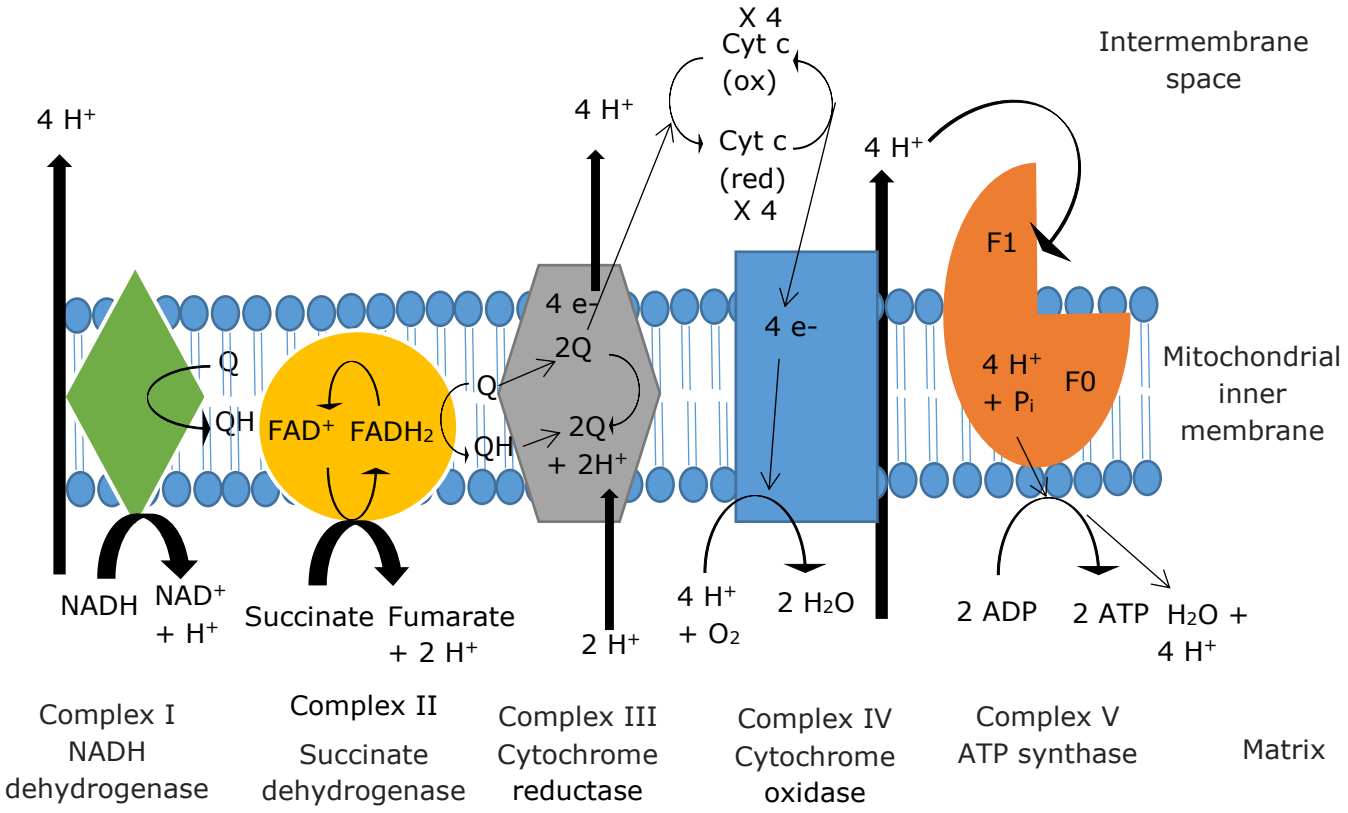

Figure 1.2: Mitochondrial oxidative phosphorylation. The enzymes of electron transport chain (complex I – IV) and complex V are embedded in the inner mitochondrial membrane. These complexes are potential targets for SRIF action which will be explored in this study.

1.3.3 Roles of ATP

ATP initiates, potentiates and maintains insulin release by blocking ATP-sensitive potassium (K_{ATP}) channels as shown in Fig. 1.1. K_{ATP} consists of eight building units, four external sulfonylurea receptors (SUR1) surrounding four internal inwardly rectifying potassium channel subunits ($K_{ir}6.2$) (Clement et al., 1997). Channel activity is blocked due to an interaction between ATP with the $K_{ir}6.2$ subunit of these channels (Tucker et al., 1997). As a result of blocking K_{ATP} channel activity, the cell membrane potential is depolarized which will lead to an opening of the voltage-gated calcium channels (VGCCs) and permits calcium ions (Ca^{2+}) to flow into the β-cells. Consequently, intracellular calcium ions concentration $[Ca^{2+}]_i$ dramatically rise and, via poorly detailed mechanisms, exocytosis of insulin vesicles occurs (Rorsman et al., 1992, Rorsman, 1997, Dou et al., 2015).

Another role for ATP was shown by Smith et al., (1989), who found that VGCCs were directly potentiated by ATP resulting from glucose metabolism, which allowed an influx of extracellular Ca^{2+} to enhance insulin exocytosis (Smith et al., 1989). Third, it is believed that ATP might potentiate exocytosis processes by energising insulin containing granules. Therefore, ATP assists mobilising and priming of the granules and making them ready for releasing insulin (Eliasson et al., 1997, Rorsman, 1997, Takahashi et al., 1999). A fourth role involves adenylyl cyclase (AC) which converts ATP into cyclic adenosine hormones monophosphate (cAMP). Activation of AC is mediated by binding of gastrointestinal or incretins such as glucagon like peptide–1 (GLP-1) and gastric inhibitory polypeptide (GIP) with their respective G-protein coupled receptors (GPCRs) which act to potentiate insulin secretion (Gromada et al., 1998, Yabe and Seino, 2011).

In mammalian cells, two kinds of AC are present, the transmembrane AC (tmAC) which is encoded by nine different genes, and a soluble AC (sAC) that is encoded by a single gene (Cooper, 2003, Sunahara et al., 1996). All isoforms of tmAC are commonly activated by $G_{s\alpha}$. Furthermore, pancreatic islets are found to express Ca^{2+}/calmodulin regulated tmAC (Tian and Laychock, 2001). On the other hand, the activity of tmAC type I, V and VI are inhibited by different types of inhibitory G protein alpha subunits ($G_{i\alpha1}$, $G_{i\alpha2}$, $G_{i\alpha3}$ & $G_{o\alpha}$) (Taussig et al., 1994). G protein beta/gamma complex ($G_{\beta\gamma}$) also can selectively regulate

various tmAC isoforms; it inhibits type I and stimulates type IV and VII (Tang and Gilman, 1991, Gao and Gilman, 1991). The level of cAMP generated by the action of AC is controlled by cyclic nucleotide-specific phosphodiesterase enzymes (PDEs) which are responsible for the hydrolysis of cAMP into 5' AMP (Beavo and Brunton, 2002, Bender and Beavo, 2006). PDEs act by hydrolysing the phosphodiester bond of cyclic nucleotides. A huge number of isoforms of PDEs exist, over 50 types encoded from 25 different genes, are known to exist in mammalian cells (Conti, 2000, Essayan, 2001). The PDE superfamily is divided into 11 subfamilies (PDE1 – PDE11) according to their regulation, structure and dynamic properties. PDEs are effective on both cyclic nucleotides, cAMP and cGMP. Isoforms which act specifically on the cAMP are PDE4, PDE7, and PDE8, while PDE5, PDE6, and PDE9 are specific for cGMP, and the rest PDE1, PDF2, PDE3, PDE10, and PDE11 are capable of hydrolysing both (Bender and Beavo, 2006, Francis et al., 2011). The pancreatic islets specifically express PDE1C, PDE3B, PDE4 and possibly PDE10A, however it is believed that PDE3B is the dominant isoform in the islets (Pyne and Furman, 2003).

Studies show that cAMP plays an important role in modulation of exocytosis in secretory cells such as neurons, endocrine, neuroendocrine and exocrine cells as a general intracellular messenger (Burgoyne and Morgan, 2003, Seino and Shibasaki, 2005, Chavez-Noriega and Stevens, 1994, Ammälä et al., 1993, Fujita-Yoshigaki, 1998). It is believed that protein kinase A (PKA) is the main but not the only target of the cAMP that enhance exocytosis. Examples for the other targets of cAMP are cyclic nucleotide-gated (CNG) channels (Kaupp and Seifert, 2002), hyperpolarization-activated cyclic nucleotide-gated (HCN) channels (Biel et al., 2002), and cAMP-specific guanine nucleotide exchange factors (cAMP-GEF)/exchange proteins directly activated by cAMP (EPAC) (Bos, 2003, Springett et al., 2004).

In pancreatic β-cells, cAMP promotes insulin exocytosis via binding and activation of two main effectors, PKA (Seino and Shibasaki, 2005, Valsecchi et al., 2013), in addition to EPAC (Holz, 2004, Seino and Shibasaki, 2005, Bos, 2003, Almahariq et al., 2014). The A-kinase anchor protein (AKAP) acts as scaffold protein where it binds PKA and other signaling proteins such as PDEs as well. AKAP tethers PKA to a specific location in the cell, permitting the cAMP to combine PKA and induce phosphorylation of proteins such as

cysteine string protein (Csp). The latter acts as a PKA substrate, which promotes insulin granules exocytosis (Evans et al., 2001, Jones and Persaud, 1998, Thompson and Shuttleworth, 2015).

Several studies suggest that the cAMP-GEF/Epac represents a PKA-independent pathway for cAMP-regulated exocytosis (Fujimoto et al., 2002, Kang et al., 2003, Kashima et al., 2001, Ozaki et al., 2000, Song et al., 2013). In addition to cAMP, Ca^{2+} is essential for the process of Epac dependent insulin secretion. There are two isoforms of EPAC expressed in pancreatic β-cells, EPAC I and EPAC II (Parnell et al., 2015, Holz, 2004, Kawasaki et al., 1998). EPAC I has a limited role in the insulin secretion process whereas EPAC II has the major effect (Song et al., 2013). The mechanism by which EPAC II mediates insulin secretion is due to direct interaction with Rim2, an isoform of Rim protein, a supposed target of the small G protein Rab3-interacting molecule that participates in exocytosis (Ozaki et al., 2000, Kashima et al., 2001, Renström et al., 1997). In the MIN6 cell line, Rim2 is found in the plasma membrane and insulin containing granules (Shibasaki et al., 2004a). In pancreatic islets and MIN6 cells, Fujimoto et al., (2002) demonstrated that piccolo protein is yet another target for EPAC II and has an essential role in cAMP dependent insulin secretion. Both Rim 2 and piccolo may act as Ca^{2+} sensors in β-cells and be involved in Ca^{2+} release. Although EPAC II also interacts with the SUR-1 subunit of the K_{ATP} channel, channel activity does not seem to be affected. However, it is believed that this interaction might be important for EPAC dependent insulin exocytosis because EPAC II might be dissociated from SUR-1 under cAMP stimulation (Shibasaki et al., 2004b). This is supported by the findings that EPAC dependent insulin secretion is impaired in SUR1 knockout islets (Nakazaki et al., 2002, Shiota et al., 2002) and that early PKA-independent exocytosis is lost in SUR1 knockout-cells (Eliasson et al., 2003).

1.4 GPCR related mechanisms of insulin secretion

GPCRs in pancreatic islets have both stimulatory and inhibitory roles by transmitting extracellular to intracellular signals. Examples of GPCRs expressed in the islets of Langerhans are receptors for the; incretin hormones GLP-1 and GIP; fatty acid activated ligands e.g. GPR40 and GPR119; neurotransmitters such as acetylcholine (Ach) that

activate muscarinic receptors (M3) and noradrenaline that activate both β_2 and α_2 adrenoceptors. Furthermore, the neuropeptides pituitary adenylate cyclase-activating polypeptide (PACAP) and vasoactive intestinal polypeptide (VIP) related to PAC1 and VPAC2 receptors, cholecystokinin which activates CCK_A receptors and neuropeptide Y (NPY Y1) receptors are also found in the islets. There are also cannabinoid (CB_1) receptors, vasopressin (V1B) receptors and P2Y receptors expressed in the islets and the hormones of islets receptors i.e. glucagon receptors and somatostatin receptors (SSTR) (Winzell and Ahrén, 2007).

In general, GPCRs exert their effects via interaction with different G proteins i.e. G_S, G_i and G_q. Each G protein consists of three subunits, α, β and γ (Neves et al., 2002). One of the important actions of GPCRs in β-cells is the formation of second messengers e.g. inositol 1,4,5 trisphosphate (IP3) and diacylglycerol (DAG). In the cell membrane, phosphatidylinositol is phosphorylated twice to produce firstly, phosphatidylinositol 4-phosphate (PIP), and then phosphatidylinositol 4,5-bisphosphate (PIP_2). The breakdown of PIP_2 by the effect of phospholipase C (PLC) enzyme which is activated under control of muscarinic receptors (M3) and G_q protein leads to IP_3 production. Consequently, IP_3 triggers Ca^{2+} release from intracellular stores (endoplasmic reticulum) joining the Ca^{2+} that has entered the cell via VGCC to stimulate exocytosis (Barker and Berggren, 2012, Berggren and Barker, 2008). Moreover, DAG is also produced as a result of hydrolysis of PIP_2 in the cell membrane where it activates one of the numerous isoforms of protein kinase C (PKC) and other signaling pathways such as Munc-13 dependent pathway as well (Berridge and Irvine, 1984, Nishizuka, 2003, Kaneko and Ishikawa, 2015). PKC has proved to play a significant role in insulin vesicle exocytosis (Nesher et al., 2002, Mendez et al., 2003, Yamazaki et al., 2010).

Glucagon has an effective role in blood glucose homeostasis because it also stimulates gluconeogenesis and glucose liberation from the liver (Jiang and Zhang, 2003). In addition to pancreatic β-cells, many other cells express glucagon receptors e.g. hepatocytes and adipocytes which make them a target for circulating glucagon (Svoboda et al., 1994, Van Schravendijk et al., 1985, Gilon et al., 2014). Different intracellular responses can be observed on the stimulation of glucagon receptors in pancreatic β-cells. First, due to the

activation of the G_s protein, AC can be activated and initiate the classical cAMP signaling pathways and potentiation of insulin secretion (Jelinek et al., 1993). Another suggestion for glucagon action is to increase intracellular $[Ca^{2+}]_i$ levels possibly by cAMP signaling pathway (Jelinek et al., 1993, Rodgers, 2012, Authier and Desbuquois, 2008, Wang et al., 2012). It is also argued that $[Ca^{2+}]_i$ level arises because glucagon might trigger either $G_{\alpha q}$, $G_{\alpha i}$ or both to produce IP_3 via PLC activation (Xu and Xie, 2009). Furthermore, studies in hepatocytes (Kimball et al., 2004) and adipocytes (Peng et al., 2012) indicate that glucagon can activate AMP-activated protein kinase (AMPK) via Ca^{2+}/calmodulin-dependent protein kinase pathway. However, in pancreatic β-cells, the Ca^{2+}/calmodulin-dependent protein kinase II may instead play a role in the modulation of insulin secretion (Niki et al., 1993).

In addition to the main effects of glucagon on glucose homeostasis, catecholamines (adrenaline and noradrenaline) have a crucial role to restore and prevent hypoglycaemia but by different mechanisms. It is well known that catecholamines have effects on the pancreatic β-cells by three ways leading to inhibition of insulin release. These methods are activation of K_{ATP} channels, inhibition of AC and a distal effect in which Ca^{2+} is prevented to induce exocytosis. It is believed that all those three effects are achieved by the pertussis toxin (PTX)-sensitive proteins G_i and G_o (Straub and Sharp, 2012). Catecholamines interact with two types of GPCR adrenoceptors (α_2 & β_2) that are expressed in the islets. Activation of β_2 adrenoceptors by noradrenaline results in stimulation of both insulin and glucagon secretion via a cAMP dependent process (Kuo et al., 1973, Lacey et al., 1991, Ahrén, 2000). In contrast, noradrenaline interacts with α_2-adrenoceptors, which results in the inhibition of insulin secretion and the stimulation of glucagon secretion (Ahrén, 2000). Clonidine (α_1 adrenoceptor agonist) also has the ability to inhibit glucose utilization and glucose stimulated insulin secretion (Laychock, 1987, Niddam et al., 1990). In conclusion, catecholamines may have dual actions on insulin secretion, stimulation through β_2-adrenoceptors and inhibition through α_2-adrenoceptors (Ullrich and Wollheim, 1985).

1.5 Physiology of Somatostatin

Somatostatin, also known as somatotropin release-inhibiting factor (SRIF), is a cyclic polypeptide secreted from various parts of the body such as the brain, gastrointestinal tract, and pancreas. In mammals, there are six different genes providing two endogenous isoforms of somatostatin according to the number of amino acids composing each form which are SRIF-14 and SRIF-28 (Pradayrol et al., 1980, Liu et al., 2010). The main source of SRIF-28 is from the gastrointestinal mucosa, while SRIF-14 has been found centrally in the brain and peripherally in pancreas, liver, lungs and other organs (Van Op den Bosch et al., 2009, Ben-Shlomo and Melmed, 2010). SRIF has many regulatory effects on neurons, endocrine and neuroendocrine glands, immune and inflammatory cells. Its secretion is regulated due to stimulation of target organs by neuropeptides, neurotransmitters, hormones and many other factors e.g. ions, nutrients, cytokines and growth factors (Pintér et al., 2006, Kim et al., 2014).

It is well known that SRIF inhibits insulin secretion. SRIF-28 is considered to be the main isoform that reduces insulin secretion *in vivo.* It is secreted as a response to food intake which induces gastrointestinal δ-cells to produce SRIF-28 (Schusdziarra et al., 1978). It is believed that this effect is responsible for the prevention of postprandial hypoglycaemia which may result from rapid insulin secretion (Ensinck et al., 1997). Nevertheless, SRIF-14 which is secreted from pancreatic δ-cells has been shown to affect β-cell function locally and inhibits insulin secretion (Tirone et al., 2003). The fact that SRIF-14 is released from the pancreas in response to a high glucose level is an indication that SRIF-14 might play a significant role in modulation of diabetes and other pancreatic dysfunctions (Sliwińska-Mossoń et al., 2014).

The physiological effects of SRIF are achieved via coupling with a group of GPCRs called somatostatin receptors (SST). There are five subtypes of receptors (SST 1-5), which have been expressed and cloned in different mammalians cells (Kumar and Grant, 2010, Patel, 1999, Olias et al., 2004). An immunocytochemistry study on human islets showed the variable distribution of the SSTRs subtypes in different islet cells. There is no absolute specificity of SSTR for any cell type in the islet, even though there is a specific localization of SST1, SST2 and SST5 receptors in human pancreatic β-cells (Kumar et al., 1999, Singh

et al., 2007). In rodents, both pancreatic β-cells and cell lines express all SSTs in their cell membrane with some variations (Smith et al., 2001, Mitra et al., 1999). According to many studies conducted on mice, rat and human, there is strong evidence that SST5 predominantly mediates the inhibitory effect of SRIF on insulin secretion (Tirone et al., 2003, Smith et al., 2001, Mitra et al., 1999, Fagan et al., 1998, Strowski et al., 2003, Zambre et al., 1999). Whereas, others suggest that activation of SST2 is responsible for inhibition of insulin secretion in isolated human islets (Brunicardi et al., 2003, Atiya et al., 1997, Moldovan et al., 1995).

1.6 Therapeutic indications of SRIF and its analogues

Somatostatin has a wide range of biological activities including inhibition of secretion in different organs such as pituitary gland, brain, thyroid, gastrointestinal, pancreas and the eye (Boehm, 2003). SRIF has a very short half-life (1-3 minutes) before being degraded by peptidases in the plasma and tissues (Benuck and Marks, 1976) which make it less useful for therapeutics. As a result, synthetic analogues (cyclic octapeptides) such as octreotide and lanreotide were developed which are more resistant to peptidases providing better biological activity and a longer half-life (1.5-2 h) than the native SRIF (Oberg, 2004). More recent studies highlight the clinical importance of SRIF and its analogues for pancreatic diseases. Sliwińska-Mossoń et al., (2014) mentioned some of these diseases such as acute and chronic pancreatitis, diabetes mellitus, pancreatic adenocarcinoma and pancreatic endocrine tumours such as insulinoma and glucagonoma (Sliwińska-Mossoń et al., 2014). In addition to pancreatic diseases, Rai et al., (2015) reviewed other therapeutic uses of SRIF and its analogues such as in the treatment of acromegaly, obesity, diabetic retinopathy, diabetic nephropathy, inflammation and pain (Rai et al., 2015).

1.7 The possible mechanisms of action of SRIF on pancreatic β-cells

To date, the mechanisms by which SRIF inhibits insulin secretion are still controversial (Fig.1.3). On the one hand, five decades since the discovery of SRIF a base of knowledge about this interesting peptide has been developed. The most widely accepted notion explained the major effect of SRIF is via the activation of pertussis toxin (PTX) sensitive G_i protein. The latter is expected to be responsible for inhibition of exocytosis by several possible mechanisms. First, it may act by activation of the potassium channels, ATP-sensitive K channels (K_{ATP}) and G protein-regulated inwardly rectifying K channels (GIRK) and the subsequent hyperpolarisation of the cell membrane (Yamada et al., 1998, Smith et al., 2001). K_{ATP} channel activation can be due to inhibition of glucose metabolism and a decrease of ATP levels (Tarasov et al., 2004, Ashcroft and Rorsman, 1989, Smith et al., 2001). Although, it is reported that K_{ATP} can also be directly activated by G proteins (Ribalet and Eddlestone, 1995). As a result, the activation of both GIRK and K_{ATP} will lead to a closure of VGCC resulting in a decrease of intracellular Ca^{2+} levels which inhibits exocytosis (Smith et al., 2001, Sims et al., 1991, Koch et al., 1988). Secondly, SRIF reduces cAMP formation by inhibition of AC activity via a direct G protein interaction; this will lead to a decrease in activation of both PKA and Epac to produce a direct inhibition of insulin exocytosis (Patel et al., 1994, Ullrich et al., 1990).

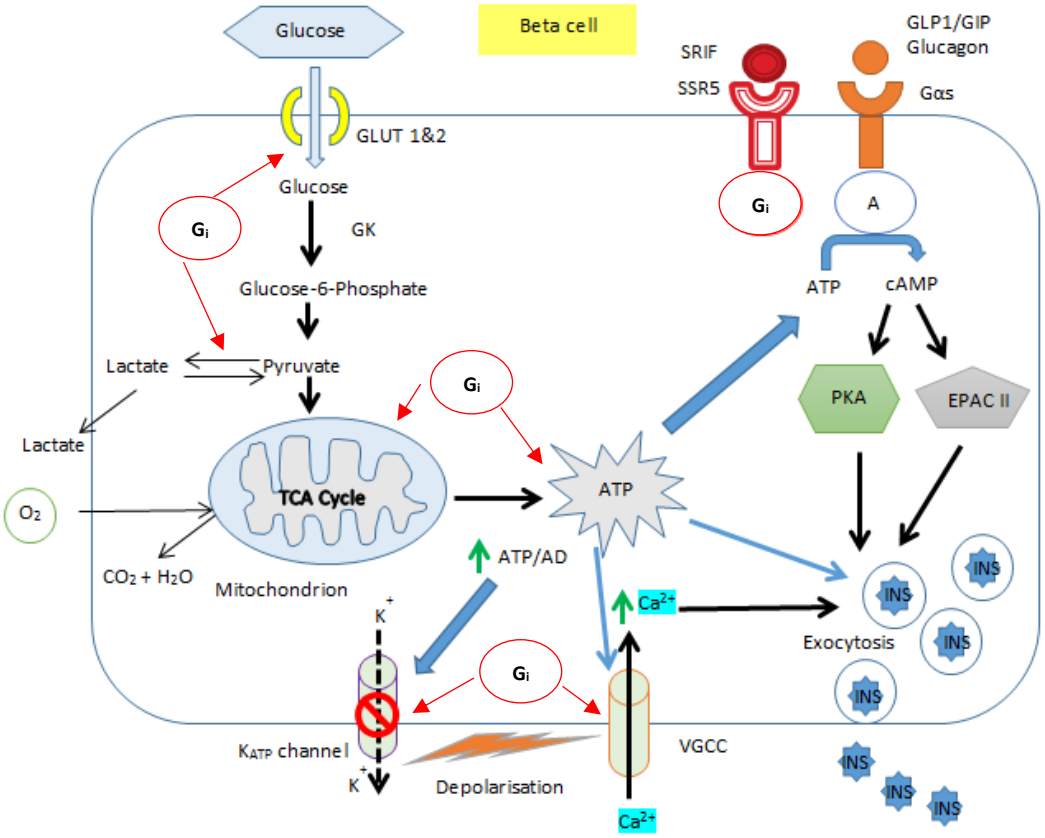

Figure 1.3: A schematic diagram shows the steps of glucose stimulated insulin secretion. The possible targets for SRIF action which will be explored in this study labelled with red arrows.

Another additional mechanism explaining the inhibitory effect of SRIF is via a direct block of both N and L-type voltage-gated Ca^{2+} channels reducing the Ca^{2+} influx (Smith, 2009, Fujii et al., 1994). Others hypothesise that in GH3 somatotropin cells, SRIF is able to activate voltage-gated K^+ channels that result in increasing K^+ efflux and decreased Ca^{2+} entry (Yang et al., 2005) an effect which might also happen in β-cells, although this has yet to be shown.

It is argued that the hyperpolarization of the cell membrane potential is probably the primary mechanism by which SRIF inhibits insulin secretion (Daunt et al., 2006). This suggests that SRIF might directly inhibit glucose metabolism because the cell membrane electrical activity is depending on ATP that results from glucose metabolism. However, to date, the mechanism of SRIF action on glucose metabolism is poorly understood.

1.8 Aims

The main aim of this project is to investigate further the mechanisms by which SRIF inhibits β-cell metabolism and subsequently insulin secretion. This includes glucose uptake and glycolysis, mitochondrial function and ATP production, in addition to the role of extracellular Ca^{2+} influx in this process Fig.1.3.

Chapter Two:
Methodology

2.1 Materials and chemicals

All chemicals were purchased from Sigma unless otherwise indicated.

2.2 Solutions

For all experiments, a modified Hank's solution was prepared which contained in mM: 5.6 KCl, 138 NaCl, 4.2 $NaHCO_3$, 1.2 NaH_2PO_4, 2.6 $CaCl_2$, 1.2 $MgCl_2$, 10 HEPES; pH adjusted by up to 11 ml of 1 M NaOH to 7.4, supplemented with 0.1% wt/vol bovine serum albumin (BSA) fraction V (Sigma).

For imaging experiments, a calcium-free Hank's solution was made as described above except 2. $CaCl_2$ was replaced with equimolar 2.6 mM $MgCl_2$ to maintain the same concentration of divalent cation in the solution. Furthermore, a high potassium Hank's solution was also used which contained in mM: 50 KCl, 92.6 NaCl, 4.2 $NaHCO_3$, 1.2 NaH_2PO_4, 2.6 $CaCl_2$, 1.2 $MgCl_2$, 10 HEPES and 1 M NaOH to obtain a pH of 7.4.

For lactate experiments, buffer A solution was prepared, which contained in mM: 10 NaH_2PO_4, 100 NaCl, 1 $MgCl_2$, and 2 glycerol, which was used for storage of Sarissaprobe®-LAC lactate electrode at 2-8^{o}C.

Stock solutions of D-glucose (Fisher scientific UK), SRIF-14 (Sigma and Peninsula Lab. Europe Ltd.), dibutyryladenosine 3',5'-cyclic monophosphate (dbcAMP) a cell penetrating cAMP analogue (Tocris®), clonidine, pertussis toxin (PTX) (Tocris®), α-ketoisocaproate (KIC), sodium azide, tertiapin LQ (Abcam)and lactate were prepared in H_2O. DMSO was used as a solvent for carbonyl cyanide-4-(trifluoromethoxy) phenylhydrazone (FCCP) (Abcam UK), forskolin, oligomycin, tolbutamide, Fluo-4 (Invitrogen), Rhodamine 123 (Rh123), cytochalasin-B, and rotenone. The protein phosphatase inhibitors cyclosporine-A and okadaic acid were dissolved in ethanol, while glucagon was dissolved in 1% (vol/vol) acetic acid.

2.3 Cell culture

2.3.1 Cell lines

Two types of cells lines were used in this project, MIN6 a mouse pancreatic β-cell line established by (Miyazaki et al., 1990) and 1.1B4, a cell line derived from human pancreatic β-cells derived by McCluskey (McCluskey et al., 2011). MIN6 originated from a transgenic

mouse insulinoma cell and is considered as a good model for studying the physiology of β-cells because MIN6 is homogenous, responsive to glucose stimulated insulin secretion within the physiological range and it expresses glucose transporter GLUT-2 and glucokinase (Ishihara et al., 1993). Furthermore, the most important reason why MIN6 is ideal for this project is that it expresses all somatostatin receptors (SSTs in their cell membrane (Smith et al., 2001, Ishihara et al., 1993). Cells were cultured in RPMI 1640 media (Gibco® of Life Technologies) which was supplemented with 11 mM glucose, 25 mM HEPES and 10% (vol/vol) foetal bovine serum (FBS). Passage numbers 24 – 48 were used in the experiments.

The 1.1B4 cell line was generated by the electrofusion of a primary culture of human pancreatic β-cells with PANC-1, an immortal human pancreatic ductal carcinoma cell line which has similar characteristics of human pancreatic β-cells (McCluskey et al., 2011). 1.1B4 cells are considered to be a good model for insulin secretion under normoglycaemic and hyperglycaemic conditions (Vasu et al., 2013). Cells were cultured in the same conditions described above for MIN6 but with the addition of 1% (wt/vol) penicillin-streptomycin. Passage numbers 36-39 were used.

Cell lines provide a sufficient amount of cells in a short period of time. Tomographic studies on adult mouse pancreas revealed that the number of pancreatic islets is around 1100 scattered through the organ tending to accumulate in the tail area (Alanentalo et al., 2007). However, the number of islets which can be harvested from whole mouse pancreas using collagenase digestion method is only around 100-200 islets, (Rorsman and Ashcroft, 2018). On the other hand, the pancreas of a human contains around one million islets and each islet contains ~200 β-cells (HELLMAN, 1959, Rorsman and Braun, 2013).

2.3.2 Starting cell culture

A cryo-vial was taken from liquid nitrogen stock and rapidly defrosted in a 37 ^{o}C water bath. Immediately after thawing, cell suspension was mixed with 1 ml of RPMI (Gibco® of Life Technologies, UK) and transferred to a 75 cm^2 TC flask (Thermo Fisher Scientific, UK) which contained 15 ml of pre-warmed RPMI medium. The flask was placed in the 37°C incubator with 5% CO_2. Since the freezing medium contains 10% DMSO, it is preferable to replace the medium within 24 h of incubation.

2.3.3 Splitting and sub-culturing

Cells were ready for sub-culturing when they reached nearly 80-90% confluence of the flask surface area. All solutions i.e. media, phosphate buffer saline (PBS) and trypsin EDTA were pre-warmed at 37 ^{o}C for 30-60 min. Under sterile conditions, the RPMI media were poured off and the cells washed with 5 ml of PBS to remove the FBS containing medium which blocks trypsin action. 3 ml of 10% trypsin EDTA (Sigma) was added to the cells and incubated at 37 ^{o}C for 3-5 min until the cells detached. Trypsin is a proteolytic enzyme which breaks down the protein molecules of the cell membrane that attach them to the plastic surface of the TC flasks, while the EDTA is to chelate Mg^{2+} and Ca^{2+} for easy cell detachment by improving the trypsin enzymatic activity (Kirkpatrick et al., 1985). Trypsin was deactivated by adding 12 ml of RPMI culture medium containing 10% FBS to the flask to obtain 15 ml of cell suspension. FBS contains protease inhibitors such as α1-antitrypsin which stop the trypsin effect.

The splitting ratio was 1:3 which was achieved by thorough mixing of the 15 ml cell suspension and the addition of 5 ml to each of three previously prepared TC flasks containing 10 ml of fresh media. The cells were incubated in a humidified atmosphere with 95% air and 5% CO_2 at 37 ^{o}C. Tissue culture media was changed every 2-3 days and the cells were split again after 5-6 days on reaching confluence.

2.4 The isolation of islets of Langerhans

A simplified version of many other protocols was used as described by (Duchen et al., 1993), in order to harvest islets rapidly and to avoid complications such as necrosis. For this Hank's solution was used, which also contained 2.8 mM glucose and bovine serum albumin (BSA) fraction V (0.5% wt/vol), which was sterilized by filtering (0.22 μm). Mice (CD-1 strain males weighed 30-35 g up to 40 days old) were stunned by cervical dislocation and killed by decapitation. There were pinned out and sprayed with 70% ethanol to improve sterility and to prevent contamination of the preparation. The pancreas was dissected out using the spleen as a handle. It was placed in a 100 mm Petri dish and carefully washed in sterile Hank's to remove any blood which might impair the action of collagenase. The pancreas was then

injected multiple times with Hank's via 0.22 µm filter and 25 gauge needle to distend the lobes.

The pancreas was then macerated into small pieces and placed into a glass scintillation vial (20 ml) which contained 3 ml of sterile filtered Hank's and 2 mg/ml collagenase V (Sigma) (Li et al., 2013). The vial was then capped and gently shaken by hand for a maximum of 15 min at a temperature of ~35 °C with vigorous shaking for 15 sec every five min until a milky digest was obtained. The digestion process was stopped by dilution of the collagenase solution with 20 ml of filtered Hank's. Then, the islets were allowed to sediment out for one minute and the supernatant removed; this left approximately 1 ml of digest in the bottom of the vial. The washing process was repeated twice and the digest was suspended again in 20 ml of Hank's. Islets were picked up by using a 20 µL Finn pipette under a binocular microscope. Islets were collected in 35 mm Petri dishes and picked up again to another 35 mm Petri dish and then into a sterile 1.5 ml Eppendorf tube. Finally, islets were either cultured or used immediately for oxygen consumption rate experiments.

2.5 Oxygen consumption rate measurement

The rate of oxygen consumption was used to measure the changes in the mitochondrial respiration. For this, the oxygen electrode (Rank Brothers, Cambridge UK) an electrochemical sensor, was used as previously described (Daunt et al., 2006). It is based on Clark electrode invented by (CLARK et al., 1953) which is also sometimes called an oxygen membrane polarographic detector (O_2-MPD) according to its mode of action.

2.5.1 Setup and principles of the oxygen electrode

The cell unit of the oxygen electrode consists of two main parts, an incubation chamber that contains the sample and a base where the working electrodes are embedded as shown in figure (2.1). The chamber content is separated from the working electrodes by 1.5 cm^2 bilayer membrane sealed by a silicone rubber O-ring. The first layer of the membrane is a gas-permeable ion-impermeable Teflon membrane, while the second layer is a tissue paper membrane that acts as a vehicle for 3 M KCl electrolyte solution that conducts ions between the two working electrodes. The main electrode is a 2 mm diameter platinum cathode which lies centrally on the base and is surrounded by a silver-silver chloride reference ring electrode (fig.2.1).

The partial pressure of O_2 (PO_2) was measured at a voltage of -0.6 V applied at the platinum cathode with respect to the reference electrode. Due to the cathode polarisation, every O_2 molecule passing through the selective membrane that reaches the electrode surface will be reduced into water according to the following equations:

$$O_2 + 2H^+ + 2e^- \longrightarrow H_2O_2$$

$$H_2O_2 + 2H^+ + 2e^- \longrightarrow 2H_2O$$

For every reduction reaction, there is oxidation at the silver reference electrode:

$$4Ag + 4Cl^- \longrightarrow 4AgCl + 4e^-$$

The overall electrochemical reaction is described by the following:

$$4Ag + O_2 + 2H_2O + 4Cl^- \longrightarrow 4AgCl + 4OH^-$$

This reaction generates a current of ~1 μA at 30 ˚C between working electrodes and this current is proportional to the partial pressure of oxygen in the chamber.

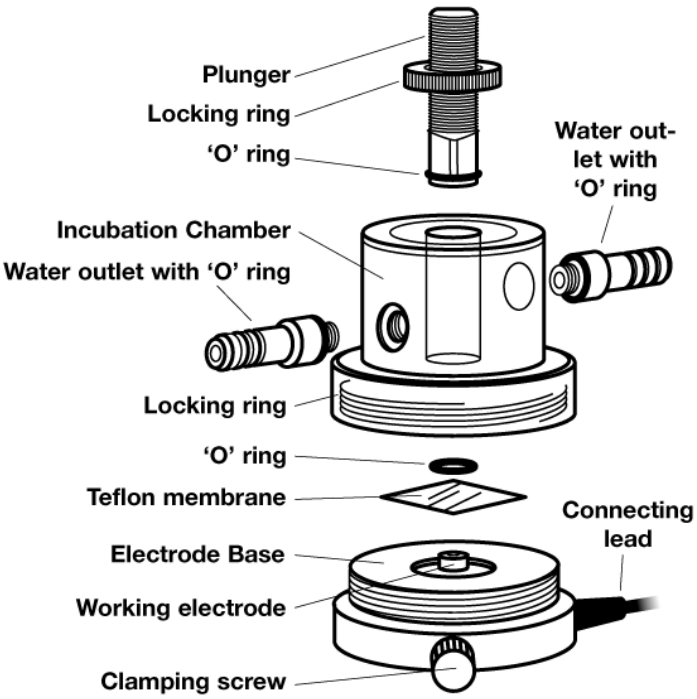

Figure 2.1: The cell unit of Perspex oxygen electrode. This illustration was adapted from and used with permission of rankbrothers.co.uk. http://www.rankbrothers.co.uk/prod1exp.htm

2.5.2 OCR measurement procedure

The electrode underwent a two point calibration before each experiment. First, 1 ml distilled water added to the chamber and a zero oxygen point was achieved by adding the fast reductant, sodium dithionate ($Na_2S_2O_4$) to the water inside the chamber. The zero point was set (0 %) and then the solution replaced with distilled water after washing the chamber several times with water to remove the sodium dithionate. The second calibration point was achieved with distilled water saturated with air (100%) which contains 0.24 mM $[O_2]_{aq}$ at 32 ˚C (Daunt et al., 2006).

After calibration, the distilled water was removed and 2 ml of cell suspension was added to each chamber with a fixed speed of stirring and was exposed to the open atmosphere for 10 min to allow gas and temperature equilibration. Meanwhile, the cell density was counted by a haemocytometer. When the equilibration was achieved, the Perspex plunger was inserted to isolate the sample from the atmosphere and the experiment begun. Care was taken to ensure that no bubble existed between the plunger and the top of the cell suspension which would greatly increase the air/liquid interface and gas-exchange to invalidate the assumption of a closed system. All additions were carefully added to the incubation chambers via a small hole in the plunger in order to avoid introduction of air bubbles inside the chamber. A closed system was used at it means only the oxygen molecules dissolved in the cell suspension inside the chamber are measured. Since the sensitivity of the oxygen electrode is temperature sensitive, with the recording signal increasing with a rise in temperature, this was controlled during the experiments by a thermostatically controlled water jacket. For all experiments, the stirring speed was fixed (number 6) at the lowest speed that was sufficient to just keep the cells floating inside the incubation chamber. Data were acquired (10 Hz) and recorded with DATAQ® instruments (Akron, Ohio). The percentage of oxygen content (PO_2) of the cell suspension in the incubation chambers was plotted versus a known period of time to produce slopes. The slopes were measured to quantify the basal respiration, glucose, and the other treatments as a rate of O_2 consumption which was expressed as nmol O_2 10^7 $cell^{-1}$ min^{-1}.

Data validation was done by excluding the values of PO_2 less than 10% in order to avoid the possible false positive results. Invalid results of O_2 consumption occurs when there is

low O_2 content in the chamber before adding the last treatment (mainly SRIF). All treatments were corrected to 6 mM sodium azide slope values because it completely blocks the cellular respiration and only allows the electrode consumption. This is achieved by subtraction of the slope values (SV) of sodium azide from the slope values of basal, substrates and the drugs. Values were corrected to the cell density i.e. the number of cells in 1 ml of suspension for 10 million cells (haemocytometer cells count) and the time for 1 min (60 s). The percentage effect of substrates, glucose and KIC in relative to basal (% E substrates) in addition to the effect of other treatments relative to substrates (% E treatment) were calculated using Microsoft Excel 2013 while the slopes were analysed by WINDAQ™ software V.2.91 to get the basic values as follows:

OCR in O_2 nmol 10^7 $cell^{-1}$ min^{-1}

$[O_2]_{aq}$ in 1ml H_2O ≈ 0.25mM converted to nmol $*10^9$

The factor = $0.25*10^{-3}*10^9$ / cell number (10^7) / 60 seconds

The factor = $0.25*10^{-3}*10^9*60$ / cell count

The factor = $15*10^6$ / cell count

OCR = SV treatments – SV sodium azide * factor

Basal OCR = (basal SV – sodium azide SV)* $15*10^6$ / cell number

Substrate OCR = (substrate SV - sodium azide SV)* $15*10^6$ / cell number

Drug OCR = (drug SV - sodium azide SV)* $15*10^6$ / cell number

% effect was calculated as follows

% E substrates = 100* (OCR substrate – OCR basal) / OCR basal

% E drug = 100* (OCR drug – OCR substrate) / OCR substrate

Basal OCR is achieved when the cells consume O_2 for 10 min without any additions

Substrate OCR is achieved after addition glucose or α-ketoisocaproate for 10 min

Drug OCR is achieved after the addition of drug for 10 min

2.6 Measurement of lactate production

An electrochemical biosensor was used to measure the rate of glycolysis of MIN6, as previously described (Sener and Malaisse, 1976). Lactate electrode Sarissaprobe® LAC in combination with previously mentioned oxygen electrode has been used to measure lactate output rate and oxygen consumption rate simultaneously. In addition to the amperometric based biosensors, there are other methods for measuring lactate e.g.: HPLC, colorimetry, fluorimetry, and chemiluminescence method. In this study and in many other studies the biosensor method has been used because it is considered as a simple, specific, fast, relatively low cost method (Rathee et al., 2016).

2.6.1 Principles of lactate biosensor

The Lactate biosensor fundamentally depends on the electrical current produced by the redox reaction that occurs between the enzymatic layer and lactate on the electrode surface. The main enzyme of Sarissaprobe® enzymatic layer is lactate oxidase which catalyses the conversion of L-lactate into pyruvate and H_2O_2 in the presence of dissolved oxygen as shown in figure 2.2. As a result of the potential between the main electrode and the reference electrode, H_2O_2 undergoes oxidation to provide the electrons which are generating the current.

$$\text{L-lactate} + O_2 \xrightarrow{\text{L-lactate oxidase}} \text{pyruvate} + H_2O_2$$

$$H_2O_2 \longrightarrow O_2 + 2H^+ + 2e^-$$

The current intensity is proportionally related to the concentration of lactate generated during the experiment. The current was recorded amperometrically using Potentiostat® and DATAQ® instruments.

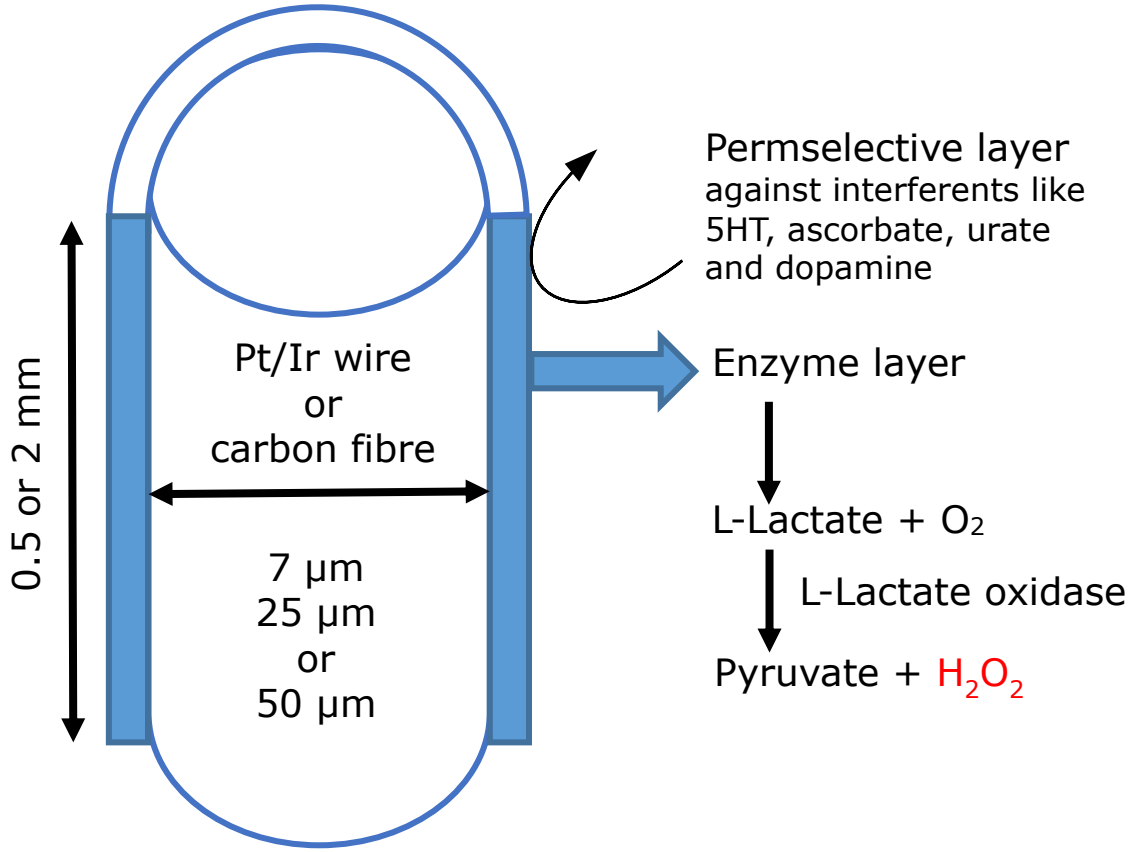

Figure 2.2: Sarissaprobe® Lactate electrode illustration is reproduced with some modifications from Sarissa biomedical website.
http://www.sarissa-biomedical.com/products/sarissaprobes/lactate.aspx

2.6.2 Calibration and measurement

The lactate electrodes were prepared according to the manufacturer's instructions. Briefly, the lactate electrode was rehydrated with buffer A which contains glycerol for 10-15 min before its first use. Dryness of the sensor was avoided after rehydration by not exposing it to the air for longer than 30 s. If for any reason prolonged exposure to air was expected, the enzyme layer of the electrode was protected by dipping it briefly in a 5 mM glycerol solution. The electrode was stored wet in buffer A at 2-8 °C which allowed effective reuse for up to 5 days. In addition to dryness, bacterial contamination was another factor that can lead to loss of electrode sensitivity, so buffer A was either filter sterilised or autoclaved before use.

After setting up the oxygen electrode (4 ml) capacity chamber, the lactate electrode and Ag/AgCl reference electrode were connected to the potentiostat as a source of an external voltage. The potentiostat was set at +500 mV to polarise the lactate electrode in relative to the Ag/AgCl reference electrode which is attached to the side of the chamber.

The electrode was initially calibrated by adding 40 µl of 10 mM sodium L-lactate (Sigma) to 4 ml Hank's solution to obtain a final concentration of 100 µM (Brown et al., 2012). After the chamber had been washed several times with Hank's, the cell suspension was then added. Recording of experiments was started after 10 min of cell equilibration by capping the chamber with the plunger as for OCR. The lactate electrode was then carefully inserted via a second orifice in the plunger to contact the cell suspension and its reading set to zero. After the experiment, a second calibration was executed with four successive additions of 40 µl of 10 mM sodium L-lactate added. A similar measurement procedure as previously mentioned in OCR (2.5.2) was applied to simultaneously measure both OCR and lactate at the same time. Data were recorded as slopes by DATAQ software and these slopes were quantified by WINDAQ^{TM} and the results of lactate production rate were expressed as a nmol lactate 10^7 cell^{-1} min^{-1} according to the following equation:

Substrate lac *60/cell number/calibration value

The substrate is the slope value of the substrate recorded for 10 min

60 s = 1 min

Calibration value = the average of response due to adding 100 µM sodium lactate.

2.7 Mitochondrial membrane potential

Mitochondrial membrane potential ($\Delta\Psi_{mit}$) of MIN6 was monitored using Rhodamine 123 (Rh123) dye. As shown previously in figure 1.2, ETC reactions lead to pumping of protons (H^+) from the matrix to the intramembrane space via the complexes of the mitochondrial inner membrane which generates a proton gradient and subsequently leads to ATP synthesis. This electrochemical gradient consists of two elements, the $\Delta\Psi_{mit}$ (~180 mV) which occurs due to the positive charges of H^+, and to a lesser extent pH gradient (~60 mV) which results from acidity rising. Thus, $\Delta\Psi_{mit}$ is considered as an indicator for mitochondrial function and cellular energy production in living cells.

2.7.1 Characteristics of Rh123

Rh123 is a lipophilic cation fluorescent dye with a specific localisation to the mitochondria (Baracca et al., 2003). It readily diffuses through the cell membrane and accumulates inside the mitochondria within 5-10 min until equilibration is reached. Rh123 uptake is

mainly controlled by $\Delta\Psi_{mit}$, therefore abolishing $\Delta\Psi_{mit}$ by protonophores or mitochondrial complex inhibitors will inhibit uptake and redistribute the dye from the mitochondria to the cytosol. The dye will be unquenched and this leads to increase the intensity of fluorescence (Gerencser et al., 2016). On the other hand, maintenance or stimulation of $\Delta\Psi_{mit}$ will reduce the fluorescence intensity because of dye quenching which occurs due to the enhancement of dye uptake (Antinozzi et al., 2002).

Although many probes have been used for monitoring $\Delta\Psi_{mit}$, Rh123 was chosen for this study for several reasons (Chen L B, 1988). Firstly, it is less toxic than other lipophilic cations such as Rh3B, Rh6G, safranin, and cyanine dyes. Moreover, it is non-toxic for the majority of cell types within the conditions of staining mitochondria i.e. incubation with 10 µg/ml at 37 ˚C for 10 min (Darzynkiewicz F et al. 1982). Secondly, Rh123 is the only dye of lipophilic cations which is easily eliminated from the mitochondria to the cytoplasm by using mitochondrial complexes inhibitors such as sodium azide and oligomycin. Finally, in contrast with the other dyes, Rh123 neither stains endoplasmic reticulum nor mitochondria in the absence of $\Delta\Psi_{mit}$ (Gerencser et al., 2016).

2.7.2 Imaging procedure

MIN6 cells were plated on 22 mm Ø glass coverslips at least 24 h prior to use. Coverslips were secured in a special chamber to be fitted later on the stage of the epifluorescence microscope. Rh123 imaging was done as previously described (Duchen et al., 1993). A stock solution of 1 mg/ml Rh123 was prepared. Cells were incubated with 10 µg/ml Rh123 in glucose free Hank's-BSA solution to room temperature for 10 min and protected from light. During the experiment, cells were continuously perfused with different treatment solutions at 32±1 ˚C. Cells were imaged with a 20X Zeiss PlanNeofluar Objective lens (Carl Zeiss Ltd). Stained cells were excited at 480 nm and the emission fluorescence was monitored at 530 nm. A CCD camera Coolsnap, Photometric was used to capture images at a sequence rate of 0.5 / s using Imaging workbench software (IW6 INDEC Biosystems, Santa Clara, CA, USA). Changes in fluorescence were recorded and the slopes were analysed by OriginLab 6.1 software (OriginLab Corporation, MA USA). Data were normalized using Microsoft Excel and statistical analysis was performed using GraphPad Prism 6.

2.8 Calcium imaging

A change in intracellular Ca^{2+} is controlled by either calcium influx from extracellular fluid or Ca^{2+} release from the intracellular stores e.g. ER and mitochondria. It is well known that Ca^{2+} influx occurs due to the opening of VGCCs of the β-cell membrane. On the other hand, Ca^{2+} release from the intracellular stores is mainly induced by ligand-gated calcium channels due to activation of cell membrane receptors e.g. GPCR which activates Ca^{2+} release second messengers such as IP_3 (Striggow and Ehrlich, 1996). Furthermore, the free cytosolic Ca^{2+} as a second messenger activated the release of stored Ca^{2+} via a calcium-induced calcium release (CICR) process. Changes in intracellular Ca^{2+} can be monitored via Ca^{2+} imaging technique using Fluo-4 AM dye.

2.8.1 Fluo-4 AM as a Ca^{2+} probe

The calcium sensitive dye Fluo-4 AM was used in this study in order to detect the rapid changes of intracellular Ca^{2+} concentration in different experimental conditions. Acetoxymethyl ester group (AM) facilitates the dye diffusion through the cell membrane which is then hydrolysed in the cytoplasm by the action of esterases. Subsequently, the free acid form of Fluo-4 is trapped inside the cell as its terminal negative charges prevent its diffusion across the plasma membrane. Moreover, the dye has negative charges that bind with free Ca^{2+}. Fluo-4 is an efficient dye for Ca^{2+} probing because it has a wide detection range with dissociation constant K_d (Ca^{2+}) of 345 nM (Gee et al., 2000). Moreover, the fluorescent intensity of Fluo-4 is insignificant at a low concentration of free Ca^{2+}, whereas the signal increases up to a 100 fold in the presence of Ca^{2+} in a concentration dependent manner.

2.8.2 Imaging procedure

To image intracellular Ca^{2+} a similar procedure to that used with Rh123 (2.7.2) was done. A stock solution of 1 mM Fluo-4 AM in DMSO was prepared and aliquoted as 5 µl each to be used later. A final concentration of 1 µM was used. MIN6 cells were incubated with 0.5 ml of dye solution for 30 min at room temperature and protected from light. Cells were excited at 480 nm and the emission fluorescence was monitored at 530 nm. Images were captured and analysed as mentioned previously in 2.7.2.

2.9 Glucose uptake assay

The Glucose Uptake-Glo™ Assay of Promega (J1341) was used to explore the effect of SRIF on the glucose uptake and glucokinase activity of pancreatic β-cells. It is a plate-based, non-radioactive and homogeneous bioluminescent assay.

2.9.1 Principles of the assay

This assay depends on the formation and accumulation of 2-deoxyglucose-6-phosphate (2DG6P) within the cell. Similar to D-glucose, 2-deoxyglucose (2DG) is transported via glucose transporters and rapidly phosphorylated with hexokinases into 2DG6P. The latter is impermeable to the cell membrane and cannot be metabolised by the usual glycolytic enzymes, therefore it accumulates inside the cells that are exposed to 2DG. Next, an acidic stop buffer is added which stops further 2DG uptake, lyses the cell membrane and destroys cellular proteins and NADPH. Before adding the 2DG6P detection reagent, the acidity was neutralised by adding an alkaline neutralization buffer. The 2DG6P detection reagent contained 125 µl glucose-6-phosphate dehydrogenase (G6PDH), 50 µl $NADP^+$, 25 µl reductase, and 3 µl reductase substrate (pro-luciferin) to 5 ml of Ultra-Glo™ recombinant luciferase reagent, prepared at least 1 h before use. G6PDH oxidizes 2DG6P to 6-phosphodeoxygluconate and at the same time, it reduces $NADP^+$ to NADPH. In the presence of NADPH, the reductase converts the pro-luciferin to luciferin which is then used by luciferase to produce light. The produced luminescent signal is proportional to the concentration of 2DG6P.

2.9.2 Procedure

MIN6 cells in a 75 ml TC flask were trypsinised and suspended with 15 ml of fresh RPMI. From this 50 µl of cell suspension was mixed well with a similar volume of trypan blue dye (BioRAD®). 10 µl of the latter mixture was injected in a cell counter slide and inserted in the BioRAD® cell counter. From a live cells count, the further desired dilution was calculated to obtain $1X10^6$ cells / ml. From this, 200 µl was added to each well of a 96 well plate to give a cell density of $2X10^5$ cells / well. Cells were then incubated for 48 h after which the tissue culture medium was removed and cells were washed with warm PBS and incubated with drugs for 5 min. Then the drugs were replaced with a combination of 2DG

and the same drugs and incubated for 10 min at room temperature. 2DG uptake was then determined by reading luminescence with a Fluoroskan Ascent™ FL Microplate Fluorometer and Luminometer (Thermo Fisher Scientific, UK) following the steps according to the instructions of the Glucose Uptake-Glo™ assay protocol as shown in fig. 2.3.

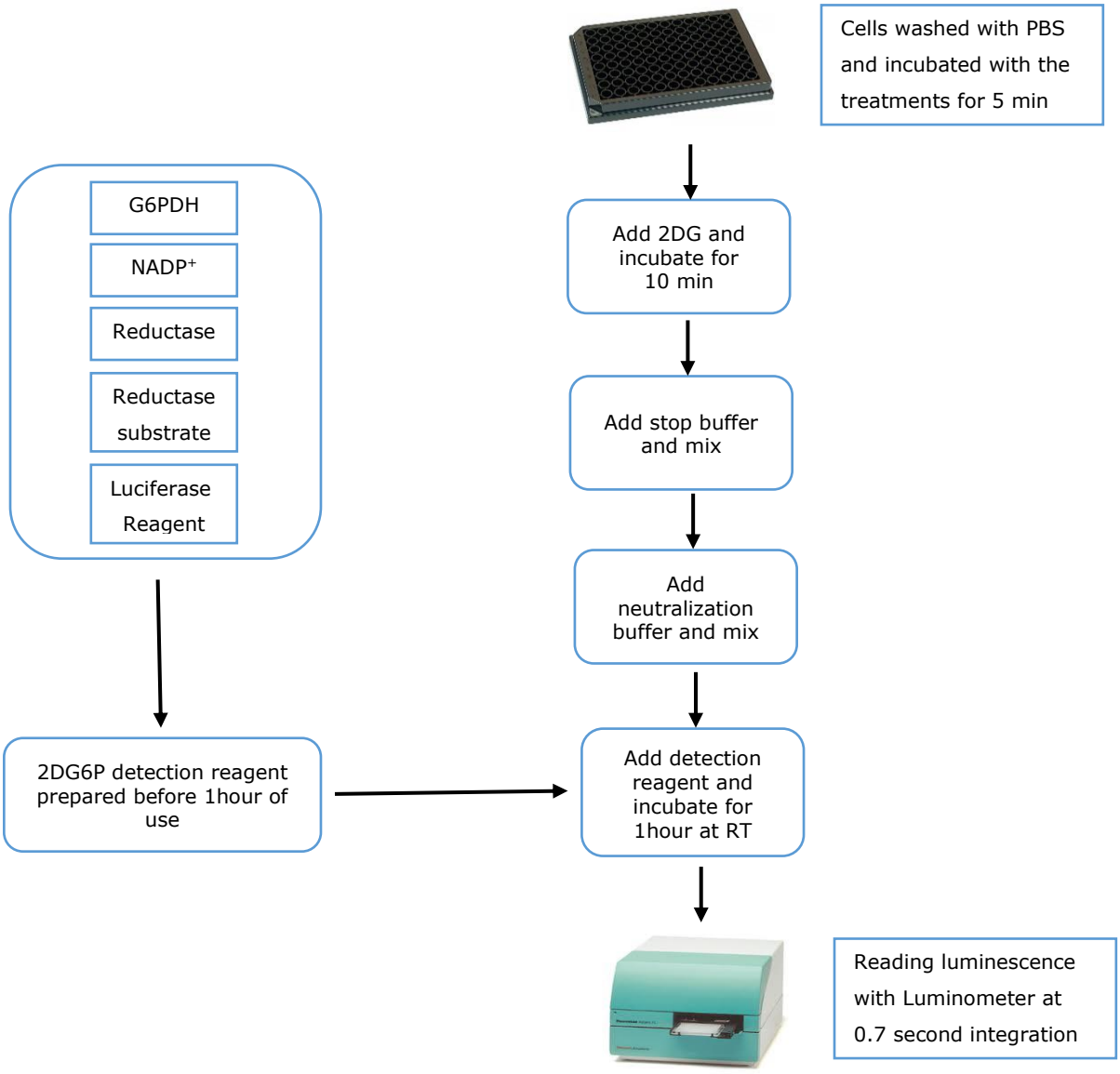

Figure 2.3: A diagram of the Glucose Uptake-Glo™ assay protocol reproduced from Promega technical manual.

2.10 Measurement of intracellular ATP

The Promega CellTiter-Glo® 2.0 Assay (G9241) was used to quantify ATP production in MIN6 cells. The reagent is ready to use and is designed to be used with a multi-well plate

in a single step. MIN6 cells were plated on an opaque wall 96 well plate (Corning®) as for the glucose uptake procedure (2.9.2). The frozen reagent was thawed in a water bath at 22 ˚C and allowed to equilibrate for 30 min at room temperature. Then it was gently mixed by inverting the content to obtain a homogenous reagent which was protected from light. In order to reverse the ATP generation associated with the 11 mM glucose of the RPMI tissue culture medium, cells were washed with warm PBS and then incubated with 100 µl/well Hank's-BSA in 37˚C for 15 min. Next, treatments were added to each group of wells according to the experimental design and incubated for 10 min at room temperature. The plate was then equilibrated to room temperature before adding 100 µl of the ATP detection reagent. The plate was shaken for 2 min by using an orbital shaker to induce cells lysis and it was incubated at RT for 10 min to stabilize the luminescent signal as shown in fig.2.4. Finally, the signal was recorded using a Fluoroskan® Luminometer at an integration time of 0.7 S.

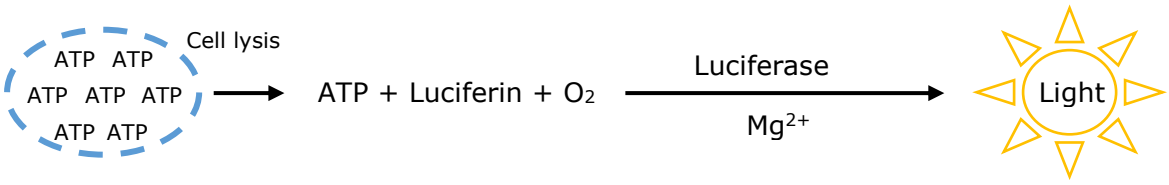

Figure 2.4: Principle of CellTiter-Glo® 2.0 ATP assay regenerated from Promega technical manual.

2.11 Statistical analysis

D' Agostino Pearson omnibus normality test has been done for all data in order to check if the samples were normally distributed or not. When the data were paired and non-normal in distribution, either one way ANOVA Friedman test with Dunn's multiple comparisons test or Wilcoxon matched-pairs signed rank t-test were used. When the data were paired and normally distributed, either repeated measured (RM) one-way ANOVA with Holm-Sidak's multiple comparisons test or students paired t-test was used. Values are considered significant at $P<0.05$ and represented with (*) on the graphs. All results expressed as a mean ± S.E.M. with n as a number of experiments. Data were normalised with Microsoft EXCEL® and statistical analysis was conducted by Prism® 6 software (Graph Pad).

Chapter Three: The Effects of Somatostatin on Mitochondrial Metabolism in MIN6 cells

3.1 Introduction

Mitochondria play an essential role in β-cell bioenergetics and subsequently insulin secretion. The main function of the mitochondria is producing energy as ATP, mainly due to glucose metabolism. ATP plays several key roles in β-cell physiology. First, it blocks K_{ATP} channels of the plasma membrane, which are responsible for membrane potential regulation. This leads to membrane depolarization and opening of VGCC allowing extracellular Ca^{2+} to enter the cell and induce insulin secretion (Ashcroft and Rorsman, 1989, Dou et al., 2015). It is also proposed that ATP directly activates VGCC and increases intracellular Ca^{2+} levels and subsequently insulin secretion (Smith et al., 1989). Third, it is believed that ATP directly potentiates the exocytosis machinery by energizing the vesicles, which leads to facilitate insulin secretion (Takahashi et al., 1999). Another important role for ATP is as a substrate for cAMP production, by the action of AC enzymes. cAMP acts as an effector to both PKA and EPACII which leads to enhanced exocytosis and insulin release (Seino and Shibasaki, 2005, Almahariq et al., 2014).

SRIF has received much attention in recent years due to its multiple inhibitory properties in pancreatic β-cells, including the inhibition of mitochondrial activity (Daunt et al., 2006, Ezzat et al., 2017). It is intuitive that any disturbance in the mitochondrial activity will be reflected on ATP production, however this notion needs more investigation to be confirmed. One of the most accepted mechanisms of SRIF action to inhibit insulin release is by decreasing Ca^{2+} influx due to cell membrane hyperpolarization, which in part is an ATP-dependent mechanism (Smith et al., 2001, Nilsson et al., 1989). This hypothesis is further investigated in chapter five of this thesis. Although some studies propose alternative mechanisms by which SRIF inhibits insulin secretion such as inhibition of cAMP production (Schuit et al., 1989) and direct inhibition of exocytosis (Ullrich et al., 1990). It is, however, the membrane hyperpolarization due to either inhibition of metabolism or/and activation of GIRK that dominates and overcomes these other mechanisms in terms of order and potency (Daunt et al., 2006).

As a result, three different techniques have been conducted in this chapter in order to explore the potential action of SRIF on the mitochondrial metabolism of MIN6 cells (Fig.

3.1). The first technique was done to evaluate the oxidative respiration by oxygen consumption rate measurement (OCR). The second technique is done to observe the mitochondrial activity by measuring the mitochondrial membrane potential. The third technique was to measure the intracellular ATP levels using the Promega CellTiter-Glo® 2.0 Assay.

The aims of this chapter were to confirm the idea that SRIF suppresses mitochondrial metabolism and to investigate the effect of SRIF on ATP production in MIN6 cells.

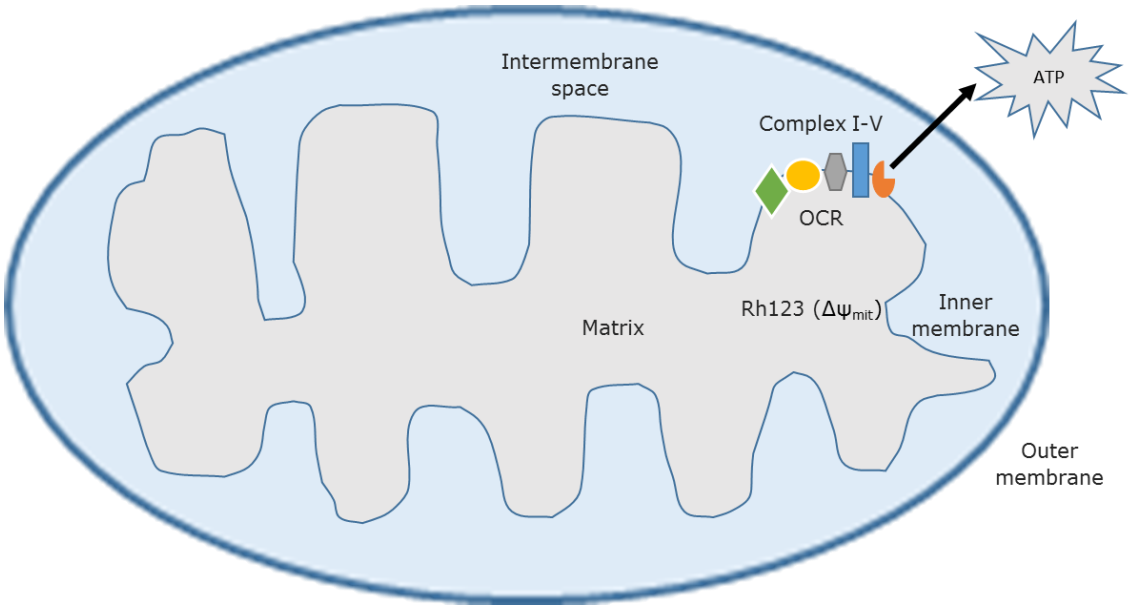

Figure 3.1: An illustration shows the measured parameters of the mitochondria in MIN6 cells. O_2 consumed in the mitochondrial complexes (I-V) which are embedded in the inner membrane. Rh123 localized in the mitochondria reflecting the inner membrane potential activity. ATP generated in the mitochondria and pumped out to the cytoplasm was also measured.

3.2 Methodology

3.2.1 Oxygen consumption rate

The method as described in chapter two, see 2.5.

3.2.2 Mitochondrial membrane potential

The method as described in chapter two, see 2.7.

3.2.3 ATP production

The method as described in chapter two, see 2.10.

3.3 Results of oxygen consumption rate (OCR)

3.3.1 Glucose stimulates OCR

Figure 3.2 shows the responsiveness of MIN6 cells to 10 mM glucose and the mitochondrial uncoupler carbonyl-cyanide-p-trifluoro-methoxyphenyl hydrazine (FCCP). Figure 3.2A illustrates that in a glucose free condition, MIN6 cells possessed a basal rate of oxygen consumption (first 10 min). Addition of 10 mM glucose to the cells produced an almost immediate increase in OCR which was maintained at a steady rate for the next 20 min data indicative of a significant 1-fold increment of OCR (Fig. 3.2B). The sharp increase in slope after adding 100 nM FCCP (Fig. 3.2A) demonstrates a further significant increase in OCR by ~ 2 fold over that of 10 mM glucose (figure 3.2B).

Addition of sodium azide (a complex IV inhibitor) blocked the consumption of cellular respiration but not that of the O_2 electrode thus the OCR measured in the presence of azide has been used as a correction factor.

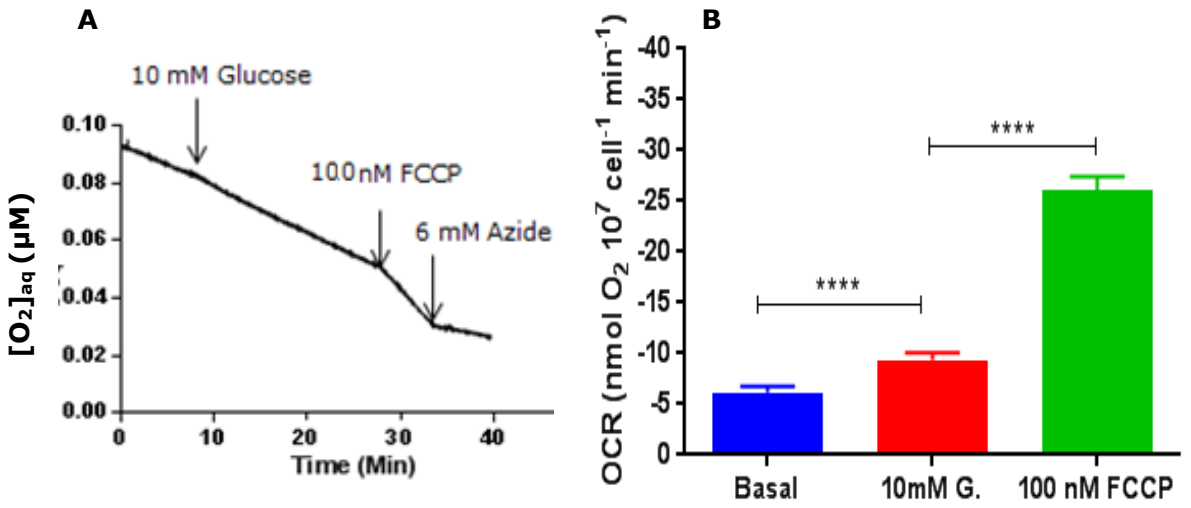

Figure 3.2: Effect of 10 mM glucose and 100nM FCCP on OCR in MIN6 cells. (A) Representative record of a single experiment of aqueous O_2 concentration in 1 ml of MIN6 cell suspension. It shows oxygen consumption under basal and the indicated additions. (B) 10 mM glucose significantly stimulated basal OCR, and 100 nM FCCP further increased OCR compared to the 10 mM glucose. Repeated measures (RM) one-way ANOVA test corrected with Holm-Sidak's multiple comparisons test (**P<0.0001, n=25).**

3.3.2 SRIF inhibits glucose stimulated OCR

Figure 3.3A&B illustrates the stimulation of OCR by 10 mM glucose and the subsequent effect of 100 nM SRIF (Fig. 3.3A) or its vehicle control (H_2O) (Fig. 3.3B). 100 nM SRIF significantly inhibited OCR (Fig. 3.3C) while the vehicle control (H_2O) failed to affect it (Fig. 3.3D). The percentage inhibitory effect of SRIF (18%), was significantly greater than that of its vehicle control, water (8%) (Unpaired t test, $P<0.01$, n=17-31).

An experimental investigation was conducted to explore if the effect of SRIF occurred in the absence of mitochondrial fuels. Figure 3.4A shows that although 100 nM SRIF reduced the basal mitochondrial respiration (43%), however, this effect was statistically insignificant relative to its vehicle control H_2O (37%) as can be seen in figure 3.4B which revealed similar results; no effect on the basal respiration (Unpaired t test, n=10-12). It is apparent from figure 3.4A that 10 mM glucose still has the ability to stimulate OCR in the presence of 100 nM SRIF (258%), ($P<0.0001$, n=12) and also in the presence of vehicle (207%) as seen in fig 3.4B ($P<0.001$, n=10). However, the percentage of glucose stimulation in the presence of 100 nM SRIF was not significantly different from the percentage of glucose stimulation in the presence of vehicle control (Unpaired t test, n=10-12).

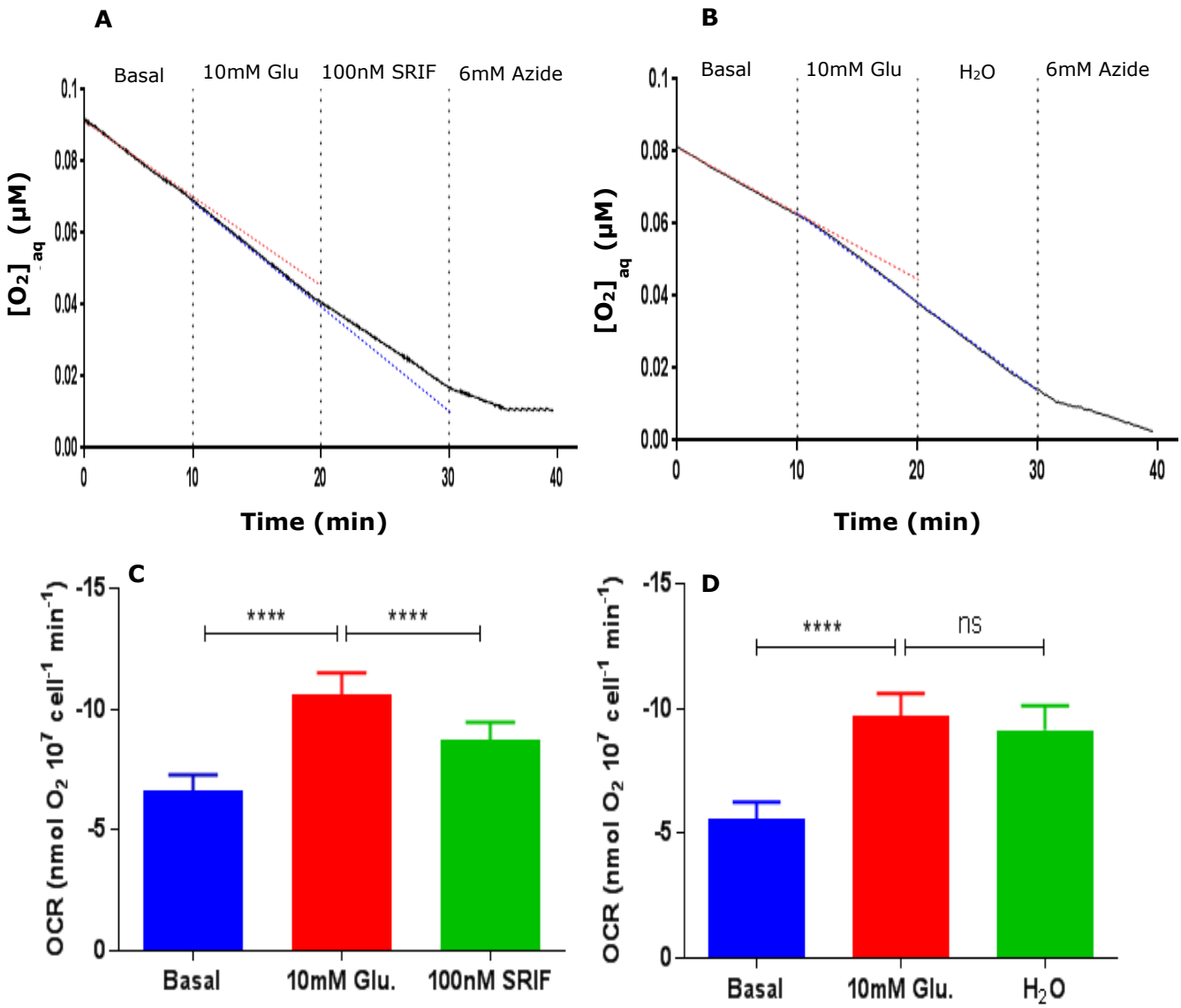

Figure 3.3: Effect of SRIF on glucose stimulated OCR in MIN6 cells. (A) Representative trace of $[O_2]_{aq}$ in response to serial additions of 10 mM glucose and 100 nM SRIF, (B) 10 mM glucose and H_2O followed by 6 mM sodium azide. (C) 10 mM glucose increased the basal respiration (P<0.0001, n=31) and 100 nM significantly decreased OCR (P<0.0001, n=31). (D) Vehicle control H_2O did not affect glucose stimulated OCR (n=17). All data were analysed with Friedman one-way ANOVA test and corrected with Dunn's multiple comparisons test). Values are mean±SEM. The red dotted lines represent a virtual slope of basal in the absence of glucose. The blue dotted line is the virtual slope of glucose in the absence of SRIF or vehicle control.

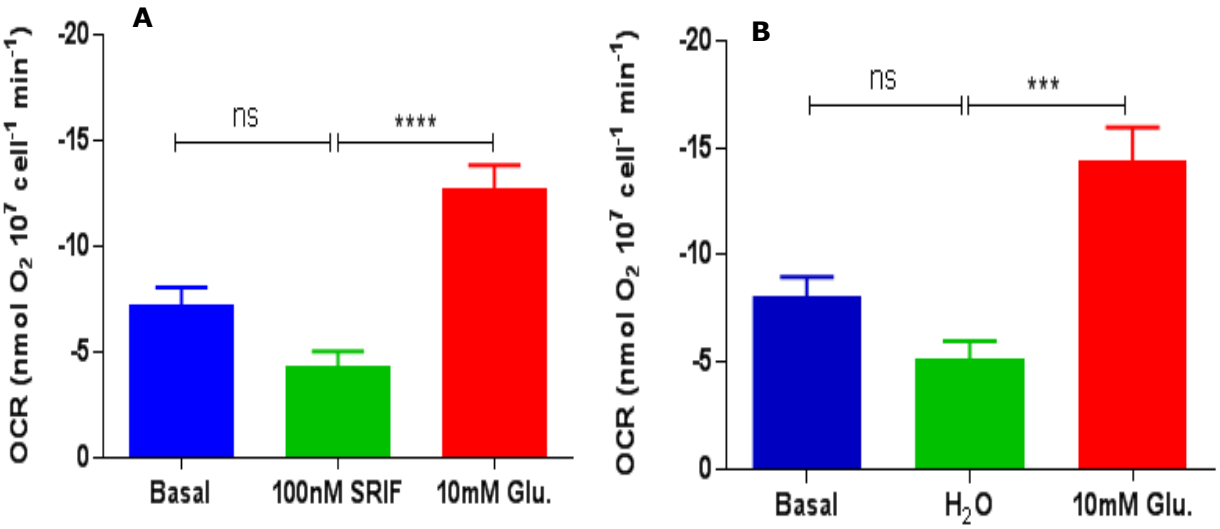

Figure 3.4: Effect of 100 nM SRIF and vehicle (H_2O) on basal OCR in MIN6 cells. (A) Serial addition of 100 nM SRIF followed by 10 mM glucose which stimulated OCR (P<0.0001, n=12). (B) Similar data were obtained by vehicle control (H_2O) and 10 mM glucose, (P<0.001, n=10). Both datasets were analysed with Friedman one-way ANOVA test corrected with Dunn's multiple comparisons test. Values are mean±SEM.

3.3.3 Effects of SRIF and dbcAMP on OCR

In this study, the ability of elevated cAMP to affect the response to SRIF was tested. As can be seen in figure 3.5A the addition of 1 mM dbcAMP in the presence of 10 mM glucose showed a significant decrease in OCR by 22% (P<0.001, n=9). In the absence of glucose, 1 mM dbcAMP decreased the basal respiration by 33% (P<0.01, n=8) as can be identified in figure 3.5C. Comparing the inhibitory effect of dbcAMP on OCR in the presence and absence of 10 mM glucose showed an insignificant difference (Unpaired t test, n=8-9). The vehicle control of dbcAMP (dH_2O) had no effect either in the presence or absence of 10 mM glucose (Fig. 3.5B&D). Data from figure 3.5 show that the overall effect of SRIF was to inhibit OCR in the presence of dbcAMP. However, in the presence of 10mM glucose, 1 mM dbcAMP did not change the magnitude of SRIF effect on OCR, since the percentage inhibition was 14% in comparison to 18% achieved without dbcAMP (Unpaired t test, n=9-31). Figure 3.5C&D shows that 10 mM glucose stimulated the basal respiration in the presence of dbcAMP by ~8% only compared to 32% in the presence of vehicle control dH_2O, however, that difference was not statistically significant (Unpaired t test, n=7-8). Moreover, 100 nM SRIF inhibited glucose stimulated OCR in the presence of 1 mM dbcAMP

by 17% and in in the presence of dH_2O by 18% which are similar to the inhibitory effect of the peptide in the absence of both.

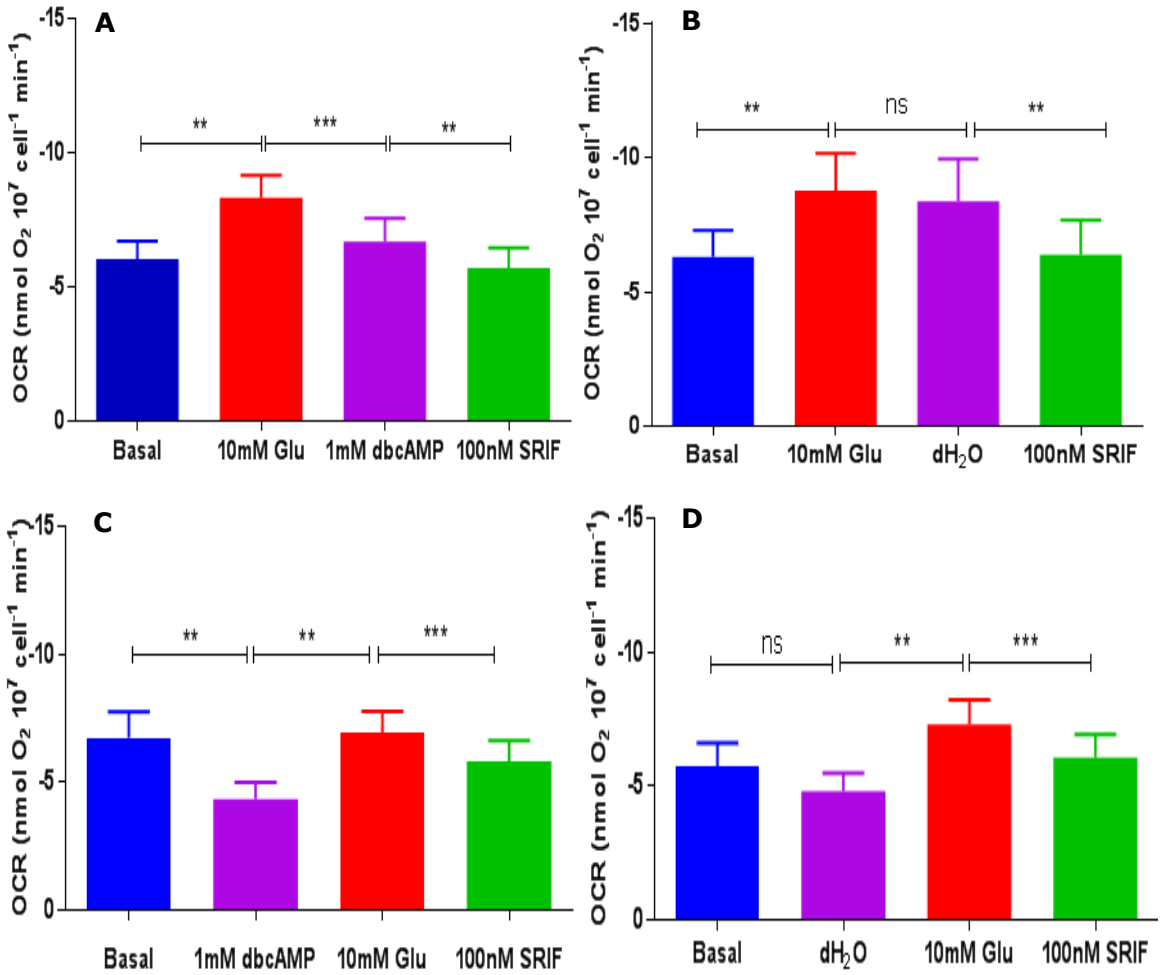

Figure 3.5: Effect of 1 mM dbcAMP and 100 nM SRIF on OCR in MIN6 cells. (A) 10 mM glucose stimulates basal OCR (P<0.01, n=9), while 1 mM dbcAMP significantly inhibited glucose stimulated OCR (P<0.001, n=9) and 100 nM SRIF reduced cells respiration (P<0.01, n=9). (B) The same steps were conducted for vehicle control of dbcAMP (dH_2O), 10 mM glucose stimulates OCR (P<0.01, n=8) while dH_2O did not change OCR (n=8) and again 100 nM SRIF significantly inhibited OCR (P<0.01, n=8). (C) Effect of swapping additions. 1 mM dbcAMP inhibited basal respiration (P<0.01, n=8), 10 mM glucose reversed the effect of dbcAMP and 100 nM SRIF inhibited glucose stimulated OCR (P<0.001, n=8). (D) dH_2O failed to affect basal OCR (n=7) and 100 nM SRIF blocked glucose stimulated OCR (P<0.001, n=7). All statistics performed with RM one-way ANOVA and corrected with Holm-Sidak's multiple comparisons test. Values are mean±SEM.

3.3.4 Effects of clonidine and glucagon on OCR

In this study, the effects of two other GPCR targeting drugs were tested on OCR of MIN6 cells. These were clonidine (Sigma) that acts via α_2-adrenoceptors to activate G_i and depress cAMP levels (Niddam et al., 1990) and glucagon that acts via glucagon receptors to activate G_s and elevate cAMP levels (Authier and Desbuquois, 2008).

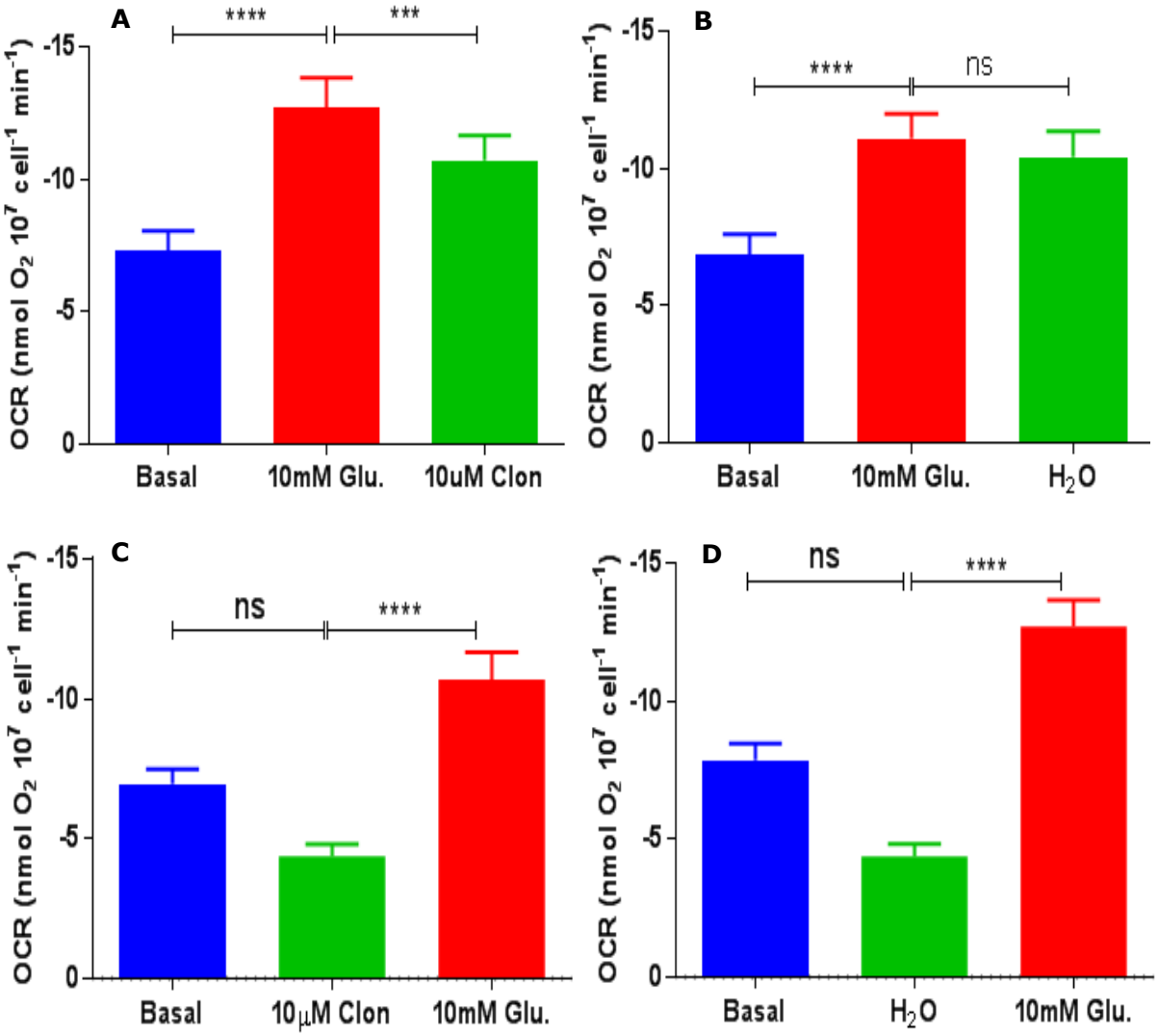

Figure 3.6: Effect of 10 μM clonidine and its vehicle control on the OCR of MIN6 cells. (A) 10 mM glucose significantly increased OCR (P<0.0001, n=24) and then 10 μM clonidine significantly inhibited glucose stimulated OCR (P<0.001, n=24). (B) 10 mM glucose stimulated OCR (P<0.0001, n=18) while the vehicle control (H_2O) was without effect (n=18). (c) Treatment with 10 μM clonidine did not affect basal OCR (n=10), subsequent 10 mM glucose significantly stimulated OCR (P<0.0001, n=10). (D) Vehicle control (H_2O) did not affect basal OCR (n=10) and subsequent 10 mM glucose stimulated it (P<0.0001, n=10). Statistics of all graphs were done by Friedman test and corrected with Dunn's multiple comparisons test. Values are mean±SEM.

Figure 3.6A indicates that 10 μM clonidine diminished the glucose stimulated oxygen consumption by 16% which is comparable to that of 100 nM SRIF (18%). The percentage inhibition of glucose by vehicle control H_2O (7%) is significantly less than that of clonidine (Unpaired t test, P<0.001, n=18-24) and it is comparable to the results of SRIF vehicle (H_2O). Furthermore, similar to SRIF (Fig. 3.4A), clonidine in the absence of substrate did not affect the basal respiration of MIN6 cells in comparison to the vehicle control (H_2O). Even though the OCR in the presence of clonidine and H_2O in the absence of glucose were apparently less than basal OCR by 38% and 45% respectively. However those effects were

not statistically significant and also the difference between the effect of clonidine and its vehicle control was insignificant (Unpaired t test, n=10). 10 mM glucose still stimulates OCR in the presence of both clonidine 155% and H_2O 214% (Fig. 3.6C& D), however, the difference was not significant (Mann-Witney t test, n=10).

Figure 3.7A shows that 100 nM glucagon significantly inhibited glucose stimulated oxygen consumption by 12% relative to 1% of its vehicle control (0.16 nM acetic acid) (Fig. 3.7B). Figure 3.7C shows that 100 nM glucagon significantly inhibited basal mitochondrial respiration (31%) which was reversed by the effect of 10 mM glucose (151%). Although the vehicle control appeared to decrease basal OCR (20%) this was statistically insignificant and 10 mM glucose still stimulated the OCR by 77% (Fig. 3.7D).

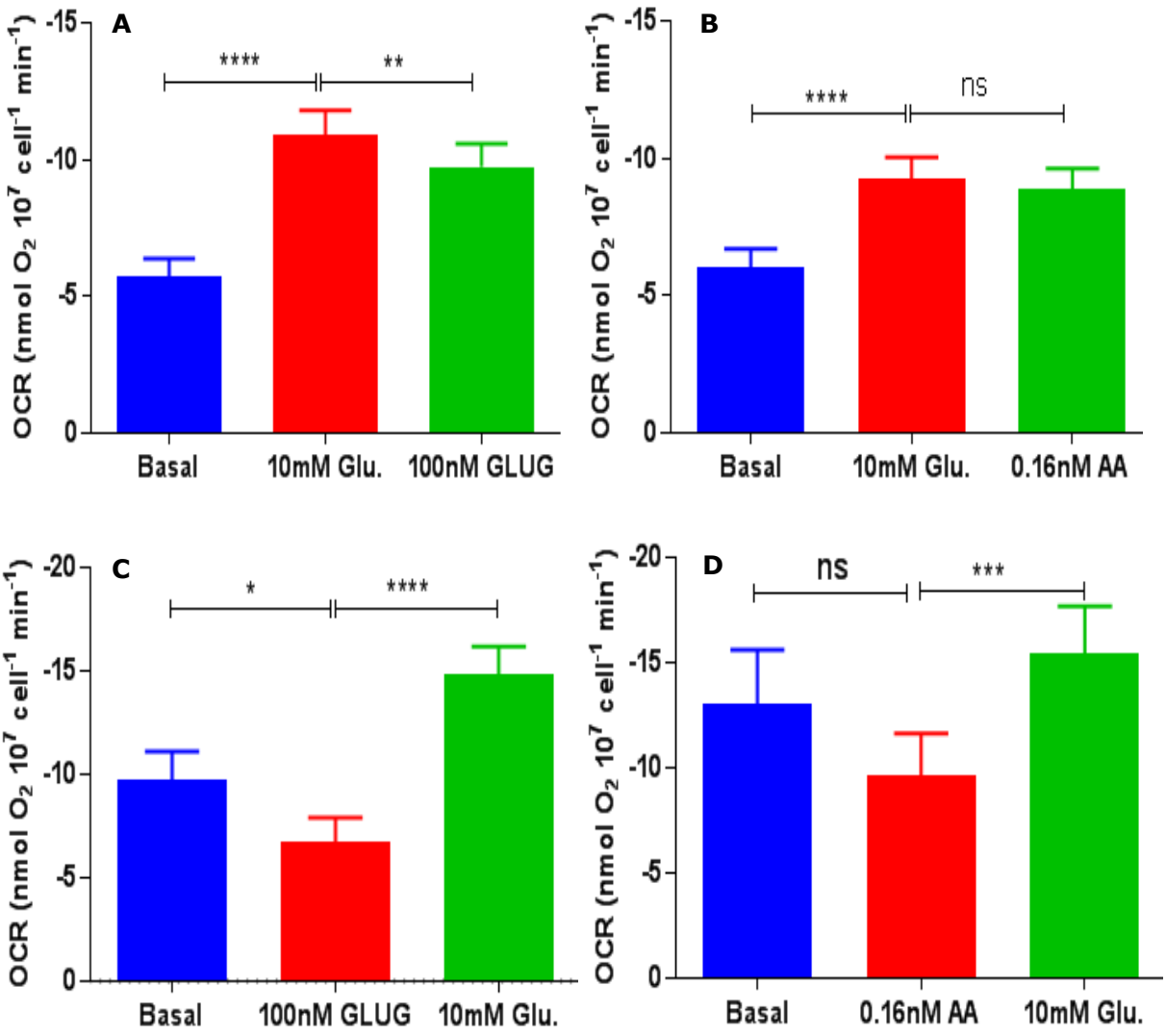

Figure 3.7: Effect of 100 nM glucagon and its vehicle control on OCR of MIN6 cells. (A) 10 mM glucose significantly increased OCR (P<0.0001, n=23), subsequent 100 nM glucagon decreased glucose stimulated OCR (P<0.01, n=23). (B) The vehicle control 0.16 nM acetic acid did not affect glucose stimulated OCR (P<0.0001, n=21). Panels A&B were analysed by RM one-way ANOVA test and corrected with Holm-Sidak's multiple comparisons test. (C) 100 nM glucagon significantly decreased basal OCR (P<0.05, n=10), but 10 mM glucose still stimulated OCR (P<0.0001, n=10). (D) Vehicle control of 0.16 nM acetic acid did not affect basal OCR (n=8) which was then stimulated by 10 mM glucose (P<0.001, n=8). For C&D statistics were done by Friedman test corrected with Dunn's multiple comparisons test. Values are mean ± SEM.

3.3.5 Effects of SRIF on KIC stimulated OCR

To determine whether SRIF was acting directly on mitochondrial function or on upstream metabolism i.e glycolysis or the pentose phosphate shunt, the effects of SRIF were tested using α-ketoisocaproate, KIC, as a direct mitochondrial fuel instead of glucose. Comparable basal respiration was recorded in a KIC experiment (-5.5 nmol O_2 10^7 $cell^{-1}$ min^{-1}) to that previously recorded (-6.6 nmol O_2 10^7 $cell^{-1}$ min^{-1}) in glucose experiments (Unpaired t test, n=13-31).

Figure 3.8A&B show that 10 mM KIC significantly increased the basal respiration by 45% in (A) versus 69% in (B), however, the difference is statistically insignificant (Mann-Whitney t test, n=10-13). 100 nM SRIF significantly inhibited the KIC stimulated OCR by 18%, while the vehicle control (H_2O) did not affect KIC stimulated OCR (4%) as shown in figure 3.8B.

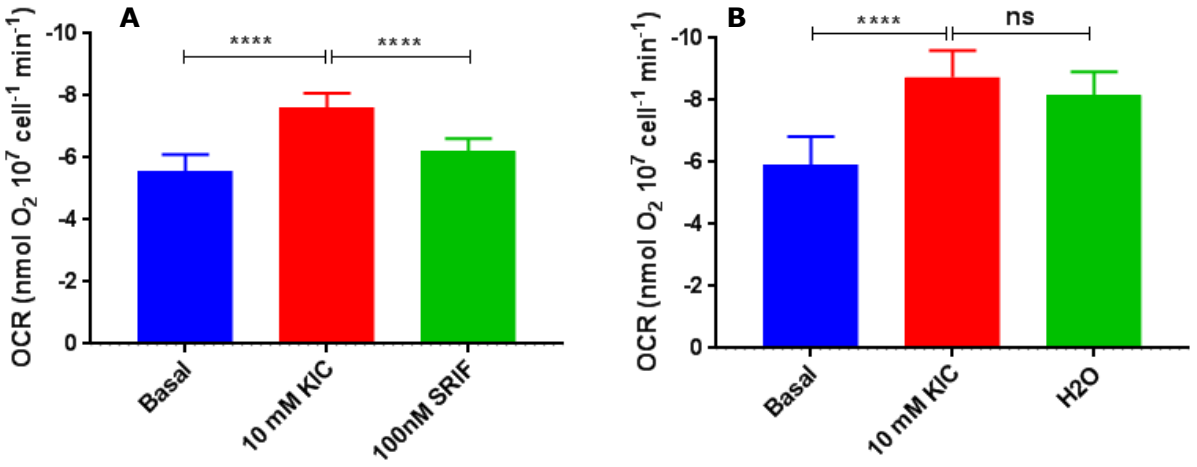

Figure 3.8: The effect of 100 nM SRIF and vehicle control (H_2O) on KIC stimulated OCR in MIN6 cells. (A) KIC stimulated OCR (P<0.0001, n=13) was inhibited by 100 nM SRIF (P<0.0001, n=13) (RM one-way ANOVA test corrected with Holm-Sidak's multiple comparisons test. (B) Insignificant effect (n=10) of vehicle control on KIC stimulated OCR (RM one-way ANOVA test corrected with Sidak's multiple comparisons test. Values are mean ± SEM.

3.4 Results of mitochondrial membrane potential

3.4.1 Effects of SRIF on glucose stimulated mitochondrial membrane potential ($\Delta\Psi_{mit}$)

From the results above, it is apparent that SRIF inhibited mitochondrial oxidative respiration of MIN6 cells. Therefore, the following experiments were done to find out whether SRIF could affect mitochondrial electron transport chain using Rh123 fluorescence as an indicator of $\Delta\Psi_{mit}$. Figure 3.9A&B shows changes in the Rh123 fluorescence represented as a percentage relative to the total change caused by 1 µM FCCP. Basal fluorescent in the absence of substrate was recorded for the first 5 min and show a constant state with a wide range of fluorescence of the selected region of interests (ROIs). When cells were treated with 10 mM glucose, a sharp decline in the signal was detected as can

be seen in figure 3.9A&B. This is a result of mitochondrial membrane hyperpolarization and quenching of the dye inside the mitochondria (Baracca et al., 2003, Duchen et al., 1993). From the data shown in Figure 3.9C, it is apparent that 10 mM glucose significantly decreased basal %Rh123 fluorescence ($P<0.0001$, n=3, ROIs=19). On the other hand, 100 nM SRIF significantly increased the %Rh123 fluorescence ($P<0.001$, n=3, ROIs=19). Vehicle control (H_2O) did not affect the glucose induced $\Delta\Psi_{mit}$ depolarization as can be seen in figure 3.9B& D. SRIF significantly increased glucose induced %Rh123 by ~6% compared to 0.5% achieved by vehicle control H_2O (Unpaired t test, $P<0.01$, n=3).

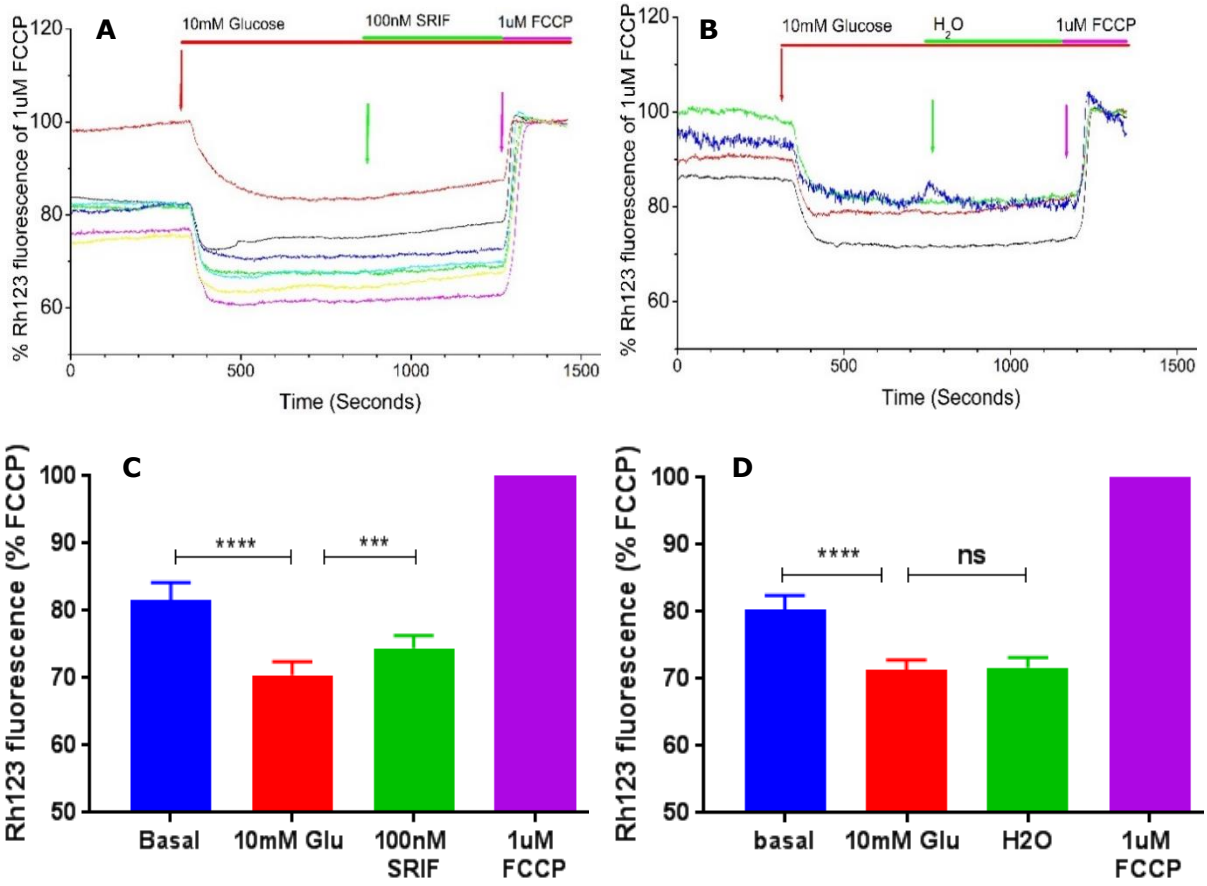

Figure 3.9: Effect of glucose and SRIF on the mitochondrial membrane potential of MIN6 cells. Representative traces of Rh123 fluorescence for MIN6 cells recorded in response to the conditions indicated. Each record is the average of several cells viewed within a given field normalised as a percentage of their response to 1 µM FCCP. (A) Effect of 10 mM glucose addition and 100 nM SRIF (B) Effect of 10 mM glucose addition and H_2O the vehicle control. (C) 10 mM glucose hyperpolarizes $\Delta\Psi_{mit}$ ($P<0.0001$) while 100 nM SRIF depolarizes $\Delta\Psi_{mit}$ ($P<0.001$). Data analysed by RM one-way ANOVA corrected with Sidak's multiple comparisons test (n=3, ROIs=19). (D) 10 mM glucose also hyperpolarized $\Delta\Psi_{mit}$ ($P<0.0001$) and the vehicle control H_2O had no effect on $\Delta\Psi_{mit}$. RM one-way ANOVA corrected with Dunnett's multiple comparisons test (n=3, ROIs=16). Data are mean ± SEM.

3.4.2 Effects of SRIF on glucose stimulated mitochondrial membrane potential ($\Delta\Psi_{mit}$) in calcium free condition

This experiment was conducted to examine the role of Ca^{2+} influx in the action of SRIF in β-cells. A Ca^{2+} free condition was obtained by replacement of the $CaCl_2$ of Hank's solution with equimolar $MgCl_2$. Figure 3.10A shows, in the continued absence of Ca^{2+}, that 10 mM glucose was still able to hyperpolarize $\Delta\Psi_{mit}$ with a sharp drop in fluorescence ($P<0.0001$, n=3, ROIs=42), however, 100 nM SRIF did not affect $\Delta\Psi_{mit}$ in the absence of Ca^{2+} as compared with its presence in figure 3.9A. By comparing the magnitude of the glucose effect in the presence of Ca^{2+} (13%) with that in the absence of Ca^{2+} (22%), it was significantly different (Unpaired t test, $P<0.001$, n=3) even though the basal fluorescence in the presence of Ca^{2+} ~82% was almost identical to the basal in Ca^{2+} free condition 86%, (Unpaired t test, n=3).

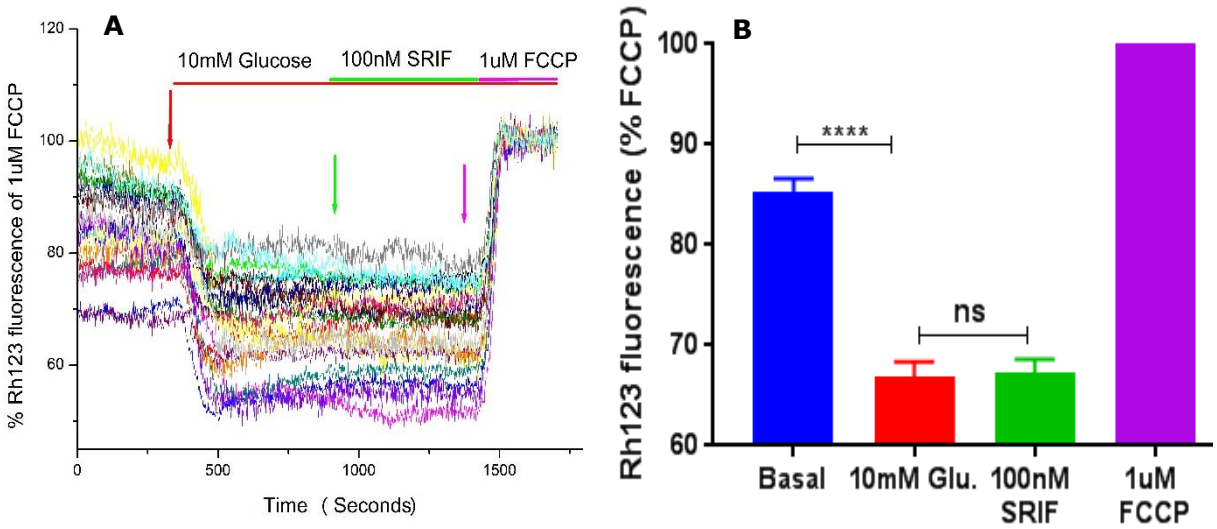

Figure 3.10: Effect of SRIF on mitochondrial membrane potential of MIN6 cells in calcium free conditions. (A) Representative trace shows that in the absence of Ca^{2+} 10 mM glucose hyperpolarized the mitochondrial membrane, however 100 nM SRIF had no effect. (B)The % basal Rh123 fluorescence significantly decreased by 10 mM glucose ($P<0.0001$) while 100 nM SRIF insignificantly effect glucose action. Data analysed by RM one-way ANOVA corrected with Sidak's multiple comparisons test (n=3, ROIs=42). Data are mean ± SEM.

3.4.3 Effects of SRIF and nifedipine on glucose stimulated mitochondrial membrane potential ($\Delta\Psi_{mit}$)

In this experiment, an attempt was done to find out the role of Ca^{2+} influx and the role of nifedipine (L-type VGCC calcium channel blocker) in the action of SRIF on MIN6 cells. 10 mM glucose hyperpolarized $\Delta\Psi_{mit}$ by around 20% then application of 20 μM nifedipine depolarised $\Delta\Psi_{mit}$ by 7%, however, this effect did not preclude the subsequent ability of SRIF to also depolarize $\Delta\Psi_{mit}$ by 4% to provide a sum of 11% in comparison to 10 mM glucose (Fig. 3.11).

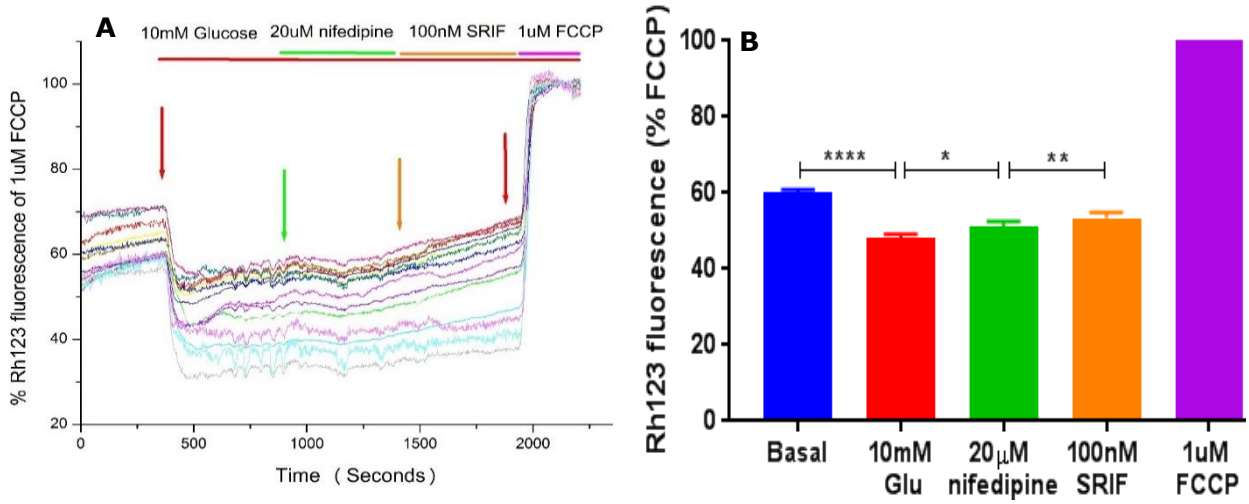

Figure 3.11: Effect of nifedipine and SRIF on mitochondrial membrane potential of MIN6 cells. (A) Representative trace of a single experiment shows that 10 mM glucose hyperpolarized the mitochondrial membrane, that effect was reversed by 20 μM nifedipine and 100 nM SRIF. (B) The % of basal Rh123 fluorescence significantly inhibited by 10 mM glucose (P<0.0001). 20 μM nifedipine significantly increased %Rh123 fluorescent (P<0.05) and 100 nM SRIF further increased the % fluorescent (P<0.01). Data analysed by Friedman one-way ANOVA test corrected with Dunn's multiple comparisons test. n=3, ROIs=50. Data are mean ± SEM.

3.5 Results of ATP production

Since SRIF inhibited OCR and the generation of $\Delta\Psi_{mit}$ the impact of the peptide on ATP production in MIN6 cells was investigated. As expected, both mitochondrial fuels, glucose ($P<0.05$, n=3) and KIC ($P<0.01$, n=3) showed significant increases in ATP production relative to fuel free conditions (fig.3.12A). However, figures 12A&B indicate that 100 nM SRIF had no effect on ATP production either in the absence or in the presence of either glucose or KIC.

Both positive controls, the ATP synthase inhibitor oligomycin and the mitochondrial uncoupler FCCP, inhibited ATP synthesis ($P<0.0001$, $n=3$) (Fig. 3.12).

Figure 3.12F illustrates the effect of 20 μM nifedipine and 100nM SRIF on glucose stimulated ATP production. 20 μM nifedipine significantly inhibited glucose stimulated ATP production ($P<0.0001$, $n=3$). In the presence of 10 mM glucose, combinations of nifedipine with SRIF and nifedipine with H_2O were significantly less than that of SRIF or H_2O alone ($P<0.0001$, $n=3$), see Fig. 3.12F.

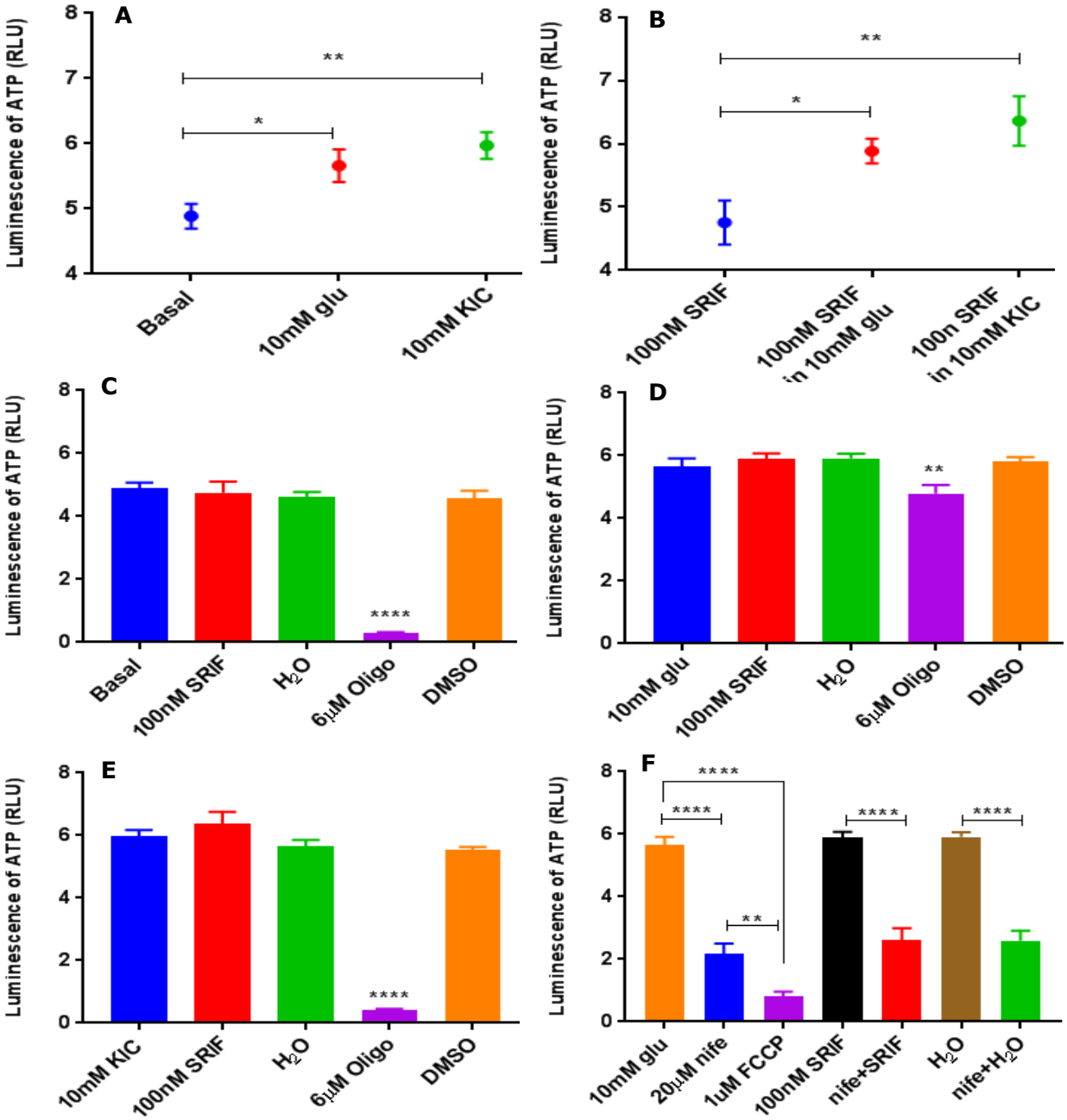

Figure 3.12: Effect of nifedipine and SRIF on ATP production in MIN6 cells. ATP luminescence was measured as relative light units (RLU). (A) Shows a comparison between mitochondrial fuels glucose and KIC as ATP generators. Both significantly induced ATP production compared to basal (substrate free condition), 10 mM KIC ($P<0.01$) and 10 mM glucose ($P<0.05$), however there was no significant difference between them. Data analysed with one-way ANOVA and corrected with Tukey's multiple comparisons test (n=3). (B) Shows a significant difference in the ATP level between 100nM SRIF in the absence of mitochondrial fuels and in the presence of fuels, 100nM SRIF with glucose ($P<0.05$) and 100nM SRIF with KIC ($P<0.01$), one-way ANOVA corrected with Holm-Sidak's multiple comparisons test (n=3). (C) ATP levels of 100 nM SRIF, H_2O and the vehicle of oligomycin (DMSO) were insignificant from basal, while 6 μM oligomycin significantly decreased ATP level, one-way ANOVA corrected with Holm-Sidak's multiple comparisons test (n=3). (D) ATP levels of 100 nM SRIF, H_2O and DMSO were insignificant of that of 10 mM glucose, except oligomycin which significantly inhibited glucose stimulated ATP level ($P<0.01$, n=3) one-way ANOVA corrected with Tukey's multiple comparisons test. (E) Only oligomycin inhibited ATP production ($P<0.0001$, n=3) one-way ANOVA corrected with Tukey's multiple comparisons test. (F) 20μM nifedipine significantly inhibited glucose stimulated ATP ($P<0.0001$) and 1μM FCCP also inhibited glucose stimulated ATP ($P<0.001$). Combinations of SRIF with nifedipine and H_2O with nifedipine were significantly less than SRIF or H_2O alone ($P<0.0001$), and it is insignificant from nifedipine alone, one-way ANOVA corrected with Sidak's multiple comparisons test (n=3).

3.6 Results of mouse islets and 1.1B4 cells

3.6.1 OCR of mouse islets

Changes in the mitochondrial respiration of isolated mice islets were investigated by measuring OCR (Fig. 3.13). Unlike MIN6 cells 10 mM glucose did not significantly raise the basal rate which was ~0.13 nmol O_2 10^2 $islet^{-1}$ min^{-1} on the contrary there was insignificant decrease in respiration. 100 nM SRIF also failed to change OCR and the trend of decrement was statistically insignificant.

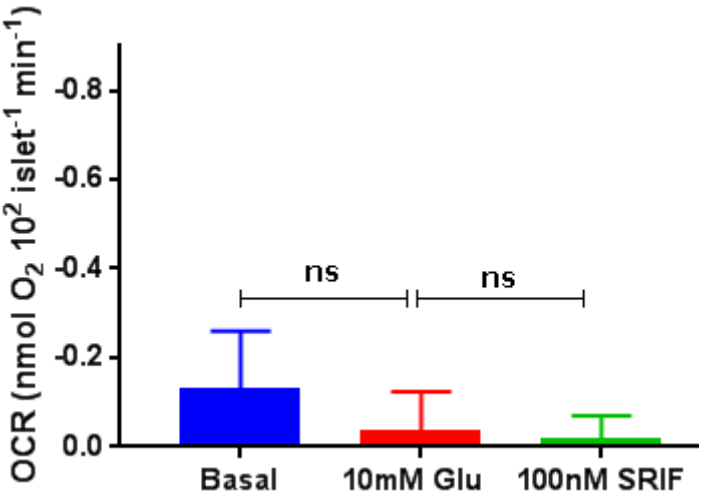

Figure 3.13: Effect of 10 mM glucose and 100 nM SRIF on the OCR in mice islets. The substrate and the peptide both insignificantly changed the OCR. Friedman test corrected with Dunn's multiple comparisons test (n=5). Values are mean±SEM.

3.6.2 OCR of 1.1B4 cells

Figure 3.14 shows the effect of 10mM glucose and 100 nM SRIF on OCR of human β–cell line 1.1B4. The values of basal respiration are comparable to that of MIN6 cells. 10 mM glucose significantly stimulated OCR as can be noticed in Fig. 3.14 A and B. 100 nM SRIF significantly inhibited glucose stimulated OCR as seen in Fig. 3.14 A, ($P<0.05$, n=10). The vehicle control H_2O insignificantly changed the glucose stimulated OCR as in Fig. 3.14 B (n=9).

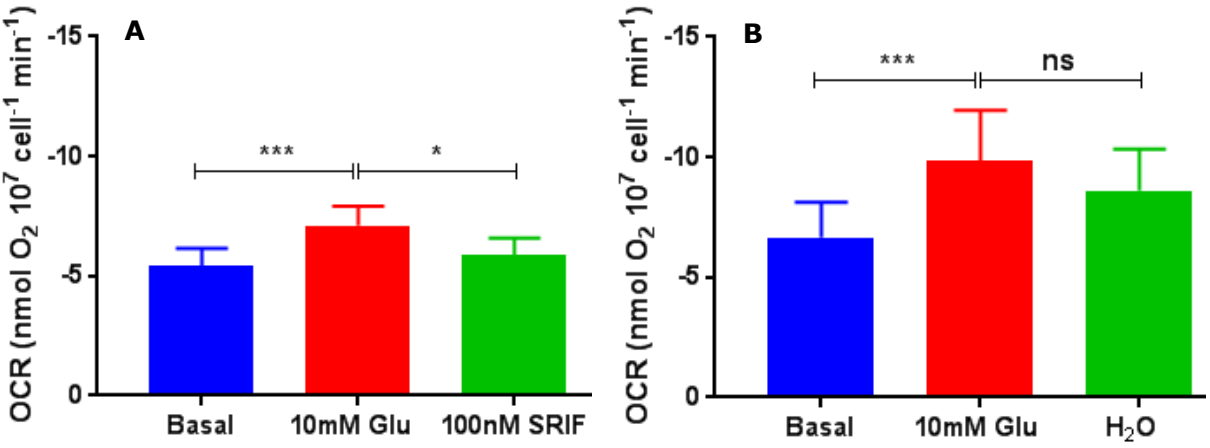

Figure 3.14: Effect of 10 mM glucose and 100 nM SRIF on OCR of 1.1B4 cells. (A) SRIF significantly inhibited glucose stimulated OCR ($P<0.05$, n=10), RM one-way ANOVA corrected with Sidak's multiple comparisons test. (B) The vehicle control H_2O did not affect the glucose stimulated OCR, Friedman test corrected with Dunn's multiple comparisons test (n=9). Values are mean±SEM.

3.7 Discussion

In this chapter, an attempt was made to find out to what extent somatostatin inhibited mitochondrial function and how this reflected on the cellular energy production (ATP) of the pancreatic β-cell. Prior studies (Daunt et al., 2006) have noted the importance of SRIF in modulating β-cell mitochondrial activity, even though they did not measure the intracellular ATP changes. In this study 100 nM SRIF-14 has been used because in the majority of previous studies they have found that the maximal effect of the peptide is ~ 100 nM (Smith et al., 2001). The current study found that 100 nM SRIF significantly inhibited glucose stimulated OCR, these results are consistent with Daunt et al., 2006. However, the specific mechanism by which SRIF achieves its action is not understood. It is well known that O_2 is consumed during the oxidative phosphorylation process in the mitochondrial inner membrane via complex IV. A possible explanation might be that SRIF inhibits one or more of the mitochondrial complexes activity in a way similar to that of complex inhibitors such as oligomycin and sodium azide. The argument against this idea is that SRIF was not as effective as established mitochondrial inhibitors e.g. oligomycin and sodium azide and the mitochondrial uncoupler FCCP. Because FCCP and oligomycin are more potent inhibitors compared to SRIF, they significantly inhibit ATP production (fig. 3.12). FCCP acts as an uncoupler to the oxidative phosphorylation by transporting the protons across the mitochondrial inner membrane to the matrix and vs versa (Benz and

McLaughlin, 1983). Oligomycin acts by blocking the proton channel F0 subunit of F1F0 ATP synthase (complex V) (Symersky et al., 2012).

In this study, SRIF blocked KIC stimulated OCR which is in contrast with Daunt et al. who found that SRIF did not inhibit the KIC stimulated OCR. The inhibition of KIC by SRIF indicates that the peptide might act on the TCA cycle because KIC directly inserts into the TCA cycle. In fact, KIC can be produced by transamination of the amino acid leucine by aminotransferase activity. Then KIC undergoes oxidative decarboxylation catalysed by keto-acid dehydrogenase to finally produce acetyl-CoA, the key product of TCA (Lynch et al., 2003, Su et al., 2012). The inhibition of TCA can explain the concomitant inhibition of both OCR and $\Delta\Psi_{mit}$ by the peptide.

This study (fig. 1.9) and the results of Daunt et al., (2006) confirm that SRIF inhibits both glucose stimulated $\Delta\Psi_{mit}$ and OCR. Despite the difference in glucose concentrations, the stimulation of OCR achieved by 10 mM glucose in this study was comparable with that produced by 20 and 25 mM glucose observed in (Daunt et al., 2006) and (Soejima et al., 1996), respectively. In MIN6 cells, glucose increased the basal respiration from around 5 nmol O_2 10^7 $cell^{-1}$ min^{-1} to approximately 10 nmol O_2 10^7 $cell^{-1}$ min^{-1} in the current and both previous studies. For $\Delta\Psi_{mit}$, 10 mM glucose decreased the Rh123 fluorescence by ~20% which is similar to that observed by Daunt et al., 2006 in MIN6 and in INS-1 cells (Maechler et al., 1997).

However, the impact of mitochondrial inhibition by SRIF on ATP production has not been reported in the literature yet. The inhibition of mitochondrial respiration and $\Delta\Psi_{mit}$ should be reflected on the ATP production. However, in this study, SRIF failed to reduce ATP production even though its ability to inhibit both $\Delta\Psi_{mit}$ and OCR. This is possibly because cells were incubated with SRIF at room temperature according to the manufacturer's recommendations which might prevent SSTs activation by the peptide. It is nevertheless mentioned in previous work (Smith et al., 2001) that SRIF activated potassium channels in a single channel experiment carried out at 22 °C. Based on that study, SRIF still able to activate SSTRs and produce an effect in the RT condition. Another possible reason is the ability of SRIF to inhibit AC activity which leads to accumulation of ATP in the cytoplasm and mask the peptide inhibitor effect. Furthermore to the above two reasons, the sample

size of this experiment is too small (n=3) which might increase the possibility of statistic errors e.g. type II error.

In an attempt to further understand the mechanism of SRIF action in pancreatic β-cell, SRIF was challenged with a high concentration of cAMP. This is because SRIF action was proposed to be mediated by the inhibition of AC and subsequently cAMP (Schuit et al., 1989). For this purpose, the cAMP activator forskolin was used (Alasbahi R. and Melzig M., 2012), however, unfortunately, the vehicle control of forskolin (DMSO) exerted similar effect of that of forskolin (data not shown), and therefore all these results were excluded. Consequently, in order to investigate the role of cAMP, the cell permeable cAMP analogue (dbcAMP) was used to elevate the intracellular cAMP level. Surprisingly, dbcAMP alone was found to inhibit basal and glucose stimulated OCR as shown in fig. 5A&C. This result may be explained by the fact that cAMP inhibits pyruvate kinase in hepatocytes (Pilkis et al., 1988). In hepatocytes, cAMP by activation of protein kinase A (PKA) enhances the phosphorylation-mediated inhibition of pyruvate kinase which leads to a decrease in the conversion of phosphoenolpyruvate to pyruvate (Pilkis et al., 1982), and less pyruvate entering into the TCA cycle leading to inhibition of oxidative phosphorylation. A similar mechanism might be applied in pancreatic β-cells.

Glucagon showed a similar effect as dbcAMP which inhibited basal and glucose stimulated OCR. This could be due to the ability of glucagon to elevate cAMP by activation of adenylate cyclase (Kawai et al., 1995). Another possible explanation is that glucagon controls blood glucose by decreasing glycogenesis and glycolysis in hepatocytes (Jiang and Zhang, 2003). There are two mechanisms suggested for glycolysis inhibiting in hepatocytes which might be happening in pancreatic β-cells. First, inhibition of phosphofructokinase-1 (PFK-1) which catalyses the phosphorylation of fructose-6-phosphate to fructose-1,6-bisphosphate, a rate limiting step in glycolysis (Castaño et al., 1979, Veneziale et al., 1976). Second, by inhibition of pyruvate kinase in the same way mentioned above (Pilkis et al., 1982, Pilkis and Claus, 1991).

As mentioned in the results section, 100 nM SRIF inhibited glucose stimulated OCR in the presence of 1 mM dbcAMP in a similar magnitude achieved by SRIF alone. This result is in line with Daunt et al. who found that cAMP analogue 8-(4-chlorophenylthio)-adenosine

3’,5’-cyclic monophosphate (8-CPT) did not affect either OCR or the ability of SRIF to inhibit OCR. However, the opposite, i.e. stimulation of OCR was not seen with clonidine nor SRIF, both of which decrease cAMP. These results suggest that elevation of cAMP did not change SRIF inhibitory action in MIN6 β–cells and the SRIF action is not mediated by cAMP.

Hyperpolarization of $\Delta\psi_{mit}$ achieved by 10 mM glucose in the absence of Ca^{2+} (22%) was significantly more than in the presence of Ca^{2+} (13%) when the basal values were comparable. This result indicates that Ca^{2+} somehow decreased glucose stimulated mitochondrial membrane potential. It is well established that mitochondria modulate both physiological and pathological Ca^{2+} signals (Hajnóczky et al., 2000, Jacobson and Duchen, 2004, Scorziello et al., 2013). Ca^{2+} uptake by the mitochondria occurs when the cytosolic [Ca^{2+}] exceeded 100 nM via the changes in the $\Delta\psi_{mit}$ during the ETC activity (Nicholls and Crompton, 1980). Mitochondria then pump out the Ca^{2+} to the cytosol via Na^{+} or H^{+} antiporters (Rottenberg and Marbach, 1990). However, the regulatory effect of Ca^{2+} on mitochondria is still controversial (Chalmers and McCarron, 2008). It is believed that Ca^{2+} uptake by mitochondria stimulates ATP production via the activation of both TCA cycle (Denton et al., 1980) and F1F0 ATP synthase in the oxidative phosphorylation process (Territo et al., 2000). On the other hand, the positive charges of Ca^{2+} might lead to $\Delta\psi_{mit}$ depolarization and subsequently reduce ATP production (Chalmers and McCarron, 2008). The latter hypothesis supports the findings of this study i.e. the magnitude of the glucose effect on $\Delta\psi_{mit}$ in the presence of Ca^{2+} is significantly less than that in Ca^{2+} free condition. In the absence of Ca^{2+}, SRIF did not depolarize the $\Delta\psi_{mit}$, data are in agreement with the observations of Daunt et al. (2006) on OCR. In addition, the blockade of L-type Ca^{2+} channels with nifedipine leads to mitochondrial depolarization and ATP reduction which emphasizes the role of Ca^{2+} in regulating mitochondrial functions. SRIF was still able to depolarize the mitochondria in the presence of nifedipine because nifedipine was not completely abolished by Ca^{2+} influx by blocking only L-type VGCCs. These data suggest that Ca^{2+} is essential for SRIF action on the mitochondria of pancreatic β-cells.

Chapter Four:

The Effect of Somatostatin on Glucose Uptake and Glycolysis of MIN6 pancreatic β-cells

4.1 Introduction

In this study, I examined the effect of SRIF on glycolytic flux, a process which can be quantified in cultured cells by measuring glucose uptake and lactate output (TeSlaa and Teitell, 2014, Sener et al., 1976). In pancreatic β-cells, glucose uptake occurs by a process of facilitated diffusion via glucose transporters GLUT 1, 2 and 3 in human and mainly by Glut 2 in rodents (van de Bunt and Gloyn, 2012, De Vos et al., 1995). Upon entering the β-cell, glucose is rapidly phosphorylated to glucose-6-phosphate by the action of glucokinase as the first step of glycolysis. Therefore, the glucose uptake quantification methods depend either on the measuring of glucose metabolites or using non-metabolised glucose analogues e.g. 2DG (Yamamoto et al., 2015).

There are several techniques to measure glucose uptake as follows: First, the enzymatic fluorimetric detection of 2-deoxyglucose-6-phosphate (2DG6P), a non-metabolized product of the glucose analogue 2-deoxyglucose (2DG) which can be measured by luminescence, fluorescence or absorbance techniques (Saito et al., 2011). Second, the detection of intracellular accumulation of a fluorescently labeled glucose analogue 2-(N-(7-nitrobenz-2-oxa-1,3-diazol-4-yl)amino)-2-deoxyglucose (2-NBDG) by fluorescence imaging techniques (Yoshioka et al., 1996, O'Neil et al., 2005).

Thirdly, measurement of accumulated radio-labelled analogues such as ^{3}H-2DG, ^{3}H-2DG6P and 3-O-methylglucose by radioactive isotope techniques (Yamamoto et al., 2015, Saito et al., 2011, Valley et al., 2016).

There is conflicting evidence from prior studies regarding whether SRIF affects glucose uptake in different cell types. Several studies found that SRIF has no effect on glucose uptake in human hepatocytes (Baron et al., 1987), rat liver, pancreas and white fat adipocytes (Cherrington et al., 1977). On the other hand, Møller et al., (1995) found that SRIF improved glucose uptake in human skeletal muscles. Therefore, in an attempt to clarify the situation in pancreatic β-cells in this study, the effect of SRIF on glucose uptake of MIN6 cells was investigated.

Lactate production due to glucose breakdown (glycolysis) is another important aspect of glucose utilization which was considered in this study. Glycolysis is an intracellular process in which one molecule of glucose is enzymatically catalysed into two molecules of pyruvate and associated with the production of two molecules of ATP. Pyruvate is the final product of glycolysis which either enters the mitochondria to produce ATP or is converted into lactate. In the presence of sufficient O_2, pyruvate has entered the mitochondria and oxidised by pyruvate dehydrogenase to acetyl-CoA. The latter enters the tricarboxylic acid cycle (TCA) to produce NADH and $FADH_2$ which donate electrons to the electron transport chain (ETC) to ultimately generate up to 34 ATP by oxidative phosphorylation. In the cytosol, mainly in the lack of O_2, lactate dehydrogenase catalyses the reduction of pyruvate into lactate which is accompanied by oxidation of NADH into NAD^+. Lactate is passively diffused outside the cell via monocarboxylate transporters (MCT), while the NAD^+ maintains the initiation of glycolysis (DeBerardinis et al., 2008). Although ATP production from the glycolytic pathway is considerably less than that of oxidative phosphorylation, glycolysis is still of value to proliferative cells and to some non-proliferative cells for energy production especially under conditions of anoxia or lack of oxygen (Pfeiffer et al., 2001).

In 1956, Warburg found that tumour cells were able to convert glucose to lactate in the presence of oxygen by anaerobic glycolysis, this behaviour is different from normal cells which depend on oxidative respiration in the presence of oxygen (Liberti and Locasale, 2016). This phenomenon has been called later the Warburg effect which happens in rapidly proliferating cells such as tumours, lymphocytes and stem cells (Vander Heiden et al., 2009). MIN6 as a cell line could be subject to the Warburg effect. Although the Warburg effect is an inefficient source of energy, it is compensated by glycolysis to provide additional metabolites essential for rapid cell proliferation (DeBerardinis et al., 2008). Warburg effect was extensively studied in cancer cells (Vander Heiden et al., 2009, Liberti and Locasale, 2016, López-Lázaro, 2008, Unwin et al., 2003, Tran et al., 2016). Moreover, studies suggest that some tumours such as large B cell lymphomas and glioblastomas are not subject to the Warburg effect (Caro et al., 2012, Marin-Valencia et al., 2012).

4.1.1 Aims

The aim of this chapter was to examine the effect of SRIF on glucose uptake and anaerobic glycolysis by measuring lactate production in MIN6 cells.

4.2 Methodology

4.2.1 Measurement of lactate production

The method as described in chapter two, see 2.6

4.2.2 Glucose uptake assay

The method as described in chapter two, see 2.9

4.3 Results of lactate production

4.3.1 SRIF inhibits glucose stimulated lactate production

10 mM glucose increased the basal lactate production (LP) in MIN6 cells (Figure 4.1 A&B). This effect was concomitant with increased oxygen consumption by the mitochondria (Figure 4.1 C&D). Figure 4.1A shows that 100 nM SRIF almost halved the lactate produced by the vehicle control H_2O in 10 mM glucose (Figure 4.1B). Figure 4.2 A&B shows that 100 nM SRIF significantly inhibited both glucose stimulated lactate production ($P<0.01$, $n=12$) and OCR ($P<0.001$, $n=12$). This effect can also be noticed in 100 µM sodium lactate solution was added as four boluses to confirm that the electrode was intact and to calibrate the electrode sensitivity. The vehicle control H_2O neither affected lactate production nor OCR (Fig. 4.2 C&D).

The ratio of glycolysis to glucose oxidation (Gly/OX) was calculated by dividing the mean of lactate production values over the mean of OCR. Figure 4.3 A shows that Gly/OX ratio of 100 nM SRIF was significantly correlated with that of 10 mM glucose, $r=0.82$ ($P<0.0001$, $n=12$). The ratio of vehicle control H_2O was also correlated with the ratio of 10 mM glucose $r=0.83$ ($P<0.0001$, $n=9$) as in figure 4.3 B.

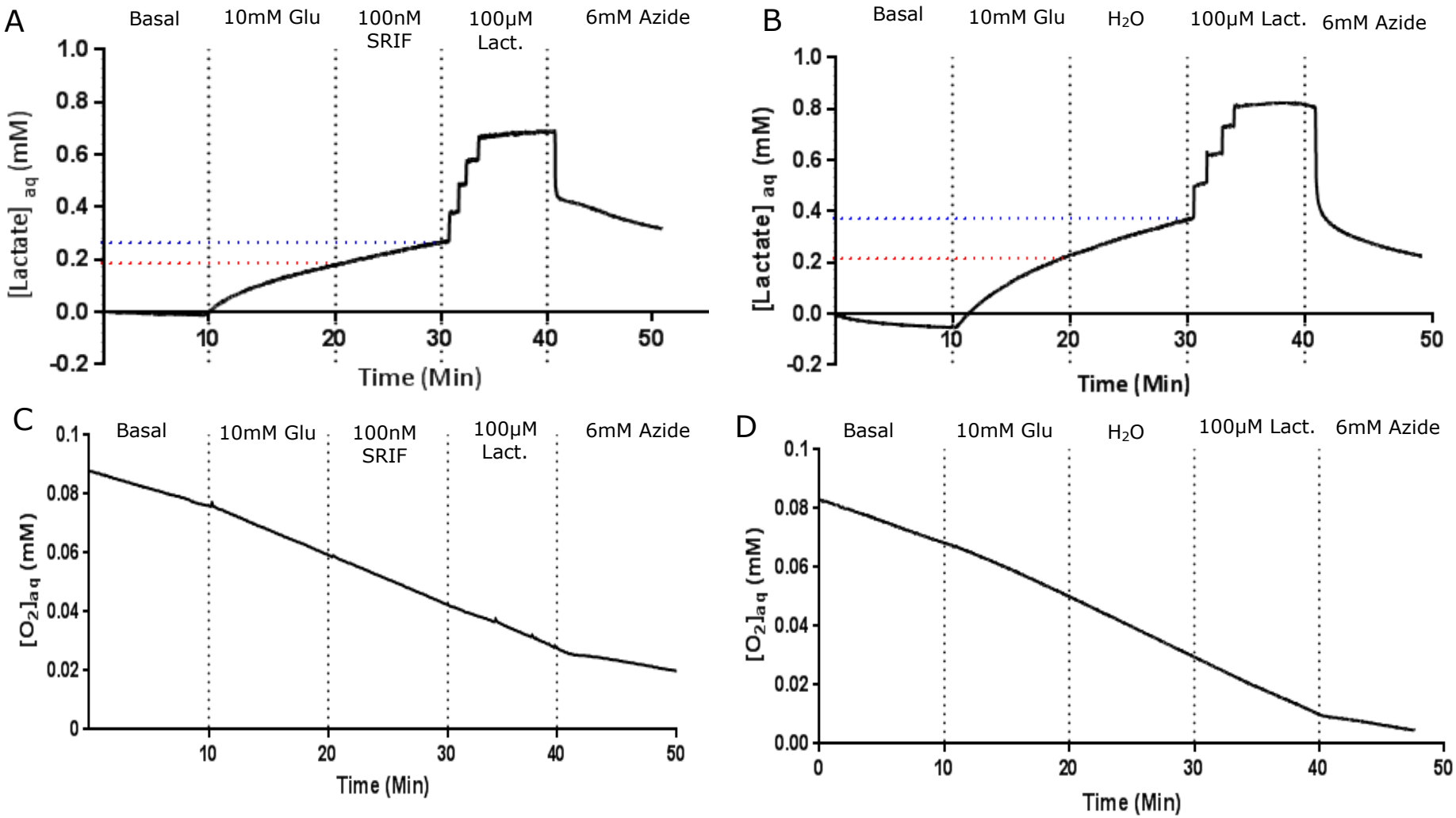

Figure 4.1: Glucose stimulates lactate production and OCR. Representative traces that show the effect of 10 mM glucose (Glu), 100 nM SRIF and 6 mM sodium azide on lactate production and OCR of MIN6 cells. (A) increase of basal lactate production by 10 mM glucose. red dotted line indicates lactate concentration after 10mM glucose treatment for 10min. (B) Inhibition of lactate production by 100 nM SRIF, which was nearly half that of the vehicle control measured at the same time. The blue dotted line represents the lactate concentration at the end of SRIF treatment in (A) and H_2O in (B). The difference between the red and the blue dotted lines shows the change in lactate production in response to 100 nM SRIF (A) or the vehicle control H_2O (B). 100 µM sodium lactate solution(Lact) added as 4 boluses to calibrate the lactate sensor. 6 mM sodium azide (Azide) decrease lactate concentration. 10 mM glucose increased OCR in (C) and (D) which was inhibited by 100 nM SRIF (C) but not by H_2O (D). 6 mM sodium azide blocks cellular respiration and only allows the electrode O_2 consumption.

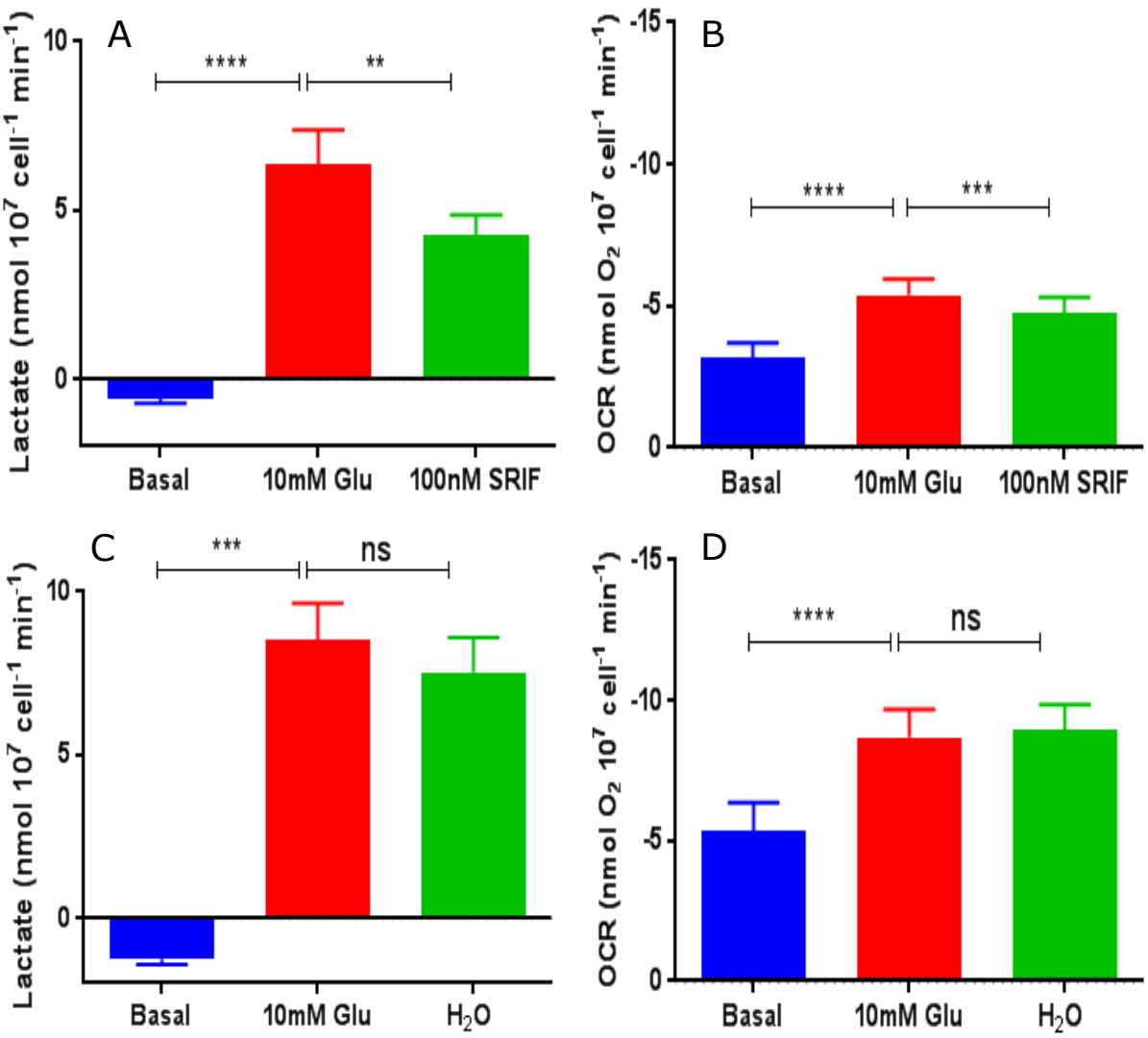

Figure 4.2: Effect of glucose and SRIF on lactate production and related OCR of MIN6 cells. (A) Lactate production was significantly increased (P<0.0001, n=12) when 10 mM glucose was introduced and was significantly decreased in response to 100 nM SRIF (P<0.01, n=12), repeated measure (RM) one-way ANOVA corrected with Holm-Sidak's multiple comparisons test. (B) The oxygen consumption was significantly increased as a result of glucose addition (P<0.0001, n=12) which was followed by a significant decrease due to the effect of 100 nM SRIF (P<0.001, n=12), RM one-way ANOVA corrected with Holm-Sidak's multiple comparisons test, n=12). (C) 10 mM glucose significantly increased lactate production (P<0.001, n=9) while the vehicle control had no effect (n=9), Friedman One way ANOVA test corrected with Dunn's multiple comparisons test. (D) Vehicle control H_2O did not affect glucose stimulated OCR, RM one-way ANOVA corrected with Holm-Sidak's multiple comparisons test (n=9). All values are mean±SEM.

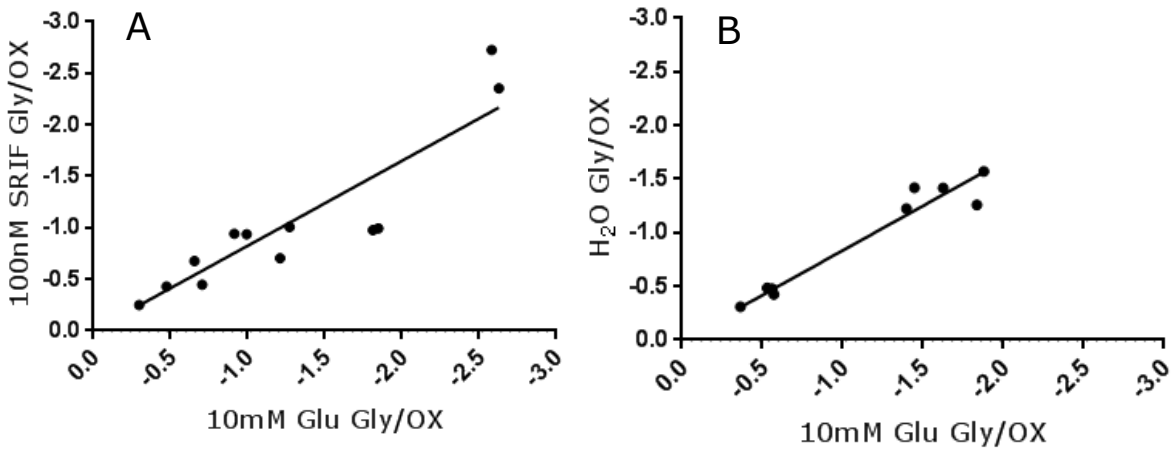

Figure 4.3: Linear regression of glycolysis (Gly) to glucose oxidation (OX) ratios of MIN6 cells. (A) Gly/OX ratios of 100 nM SRIF and 10 mM glucose were significantly correlated (P<0.0001, n=12). (B) Gly/OX ratios of vehicle control H_2O and 10 mM glucose were also significantly correlated (P<0.0001, n=9). Data analysed with linear regression XY and all values are mean±SEM.

4.3.2 Effects of cyclosporine A and SRIF on lactate production

Since the inhibitory effect of somatostatin is proposed to be mediated by activation of the protein phosphatase calcineurin in pancreatic α-cells (Gromada et al., 2001) and β-cells (Renström et al., 1996), the effect of the peptide in the presence of calcineurin inhibitors e.g. cyclosporine A and okadaic acid was investigated. Figure 4.4A shows that 1 μM cyclosporine A (CSA) neither affected the ability of glucose to stimulate lactate production (LP) nor 100 nM SRIF inhibition of glucose stimulated LP (P<0.01, n=8). Figure 4.4B shows the associated OCR in which 1 μM CSA neither affected glucose stimulated OCR nor its inhibition by 100 nM SRIF (P<0.0001, n=8). These data suggest that SRIF inhibits glycolysis and mitochondrial respiration via a protein phosphatase independent pathway. Vehicle control (ethanol) of both CSA and OKA was tested in this study and no significant changes either in LP or in OCR were noticed as can be seen in figure 4.4 C&D. Although in the presence of ethanol, 100 nM SRIF significantly inhibited glucose stimulated OCR (P<0.001, n=7), however it failed to reduce glucose stimulated LP (figure 4.4 C&D). 100 nM SRIF inhibited glucose stimulated LP in the presence of CSA by 19% which is insignificantly different from that of the vehicle control ethanol 14% (Unpaired t test, n=8).

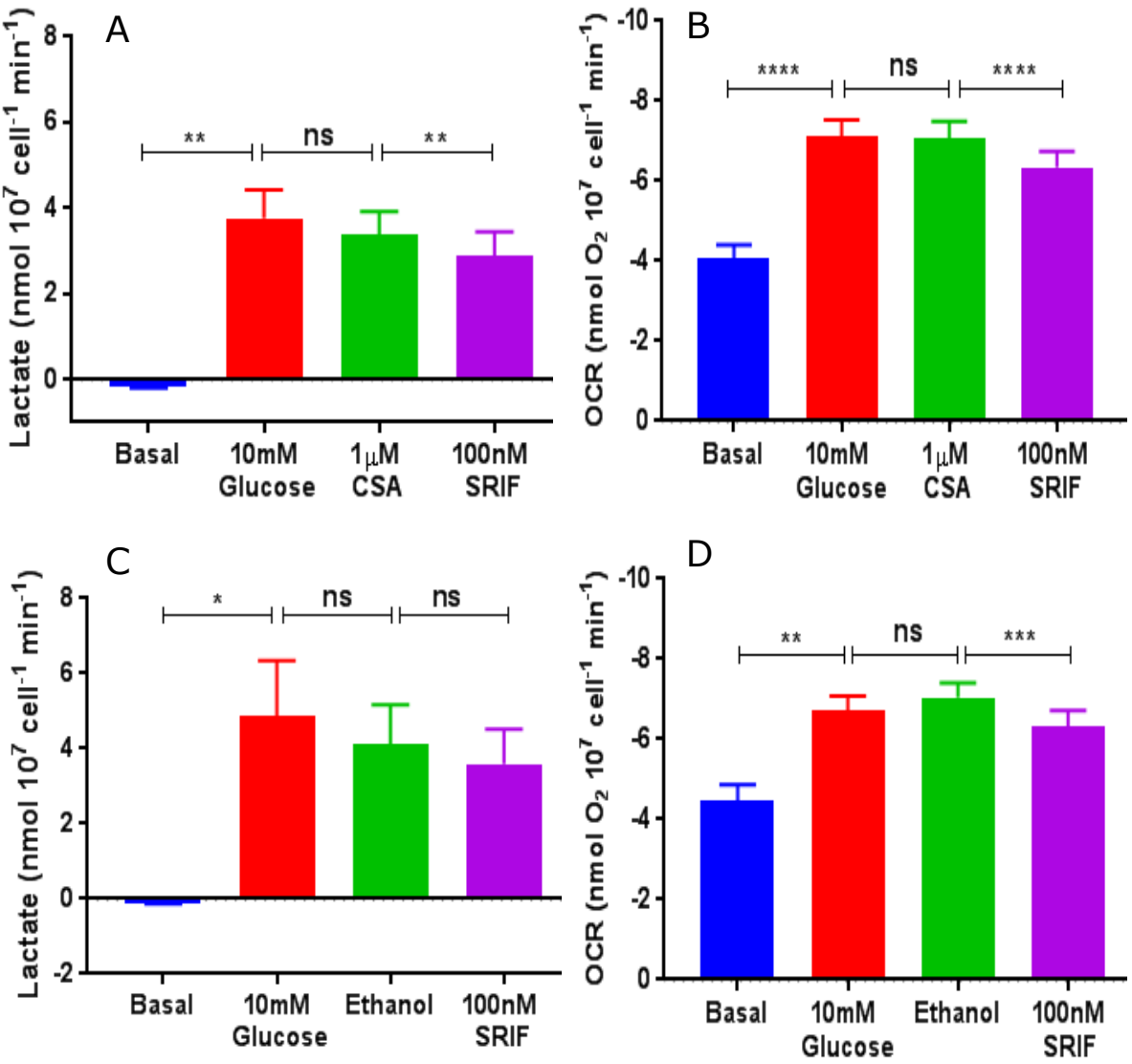

Figure 4.4: Effect of SRIF, cyclosporine A (CSA) and ethanol on glucose stimulated lactate production and related OCR of MIN6 cells. (A) lactate production significantly increased (P<0.01, n=8) by 10 mM glucose which was unaffected by 1 μM CSA. Lactate still was significantly decreased in response to 100 nM SRIF (P<0.01, n=8), RM one-way ANOVA and corrected with Sidak's multiple comparisons test. (B) Basal oxygen consumption was significantly increased by 10 mM glucose (P<0.0001, n=8), with no effect of 1 μM CSA. 100 nM SRIF significantly inhibited OCR (P<0.0001, n=8), RM one-way ANOVA corrected with Holm-Sidak's multiple comparisons test. (C) 10 mM glucose significantly increased lactate production (P<0.05, n=7), while the vehicle control ethanol and SRIF had no effect, RM one-way ANOVA corrected with Holm-Sidak's multiple comparisons test. (D) Vehicle control ethanol did not affect glucose stimulated OCR, while 100nM SRIF significantly inhibited OCR (P<0.001, n=7) RM one-way ANOVA corrected with Holm-Sidak's multiple comparisons test. All values are mean±SEM.

4.3.3 Effects of okadaic acid and SRIF on lactate production

100 nM okadaic acid (OKA), like CSA, did not affect glucose stimulated LP and OCR as can be seen in figure 4.5A&B respectively. In the presence of 100 nM OKA, SRIF failed to change glucose stimulated LP, on the other hand, it inhibited glucose stimulated OCR

(P<0.05, n=8). The effect of vehicle control ethanol on glucose stimulated LP (Fig. 4.4C) was comparable with that of OKA (Fig. 4.5A) and both of them abolished the inhibitory effect of SRIF. 100 nM SRIF inhibited glucose stimulated LP in the presence of OKA by 9% which is insignificantly different from that of the vehicle control ethanol 14% (Unpaired t test, n=8).

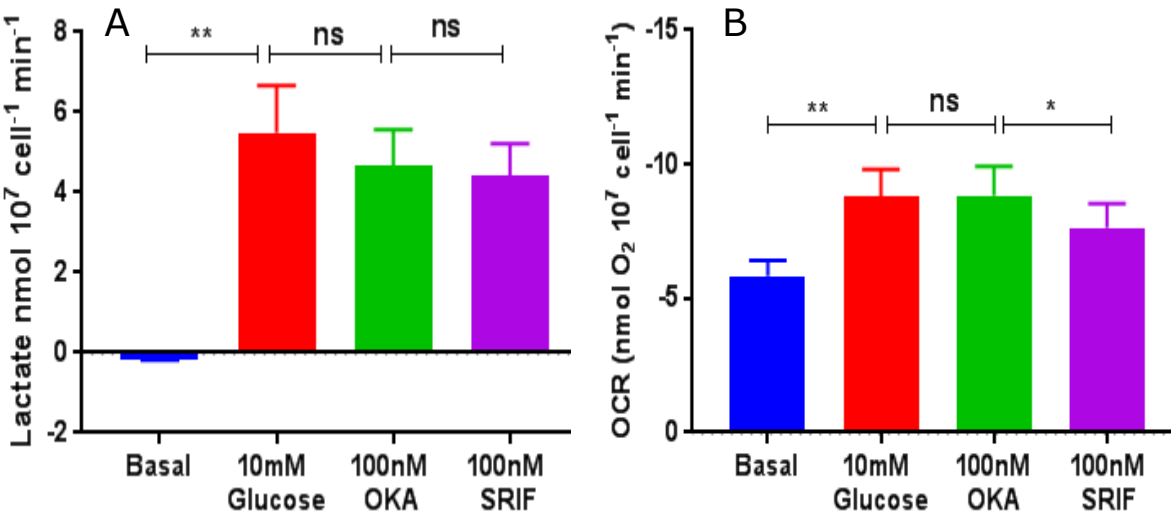

Figure 4.5: Effect of SRIF and Okadaic acid (OKA) on glucose stimulated lactate production and related OCR of MIN6 cells. (A) 100 nM OKA abolished SRIF inhibitory action, RM one-way ANOVA corrected with Holm-Sidak's multiple comparisons test. (B) 100 nM OKA neither changed the 10 mM glucose stimulation nor the ability of 100 nM SRIF to inhibit OCR (P<0.05, n=8), RM one-way ANOVA corrected with Sidak's multiple comparisons test. All values are mean±SEM.

4.4 Results of glucose uptake assay

4.4.1 Effects of SRIF on 2-deoxyglucose uptake

The potential ability of SRIF to affect glucose transporters, glucose uptake and glucokinase activity were investigated in this study using a plate based technique of the Glucose Uptake-Glo™ assay of Promega®. Figure 4.6A illustrates the response of MIN6 cells incubated with 2-deoxyglucose (2DG), 100 nM SRIF and 50 µM cytochalasin B (CB) which was measured according to the provided protocol every half an hour for 5 hours. As can be noticed from figure 4.6A, the highest level of luminescence was recorded after one hour incubation at room temperature. Based on the result of this experiment (figure 4.6A), all the latter experiments were measured after one hour incubation. Data from figure 4.6B show that neither 100 nM SRIF nor DMSO changed the basal 2DG uptake. On the other

hand, cytochalasin B (glucose transport inhibitor) significantly inhibited basal 2DG uptake (P<0.0001, n=3, 17 repeats).

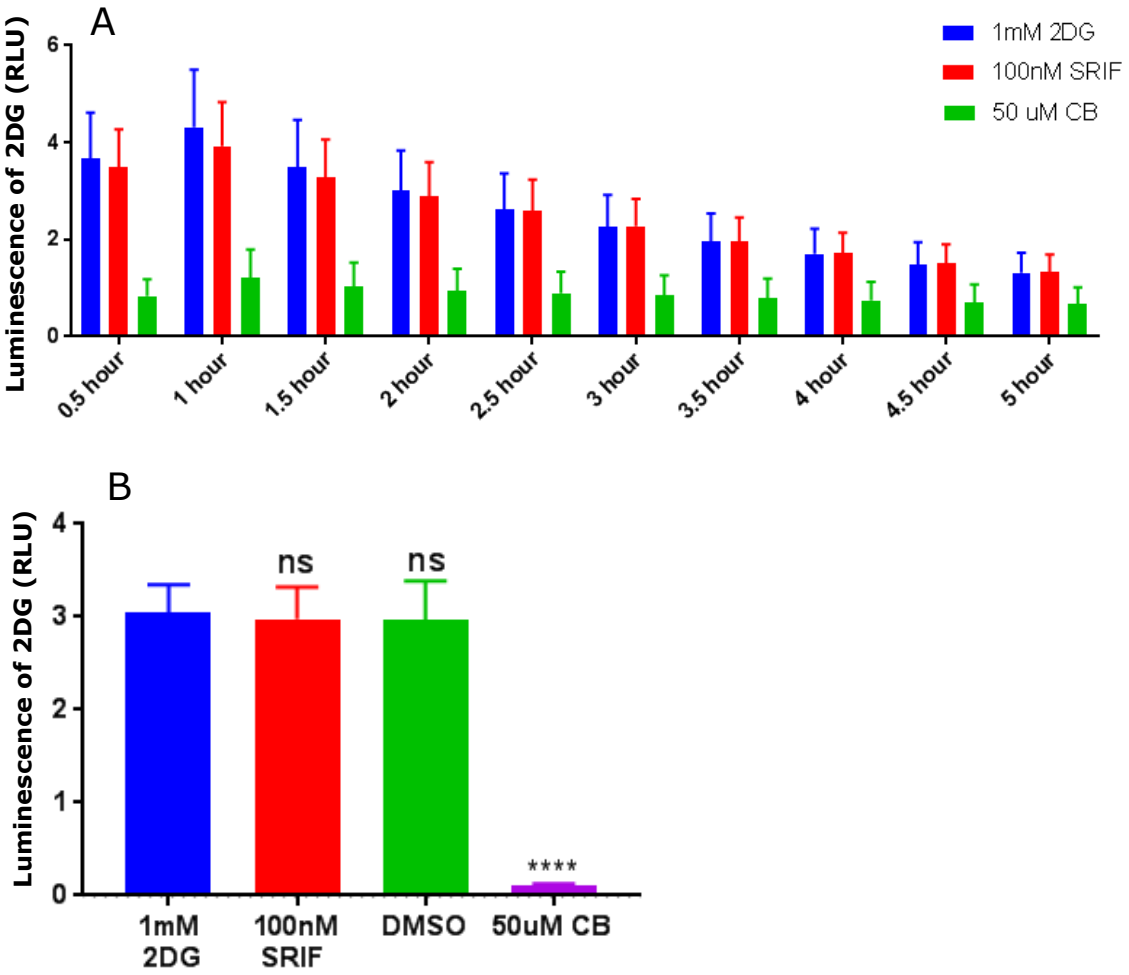

Figure 4.6: Effect of SRIF, cytochalasin B (CB) and DMSO on 2DG uptake of MIN6 cells. (A) Luminescence measured as relative light units (RLU) every 30 min for 5 hours at room temperature. Results show that the largest response was achieved after 1 hour incubation. Statistics done by two-way ANOVA and corrected with Sidak's multiple comparisons test (the data are from a single pilot experiment with 10 repeats of each treatment). (B) Luminescence of 2DG uptake in the presnce of 100 nM SRIF and DMSO (the vehicle of CB) were insignificant in comparison with 1 mM 2DG alone, while 50 µM CB significantly inhibited 2DG uptake (P<0.0001, n=3, 17 repeats) one-way ANOVA corrected with Holm-Sidak's multiple comparisons test. Values are mean±SEM.

4.5 Discussion

In this study, 100 nM SRIF did not affect glucose uptake into MIN6 cells as can be seen in figure 5B. This result is consistent with a previous study performed on pancreatic α and β cells (Gorus et al., 1984). Moreover, SRIF failed to change glucose uptake in rat skeletal muscles, hepatocytes and adipocytes (Cherrington et al., 1977). On the other hand, a study carried out on human skeletal muscle found that locally injected, but not systemic, SRIF significantly improved insulin stimulated glucose uptake (Møller et al., 1995). However, the locally perfused SRIF did not change the basal glucose uptake unless hyperinsulinemia condition was applied. Therefore, their results can be interpreted as SRIF may enhance insulin sensitivity (Orskov et al., 1996) and subsequently glucose uptake. Due to the dual inhibitory effect of SRIF on both LP and OCR found in the current study, we can infer that the peptide may inhibit glucose uptake and or the early glucokinase phosphorylation step of glycolysis. Since the principle of the Glucose Uptake-Glo™ assay depends on the conversion of 2DG into 2-deoxyglucose-6-phosphate (2DG6P) by glucokinase activity in MIN6 cells. The failure to see an effect of SRIF on 2DG6P refutes an action of the peptide either on glucose uptake or phosphorylation by glucokinase in MIN6 cells.

Undoubtedly, the measurement of lactate in the extracellular fluid could not provide a complete picture of glucose metabolism, however, it can show realistic information of glycolytic flux assuming that the treatments do not influence the monocarboxylate transporters (MCT1–MCT4) at the cell membrane. In the current study, 100 nM SRIF significantly inhibited lactate production, the data are in agreement with Møller et al. (1995) who found that SRIF decreased lactate production from human skeletal muscle. Although a study of Cherrington et al. (1977) hypothesized that the inhibitory effect of somatostatin is according to an effect on the endocrine system rather than to its direct effects on glucose metabolism. However, the inhibition of lactate production in this study refutes Cherrington's hypothesis and confirms that there is a direct interaction of SRIF with glucose metabolism at the final step of glycolysis. Furthermore, Steták et al., (2007) found in COS cells that SRIF and its analogue TT-232 interact with pyruvate kinase (PK), a glycolytic rate-limiting enzyme. They were suggested that TT-232 has a dual pathway

which are receptor activation that causes cell cycle arrest and another undefined mechanism that induces apoptosis. Add to that the same study showed that TT-232 induced nuclear translocation of the pyruvate kinase M2 (PKM2) isoenzyme which leads to stimulation of cell apoptosis (Steták et al., 2007). Even though the cell death induced by PKM2 translocation is not related to its enzymatic activity, however, the ability of SRIF and its analogue to modify this glycolytic enzyme is the most important part in this context. Another glycolytic enzyme, phosphoglycerate dehydrogenase could also be affected by the action of SRIF. Previous studies suggested that activation of this enzyme leads to a shift of glucose utilization via glycolysis from pyruvate production into serine synthesis pathway (Locasale et al., 2011, Possemato et al., 2011) which provides a reasonable explanation of the concomitant decrease of both OCR and LP in the current study. However, this explanation needs to be confirmed by testing the peptide on the phosphoglycerate dehydrogenase enzyme activity in pancreatic β–cells.

In this study, 10 mM glucose stimulated OCR of MIN6 cells similar to that published previously by Daunt et. al., (2006). Glucose also stimulated lactate production in MIN6 cells which were comparable to that of rat islets reported by Sener et al., (1976). In the current study, the ratio of glycolysis to glucose oxidation (Gly/OX) obtained from 10 mM glucose in MIN6 was 2.5. This is similar to the ratio of 2.4 obtained from 16.7 mM glucose in rat islets (Sener et al., 1976). 100 nM SRIF changed the (Gly/OX) ratio of 10 mM glucose from 2.5 to 2.0, which is statistically insignificant (Mann Whitney t test, n=12). These results provide evidence that SRIF inhibits both glycolysis and glucose oxidation in the same magnitude. This is also indicating that the mitochondrial inhibition by the peptide may be in part due to the inhibition of glycolysis.

Interestingly, 6 mM sodium azide, a mitochondrial complex IV inhibitor, concomitantly blocked the OCR and rapidly decreased the extracellular lactate concentration. Logically in the presence of glucose, blockade of the mitochondrial electron transport chain must lead to accumulation of pyruvate in the cytoplasm and subsequently increase the lactate production. However, the opposite was noticed in this study since the lactate concentration significantly decreased. One possible explanation of this behaviour is that MIN6 cells might be metabolically switched from oxidative respiration to glycolysis by using the extracellular

lactate as a source of energy. Moreover, MIN6 as a cell line, it could be subjected to the Warburg effect.

CSA and OKA were used to examine whether the inhibitory effect of somatostatin is mediated by the activation of protein phosphatases. In this study, acute treatment of MIN6 with 1 μM CSA neither changed glycolysis nor mitochondrial respiration even though a long term high doses of CSA reported to be toxic to the pancreatic β–cells in rats (Helmchen et al., 1984). Previous studies reported that 1 μM CSA abolished the inhibitory effect of SRIF on exocytosis in pancreatic α cells (Gromada et al., 2001). However, in this study 1 μM CSA did not prevent the inhibitory action of SRIF on both LP and OCR of MIN6. In addition, the current study found that 100 nM OKA successfully abolished the inhibitory effect of 100 nM SRIF on LP. The vehicle control ethanol produced a similar effect. As a result, this study could not confirm that the inhibitory effect of SRIF on glycolysis is mediated by protein phosphatase activation. Therefore, further investigation of SRIF action on glycolytic enzymes in the pancreatic β-cells is recommended.

Chapter Five:
The Effect of Somatostatin on Glucose Stimulated Ca^{2+} Influx of MIN6 cells

5.1 Introduction

The increase in the intracellular free Ca^{2+} level is one of the most important factors that regulate insulin secretion from pancreatic β-cell. Ca^{2+} influx from extracellular fluid occurs via voltage gated calcium channels (VGCCs) distributed on the plasma membrane of β-cells mainly in response to secretagogues such as glucose (Ashcroft and Rorsman, 1989). Somatostatin decreases the intracellular free Ca^{2+} level predominantly by inhibition of Ca^{2+} entry to the β-cells, however, the mechanism of inhibition is still controversial. Previous studies suggest that SRIF inhibits Ca^{2+} influx into β-cells by a direct effect on VGCCs (Smith, 2009, Fujii et al., 1994). Others suggest that SRIF inhibits Ca^{2+} influx by blocking VGCCs but without stimulation of ATP-sensitive K^+ channels (K_{ATP}) (Hsu et al., 1991, Abel et al., 1996). A study of Ribalet and Eddlestone (1995) claimed that SRIF mostly activates K_{ATP} channels, however, in some experiments it blocked the channels, and this block was reversed by dbcAMP. On the other hand, other researchers have confirmed that SRIF-induced hyperpolarisation of the β-cell plasma membrane occurs not only by activation of K_{ATP} channels but also by G protein-coupled inwardly rectifying K^+ (GIRK) channels (Smith et al., 2001, Ribalet and Eddlestone, 1995) which subsequently blocks VGCCs by preventing their activation (Ashcroft and Rorsman, 1989, Rorsman and Ashcroft, 2018).

Ca^{2+} plays a key role in the regulation of some cellular functions including plasma membrane potential, apoptosis and cell proliferation (Petrou et al., 2017, Berridge et al., 2000). Since these cellular functions are also regulated by SRIF (Liu et al., 2000, Patel, 1999), this provides another rationale to study the relation between SRIF and intracellular Ca^{2+} level.

Like neurons, pancreatic β-cells are electrically excitable that undergo changes in the plasma membrane potential, mainly according to alterations of blood glucose concentration (Drews et al., 2010, Henquin and Meissner, 1984, Rutecki, 1992). Glucose metabolism depolarises the plasma membrane and leads to an influx of Ca^{2+} through VGCCs which is essential for exocytosis (Eliasson et al., 2008). This is consistent with the findings of Meissner in 1976 who mentioned the correlation between glucose stimulated insulin secretion and plasma membrane electrical activity (Meissner, 1976, Meissner and Schmidt,

1976, Meissner and Atwater, 1976). It is believed that the pulsation of insulin secretion occurs due to Ca^{2+} oscillation (Gilon et al., 1993) which is associated with the plasma membrane electrical activity (Valdeolmillos et al., 1989).

An electrophysiological study of MIN6 cells using patch clamp techniques conducted by Smith et.al. (2001) demonstrated that SRIF inhibits glucose stimulated electrical activity by activation of two types of K^+ channels (K_{ATP} and GIRK). Although SRIF has other proposed mechanisms for inhibition of insulin secretion such as direct block of VGCCs, inhibition of cAMP production by blocking AC activity and direct inhibition of the exocytotic machinery, it is believed that activation of K^+ channels and blocking of VGCCs are dominant because SRIF ionic action is more potent and precedes the non-ionic distal events (Smith et al., 2001).

K_{ATP} channels play an important role in pancreatic β-cell functions because they connect the cell metabolism with the plasma membrane electrical activity and subsequently control Ca^{2+} mobilisation and insulin secretion (Ashcroft, 2005). The K_{ATP} channel is composed of eight subunits, four $K_{ir6.2}$ subunits forming a pore located centrally which are surrounded by four regulatory SUR1 subunits (Mikhailov et al., 2005, Puljung, 2018). Cytosolic adenine nucleotides, i.e. ATP and ADP, regulate K_{ATP} channels by closing and opening the channels, respectively (Kakei et al., 1986). Endogenous substrates e.g. glucose provide a high concentration of cytosolic ATP which binds with the binding site of $K_{ir6.2}$ subunit and lead to a closure of the channel. On the contrary, in the lack of substrates, ADP concentration arises which activate the channels by binding with nucleotide binding domains of SUR1 subunit (Tucker et al., 1997). The therapeutic mode of action of sulphonylurea drugs such as tolbutamide and glibenclamide emphasises the importance of the K_{ATP} channels in β-cell physiology: because they block channel activity by binding with the SUR1 subunit (Gribble and Reimann, 2003, Martin et al., 2017). Studies of genetics have linked mutations and the functional defects in the K_{ATP} channel activity with hyperinsulinaemia and diabetes which confirm the importance of K_{ATP} channels for the insulin secretion process (Stanley, 2016, Nichols and Remedi, 2012).

SRIF inhibits the electric conductivity of neurons mainly via a direct effect on different types of VGCCs (Tedford and Zamponi, 2006, Beech et al., 1992, Shapiro and Hille, 1993).

It seems that SRIF has a similar inhibitory effect on pancreatic β-cell secretion which is also mediated by blockade of VGCC (Hsu et al., 1991, Smith, 2009). This makes SRIF and its analogues of great value for studying different calcium related pathologies including tumours and diabetes (Boehm, 2003, Rai et al., 2015, Appetecchia and Baldelli, 2010).

5.1.1 Aims

The aim of this chapter was to understand the molecular mechanisms by which SRIF decreases Ca^{2+} influx. This includes exploring whether the peptide blocks the central route of glucose stimulated Ca^{2+} entry i.e. activity of K^+ channels and hyperpolarisation of the plasma membrane or directly blocks the VGCCs.

5.2 Methodology

5.2.1 Calcium imaging

The method as described in chapter two, see 2.8.

5.3 Results

5.3.1 SRIF inhibited basal and glucose stimulated calcium entry

MIN6 cells were loaded with the calcium sensitive dye Fluo-4 AM and treated with glucose free medium (Hank's supplemented with 0.1% BSA) for ~300 seconds which was recorded as basal fluorescence. Figure 5.1 shows the changes in fluorescence intensity due to the application of different treatments. 10 mM glucose (5.1B) clearly increased the fluorescence intensity compared to the basal (5.1A). While the application of 100 nM SRIF (5.1C) decreased fluorescence in the presence of 10 mM glucose. Adding 50 mM K^+ produced a maximum increase of the fluorescence as can be seen in figure 5.1D.

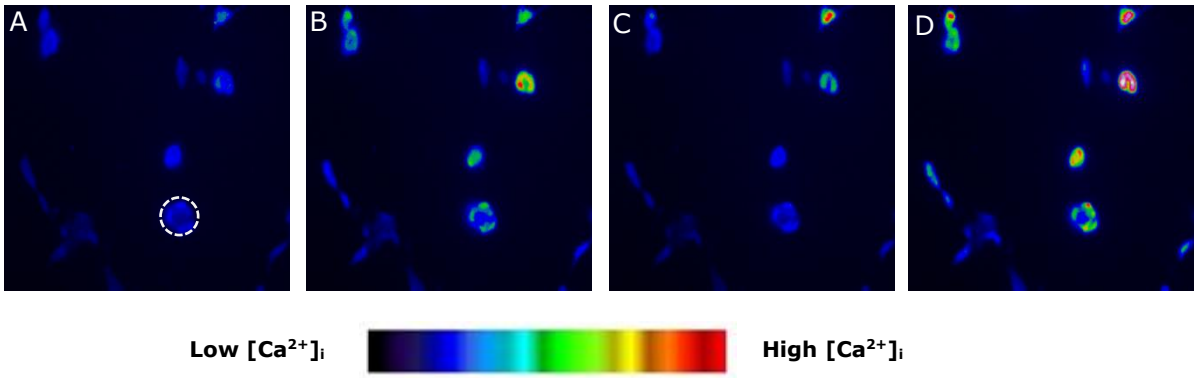

Figure 5.1: Fluorescent images for MIN6 cells show the response of cells to different treatments during one experiment. Intracellular Ca^{2+} levels represented as Fluo-4 fluorescence of the basal (A) and the effect of 10 mM glucose (B), 100 nM SRIF (C) and 50 mM K^+ (D). The white dashed circle in (A) denotes a region of interest (ROI).

As shown in figure 5.2A&B, there were variations in basal fluorescent levels among the selected ROIs (single cells and clusters) which were accompanied by variable responses to 10 mM glucose. However, most of the cells responded to treatments in the same manner. Three phases of response can be noticed after the exposure of cells to 10 mM glucose which started with a decrease in Ca^{2+} level for ~200 seconds. Then the second phase (peak formation) occurs when a rapid increase of the signal with spiking is followed by a gradual decrease for ~400 seconds. The third phase of the glucose effect appeared as a steady state with continuous spiking, see figure 5.2A&B. Perfusion of 100 nM SRIF solution provoked a rapid and significant decrease in calcium level accompanied by either cease or interruption of spiking as can be seen in figure 5.2A&C. On the other hand, the vehicle control (H_2O) neither affected the calcium level nor the signal spiking as appeared in figure 5.2B&D. 100 nM SRIF inhibited glucose stimulated Ca^{2+} influx by 23% in comparison to the vehicle control H_2O which stimulated Ca^{2+} entry by 3%, Mann-Whitney t test ($P<0.0001$, n=9-10). In the presence of 10 mM glucose, 100 nM SRIF had a magnitude of 18% more than the basal indicating that SRIF impaired but not completely blocked the stimulatory effect of glucose. However, the SRIF magnitude to basal is significantly less than that of vehicle control H_2O 54%, Mann-Whitney t test ($P<0.0001$, n=9-10). Lastly, perfusion of 50 mM K^+ Hank's to the bath produced a maximum increase of calcium level which consisted of the signal due to inactivation of K_{ATP} channels and plasma membrane depolarization.

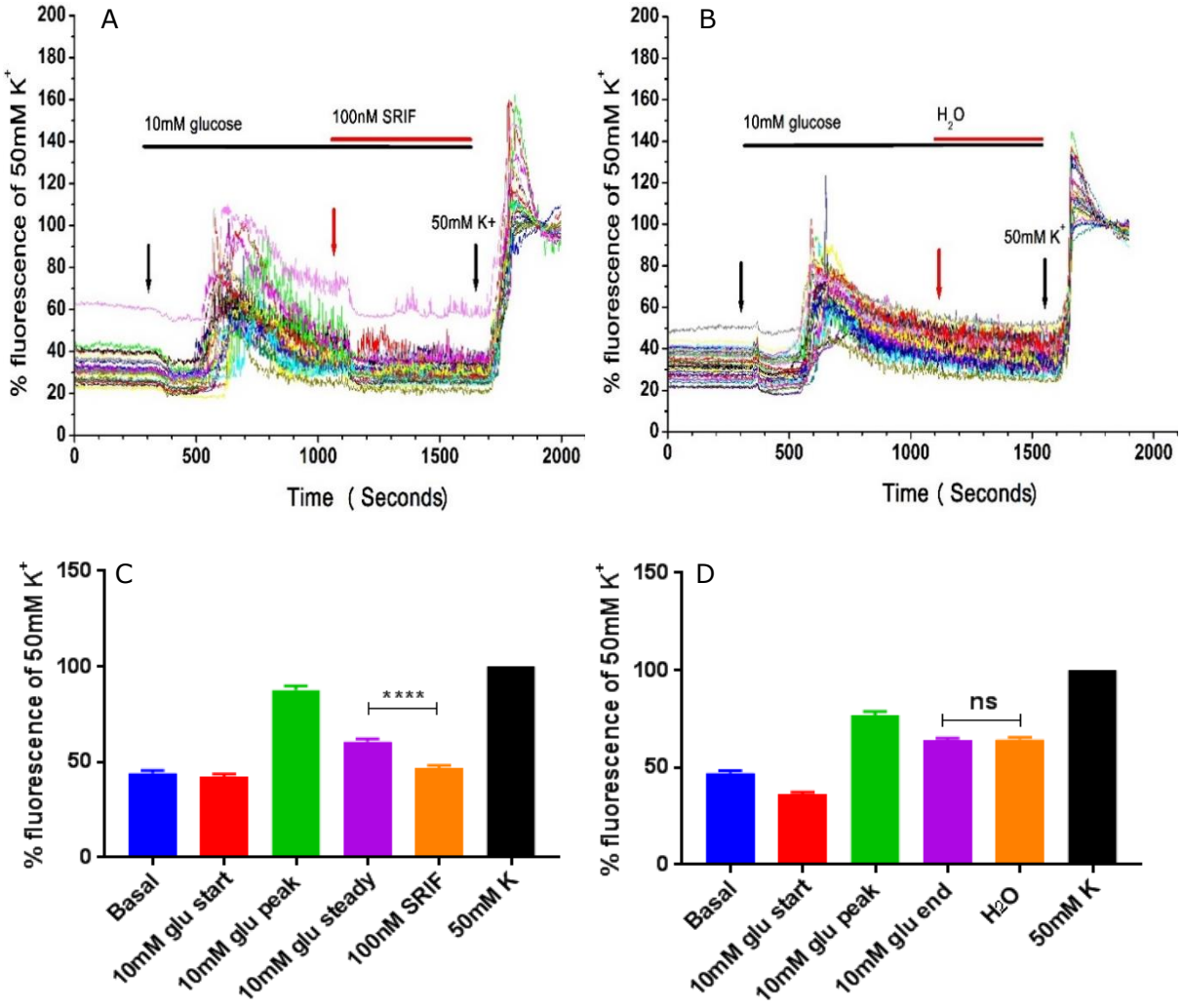

Figure 5.2: Intracellular Ca^{2+} levels as a percentage of 50 mM potassium Hank's for glucose, SRIF, and H_2O in MIN6 cells. Cells treated with glucose free Hank's for the first 300 seconds of each experiment and recorded as a basal. The representative traces (A) and (B) show three phases of response which can be noticed after perfusion of 10 mM glucose. Adding 100 nM SRIF with 10 mM glucose significantly inhibited Ca^{2+} entry as can be seen in (C) Friedman one way ANOVA test corrected with Dunn's multiple comparisons test ($p<0.0001$, n=10, ROIs=186). Vehicle control (H_2O) with 10 mM glucose had no effect on Ca^{2+} levels (D) Friedman one way ANOVA test corrected with Dunn's multiple comparisons test (n=9, ROIs=140). Arrows indicate the time of treatments.

An experiment was conducted to examine the effect of SRIF on basal Ca^{2+} in the absence of substrates. The basal fluorescence originates from the binding of Fluo-4 to cytoplasmic free Ca^{2+} ions which are physiologically maintained at around 100 nM in mammalian cells (Barrett et al., 2012, Clapham, 2007). Application of 100 nM SRIF significantly decreased basal fluorescence (Fig.5.3A&C), while the vehicle (H_2O) failed to affect basal fluorescence as seen in Fig.5.3B&D. In the presence of 100 nM SRIF, 10 mM glucose reversed the inhibitory effect of the peptide in the same manner (tri-phasic response) as previously demonstrated in the absence of the peptide, see Fig 5.2. The peak glucose stimulatory effect in the presence of 100 nM SRIF (84%) was significantly less than that of glucose

peak effect in the presence of H_2O (181%), Unpaired t test ($P<0.05$, n=3). Similar results observed with a steady state of glucose in the presence of SRIF (38%) which was significantly less than that of H_2O (80%) ($P<0.05$, Unpaired t test, n=3).

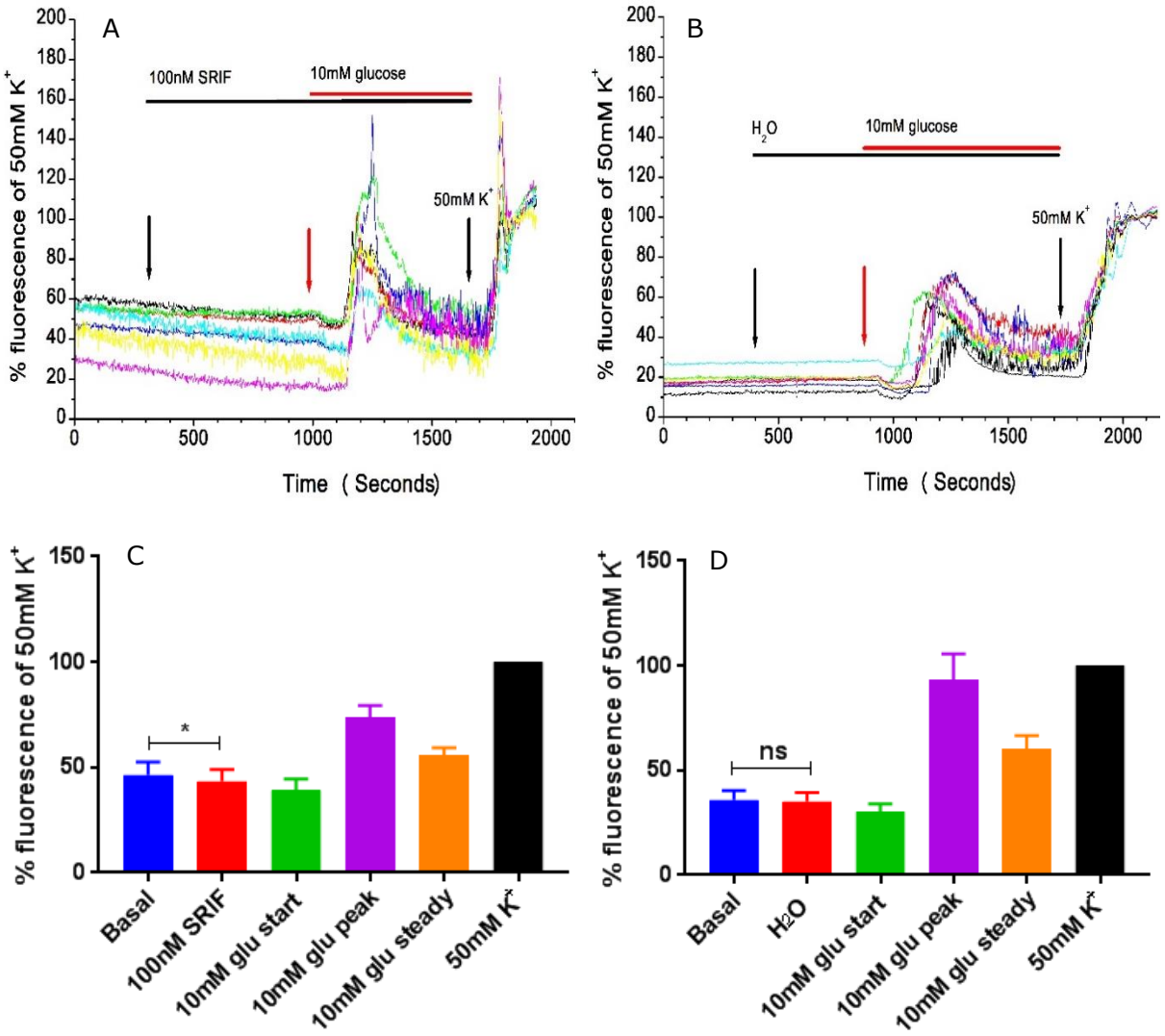

Figure 5.3: Intracellular Ca^{2+} levels as a percentage of 50mM potassium Hank's induced fluorescence for SRIF and H_2O followed by 10 mM glucose in MIN6 cells. Graphs (A) and (B) showed that 10 mM glucose stimulated Ca^{2+} entry and reversed the effect of both SRIF and vehicle control. 100 nM SRIF significantly inhibited basal Ca^{2+} level as shown in (C) RM one way ANOVA corrected with Holm-Sidak's multiple comparisons test ($p<0.05$, n=3, ROI=25). Unlike SRIF, the vehicle (H_2O) did not affect basal Ca^{2+} levels (D) RM one way ANOVA corrected with Holm-Sidak's multiple comparisons test (n=3, ROI=14).

5.3.2 PTX abolished the inhibitory effect of SRIF

This experiment was conducted to investigate whether the SRIF effect was mediated through PTX-sensitive Gαi/o proteins. MIN6 cells were incubated with 100 ng/ml PTX for 18-24 h (Yoshitomi et al., 1997) and basal Ca^{2+} fluorescence was recorded in glucose free

Hank's medium. The basal percentage fluorescence of PTX treated cells (42%) was comparable with the baseline level of non-treated cells (46%) (Unpaired t test, n=3). Cells incubated with PTX responded to 10 mM glucose and 50 mM K^+ treatments similarly to non-incubated cells, however, 100 nM SRIF did not affect the intracellular Ca^{2+} levels as can be noticed in (Fig. 5.4A&B). This result indicates that SRIF inhibited Ca^{2+} mobilisation by a Gαi/o protein dependent pathway.

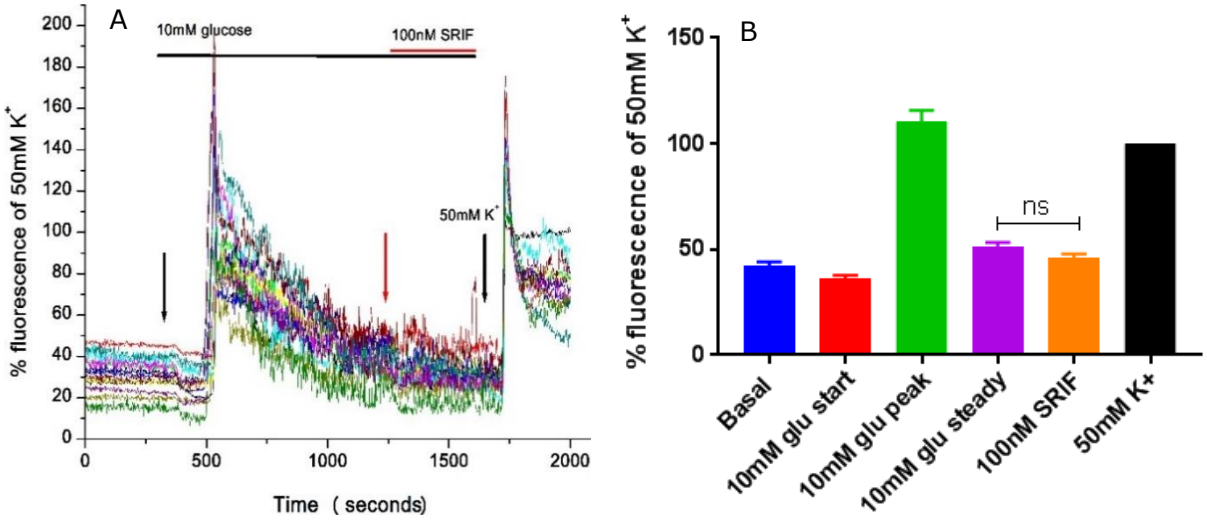

Figure 5.4: Intracellular Ca^{2+} levels as a percentage of 50 mM K^+ Fluo-4 fluorescence for glucose and SRIF in MIN6 cells incubated with 100 ng/ml PTX. Cells were treated with 100 ng/ml PTX for 18-24 hours before conducting the experiments. 10 mM glucose showed similar effect to cells not treated with PTX (A). As can be seen in graph (B), PTX abolished the inhibitory effect of 100 nM SRIF on calcium influx, Friedman one way ANOVA test corrected with Dunn's multiple comparisons test (n=3, ROIs=39).

5.3.3 SRIF inhibits KIC stimulated calcium entry

A direct mitochondrial fuel, KIC, was used to exclude the possible sequence effect of SRIF on glycolysis or glucose uptake that might be reflected on the mitochondria. 10 mM KIC stimulated Ca^{2+} entry in a similar manner to that of glucose, three phases of response and signal spiking can be recognised as shown in Fig. 5.5A&B. The steady state level of 10 mM KIC stimulation of basal (43%) was not different from that of 10 mM glucose 59%, (Mann Whitney t test, n=3). 100 nM SRIF significantly inhibited KIC stimulated Ca^{2+} levels (Fig. 5.5C) and the signal spiking discontinued (Fig. 5.5A). The vehicle control H_2O did not change the KIC stimulated Ca^{2+} entry as in figure 5.5B&D. The magnitude of SRIF inhibition of KIC stimulated Ca^{2+} influx (~26%) was significantly more than that achieved by 10 mM glucose (23%) (Mann Whitney t test, $P<0.05$, n=3).

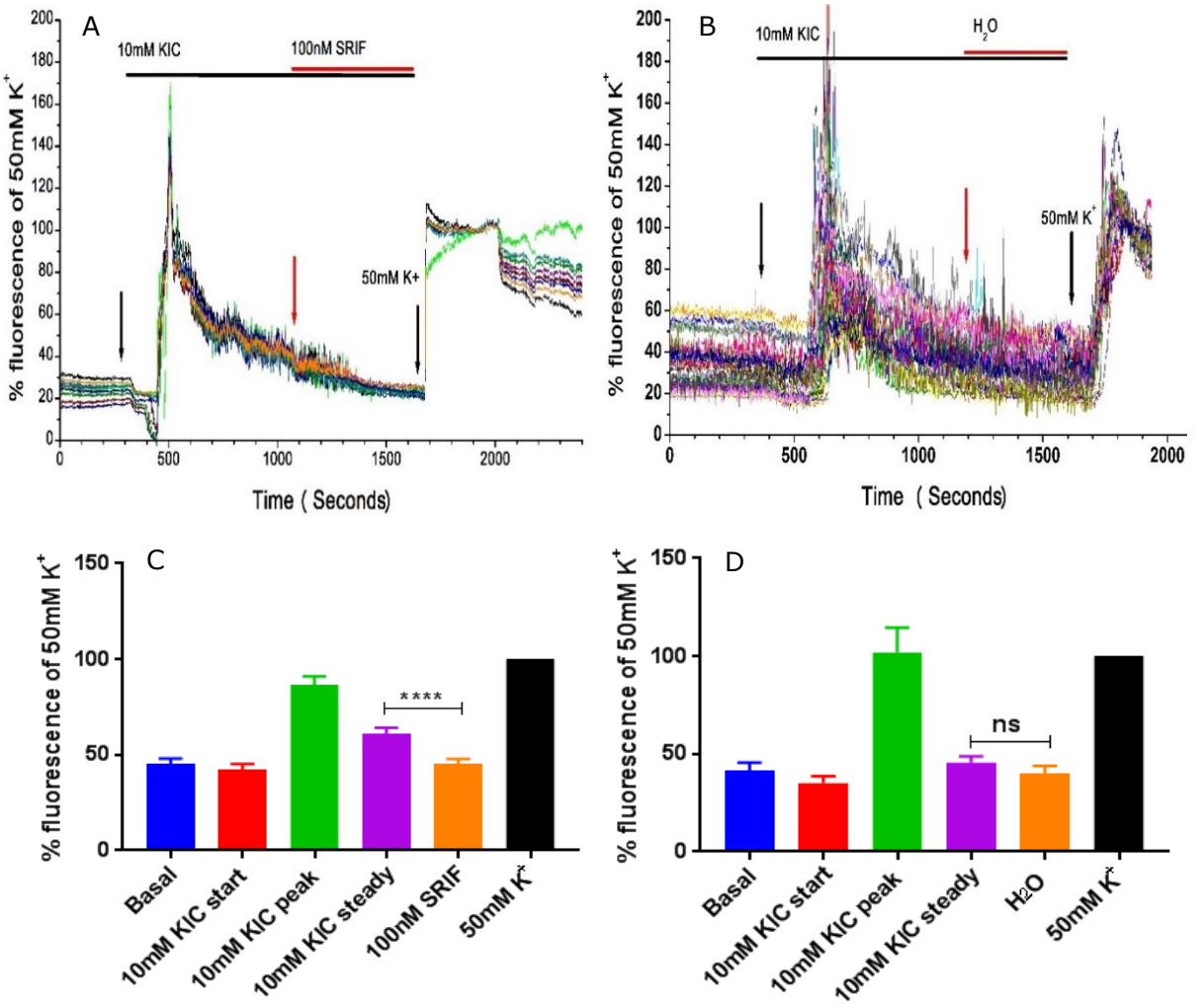

Figure 5.5: Intracellular Ca^{2+} levels as a percentage of K^+ Fluo-4 fluorescence for KIC, SRIF and vehicle (H_2O) in MIN6 cells. 10 mM KIC showed a similar response to 10 mM glucose which can be noticed in graph (A) and (B). 100 nM SRIF significantly inhibited KIC stimulated Ca^{2+} entry as shown in (C) Friedman one way ANOVA test corrected with Dunn's multiple comparisons test ($p<0.0001$, n=7, ROIs=50). While the vehicle control (H_2O) had no effect on Ca^{2+} levels (D) Friedman one way ANOVA test corrected with Dunn's multiple comparisons test (n=3, ROIs=27).

5.3.4 SRIF and dbcAMP inhibited glucose stimulated calcium entry.

To test the hypothesis claimed that SRIF action is mediated by cAMP, experiments were performed in the presence of excess intracellular cAMP, to investigate if the effect of SRIF on Ca^{2+} was mediated by a reduction in cAMP. At first, forskolin was used to stimulate the production of cAMP, but because the vehicle (DMSO) exerted a similar effect to that of

forskolin, these data were excluded (data not shown). As an alternative, the cell permeable cAMP analogue dbcAMP was used to mimic the elevation of intracellular cAMP levels (Yaekura and Yada, 1998). Surprisingly 1 mM dbcAMP significantly inhibited glucose stimulated Ca^{2+} entry ($P<0.01$, $n=3$) as shown in figure 5.6C, however it did not affect the signal spiking (oscillation) (Fig. 5.6A). Further inhibition of Ca^{2+} levels were achieved on the addition of 100 nM SRIF in the presence of 1 mM dbcAMP (Fig. 5.6A&C). Similar to previous results, the vehicle H_2O had no effect on glucose stimulated Ca^{2+} entry. Although the inhibitory effect of 100 nM SRIF, when combined with the vehicle, was more obvious than that with dbcAMP, they were not significantly different, (Unpaired t test, $n=3$) this can be noticed in figure 5.6A&B. The inhibitory effect of SRIF in the presence of dbcAMP (15%) was significantly less than that of SRIF alone (23%), (Mann Whitney t test, $P<0.01$, $n=3$).

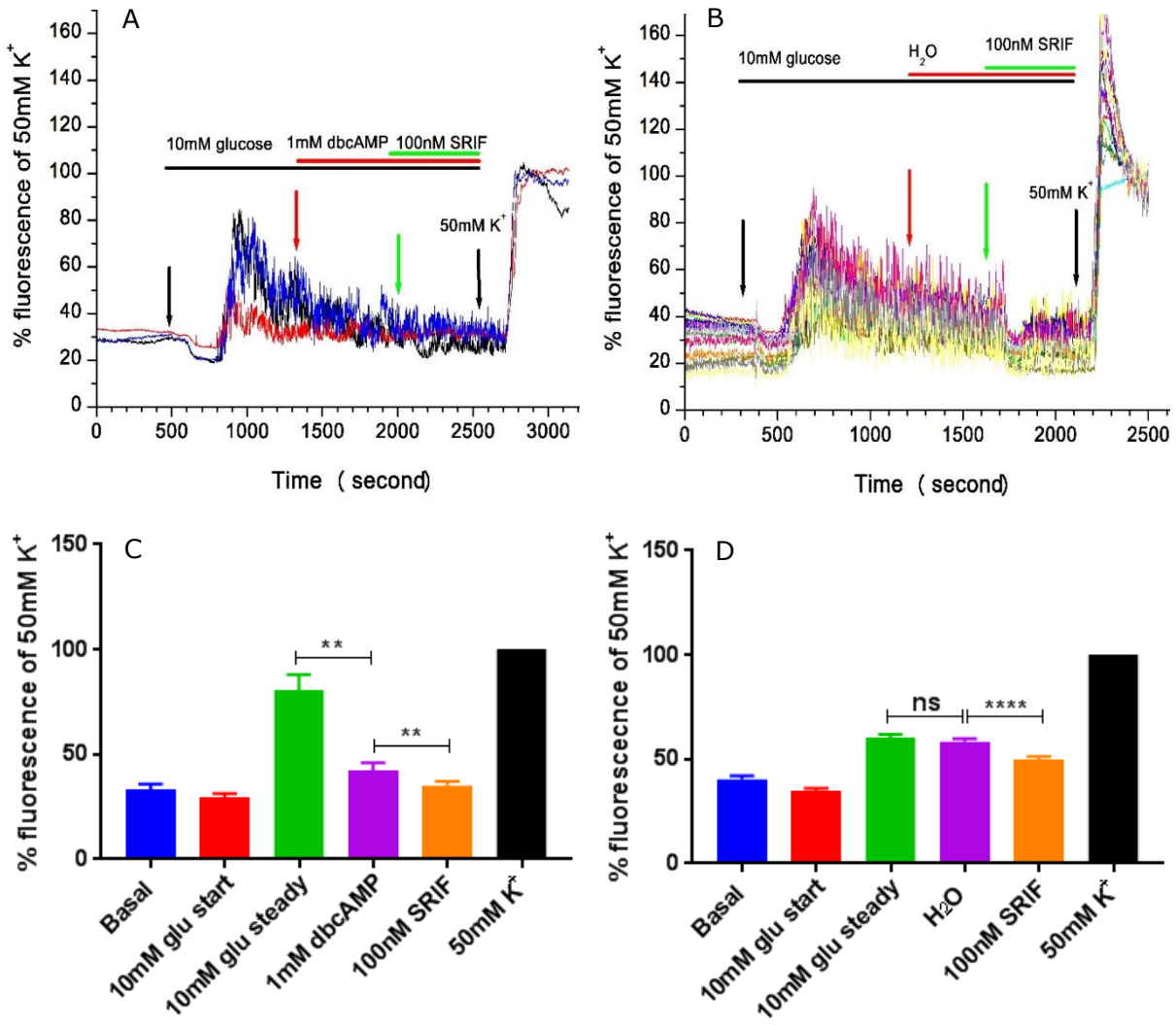

Figure 5.6: Intracellular Ca^{2+} levels as a percentage of 50 mM K^+ Fluo-4 fluorescence for glucose, 1 mM dbcAMP, vehicle (H_2O) and SRIF in MIN6 cells. 1 mM dbcAMP significantly inhibited glucose stimulated Ca^{2+} entry, in addition SRIF inhibited glucose stimulation in the presence of dbcAMP as in (A) and (C) RM one way ANOVA test corrected with Sidak's multiple comparisons test ($P<0.01$, n=3, ROIs=14). In (B) and (D) vehicle H_2O did not affect Ca^{2+} entry while SRIF significantly inhibited Ca^{2+} levels Friedman one way ANOVA test corrected with Dunn's multiple comparisons test ($p<0.0001$, n=3, ROIs=54).

5.3.5 SRIF inhibited calcium levels stimulated by glucose and tolbutamide

This experiment was done to examine if the SRIF action was mediated by activation of K_{ATP} channels. Basal fluorescence was recorded for 300 s followed by the addition of 10 mM glucose which showed a significant increase in basal Ca^{2+} influx. Next 200 µM tolbutamide was added with glucose and a further peak in Ca^{2+} levels was noticed which can be seen in Fig. 5.7A. This increment was expected because there is an additive but not synergistic effect of glucose and tolbutamide on K_{ATP} channels (Trube et al., 1986). However, the

steady Ca^{2+} level for 200 μM tolbutamide was insignificant from that of 10 mM glucose, (Mann Whitney t test, n=3) as seen in figure 5.7C. Although DMSO 0.1% (Vol/Vol) significantly inhibited glucose stimulated Ca^{2+} entry as seen in Figure 5.7D. However, it seems that the effect of tolbutamide is more powerful than that of DMSO to inhibit it on membrane channel activity because tolbutamide was still able to potentiate the effect of glucose. Figure 5.7 shows that 100 nM SRIF significantly inhibited Ca^{2+} levels in the presence of both tolbutamide and DMSO. This result confirms the notion that K_{ATP} channels are not the sole target of SRIF action since they are presumed blocked to fully activate β-cell electrical activity. Therefore, other channels e.g. GIRK and/or VGCCs are considered as potential targets of SRIF action. The percentage inhibition of SRIF in the presence of tolbutamide (21%) was not significantly different from that in the presence of DMSO (17%) (Mann-Whitney t test, n=3).

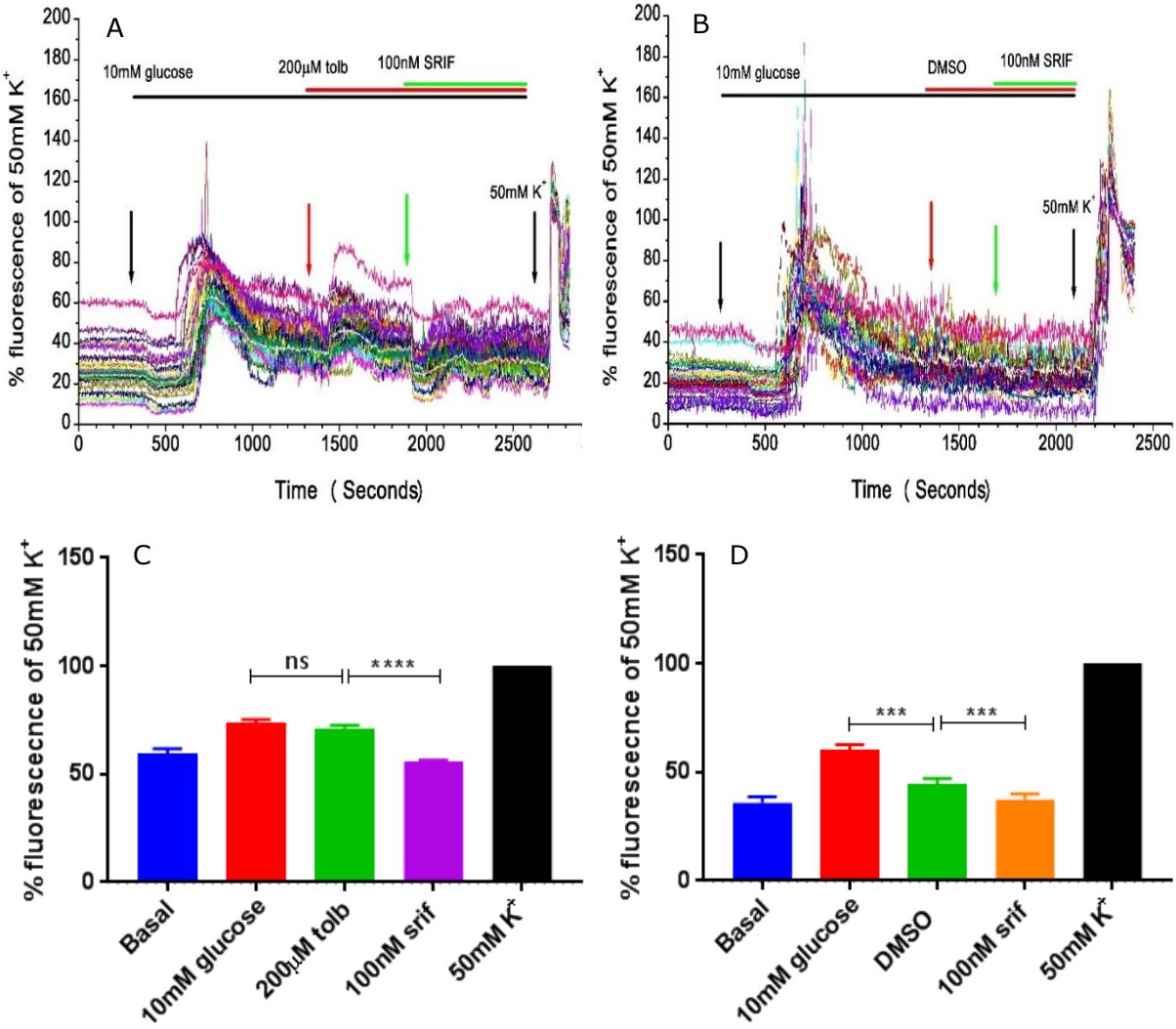

Figure 5.7: Intracellular Ca^{2+} levels as a percentage of 50 mM K^+ Fluo-4 fluorescence for glucose, 200 µM tolbutamide, vehicle (DMSO) and 100 nM SRIF in MIN6. (A) 200µM tolbutamide maintained the glucose stimulated Ca^{2+} entry. In graph (C) and (D) the bars of glucose, tolbutamide and DMSO are representing the steady state fluorescence. 100 nM SRIF significantly inhibited tolbutamide stimulated Ca^{2+} entry as shown in (C) Friedman one way ANOVA test corrected with Dunn's multiple comparisons test ($p<0.0001$, n=6, ROIs=186). DMSO 0.1 µl/ml (V/V) significantly decreased glucose stimulated Ca^{2+} entry Friedman one way ANOVA test corrected with Dunn's multiple comparisons test ($p<0.001$, n=3, ROIs=68) as shown in (B) and (D). The same graphs show that 100 nM SRIF significantly inhibited Ca^{2+} level of DMSO, Friedman one way ANOVA test corrected with Dunn's multiple comparisons test ($p<0.001$, n=3, ROIs=68).

5.3.6 SRIF inhibited calcium levels stimulated by glucose and tertiapin LQ

To investigate the role of GIRKs in SRIF mode of action, the basal and 10 mM glucose fluorescence were recorded before 100 nM tertiapin LQ that is a selective $K_{ir}1.1$ channel blocker. It was found that 100 nM tertiapin LQ did not affect the steady state of Ca^{2+} fluorescence produced by 10 mM glucose as in Fig. 5.8A&C. Similar to the previous experiments, the vehicle of tertiapin (H_2O) also did not change the Ca^{2+} level see figure

5.8B. The graphs (C) and (D) showed that 100 nM SRIF significantly inhibited the Ca^{2+} level of both tertiapin LQ and H_2O treated cells, even though the inhibition by SRIF was significantly less in magnitude in case of tertiapin-LQ (12%) than that of H_2O (20%), (Mann-Whitney t test, P<0.001, n=3-4).

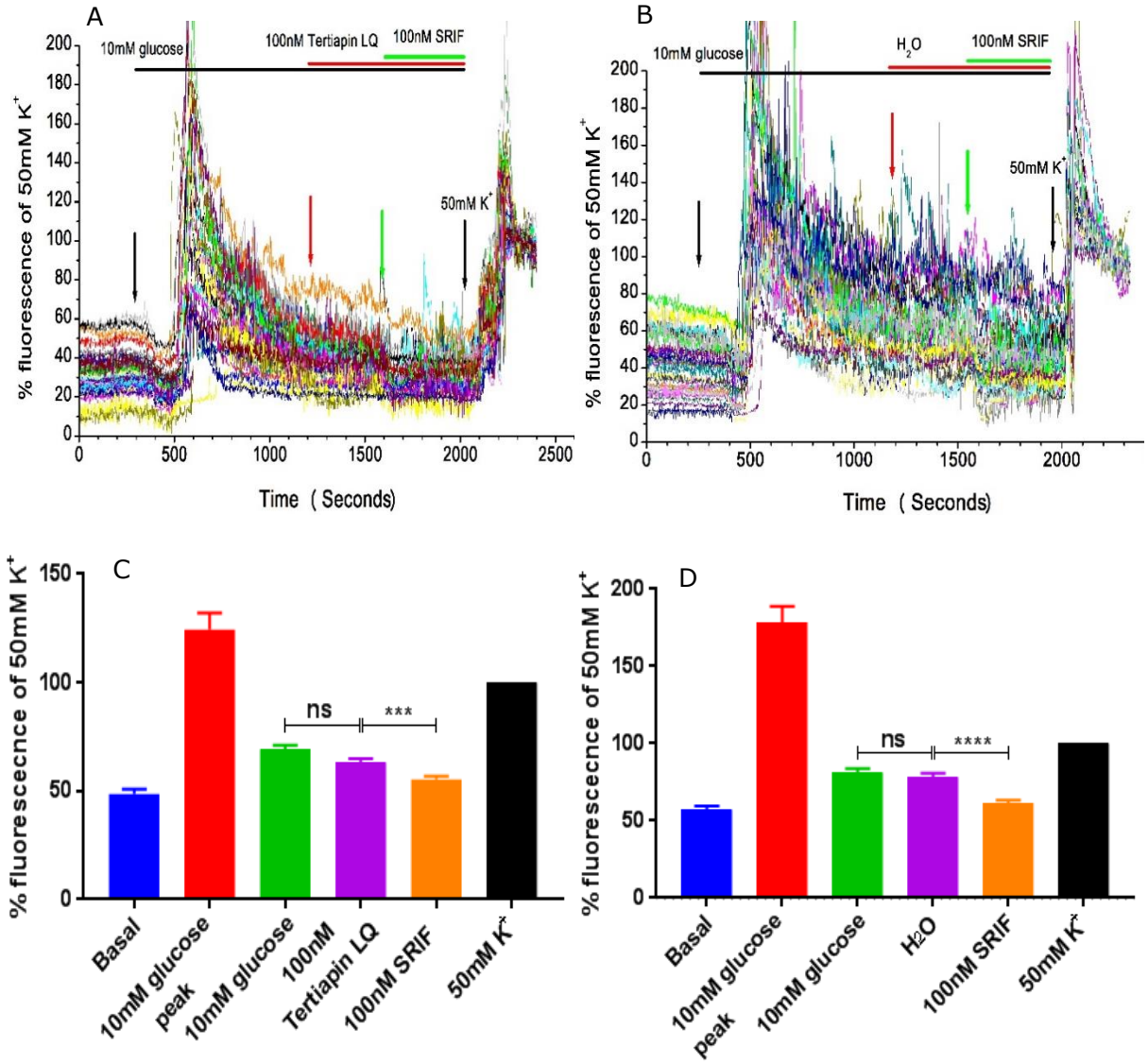

Figure 5.8: Intracellular Ca^{2+} levels as a percentage of 50 mM K^+ Fluo-4 fluorescence for glucose, 100 nM Tertiapin LQ, vehicle (H_2O) and 100 nM SRIF in MIN6. In (A) and (B) 10 mM glucose stimulates Ca2+ influx while neither 100 nM tertiapin LQ (A) nor its vehicle H_2O (B) were affected glucose stimulated Ca^{2+} level. 100 nM SRIF significantly inhibited Ca^{2+} levels of tertiapin LQ treated cells (C) Friedman one way ANOVA test corrected with Dunn's multiple comparisons test (p<0.001, n=4, ROIs=82) and also of H_2O treated cells (D) Friedman one way ANOVA test corrected with Dunn's multiple comparisons test (p<0.0001, n=3, ROIs=70).

5.3.7 SRIF inhibited calcium levels stimulated by glucose, tolbutamide & tertiapin LQ

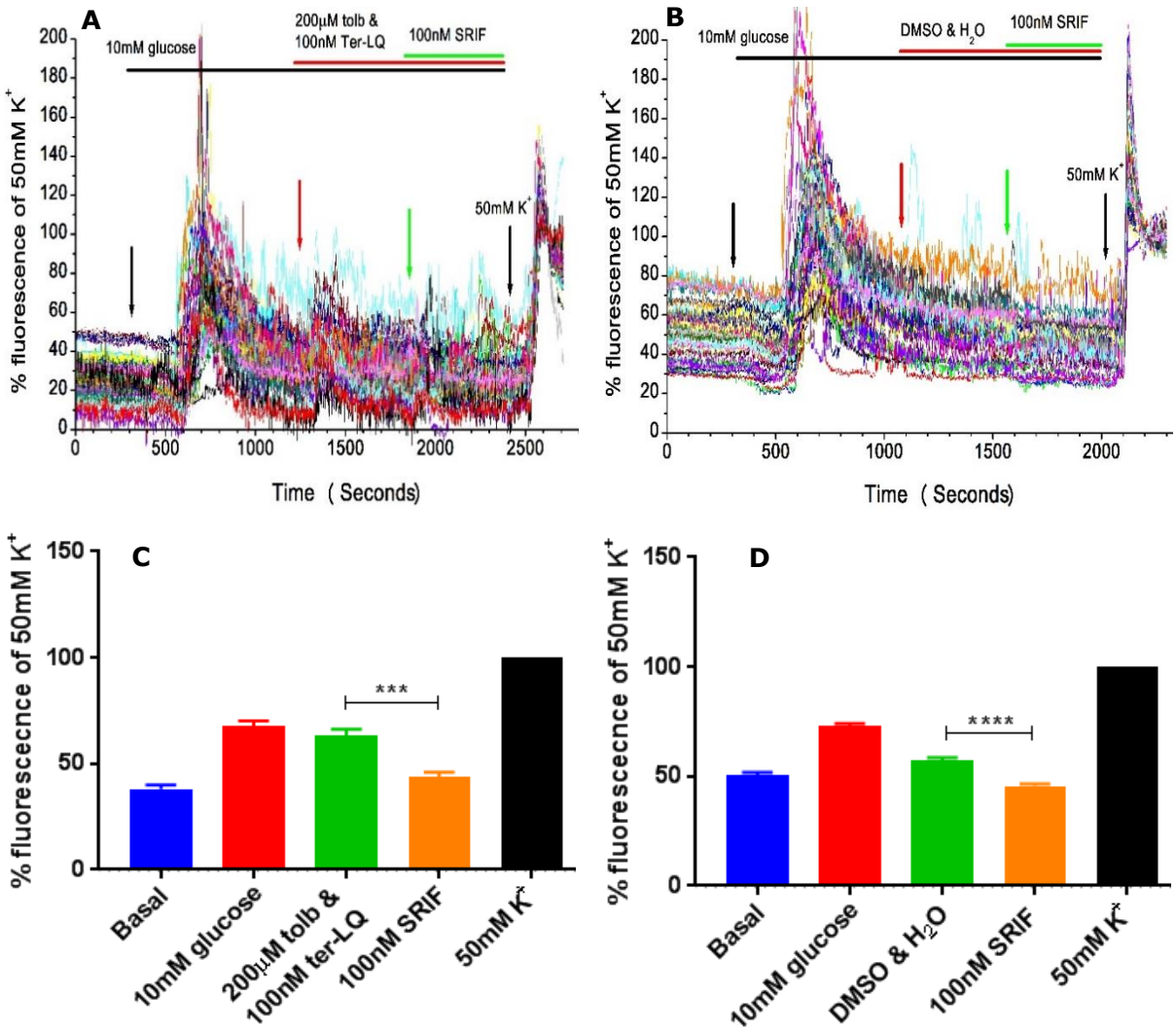

Figure 5.9: Intracellular Ca^{2+} levels as a percentage of 50 mM K^+ Fluo-4 fluorescence for glucose, SRIF tolbutamide (tolb) and tertiapin LQ (ter-LQ), and their vehicles (DMSO and H_2O) in MIN6 cells. In (A) and (B) 10 mM glucose stimulated Ca^{2+} influx but the combination of 200 µM tolb and 100 nM ter-LQ showed further peak of stimulation of Ca^{2+} entry (A) while the combination of vehicles 0.1% V/V DMSO and H_2O did not as shown in (B). In (C) 100 nM SRIF has significantly inhibited Ca^{2+} levels of cells treated with the combination of tolb and ter-LQ, Friedman one way ANOVA test corrected with Dunn's multiple comparisons test ($p<0.001$, n=4, ROIs=81). (D) SRIF has also inhibited calcium levels of the cells treated with vehicles, Friedman one way ANOVA test corrected with Dunn's multiple comparisons test ($p<0.0001$, n=4, ROIs=184).

The role of VGCC channels as a target for SRIF action was investigated by simultaneously blocking both K_{ATP} and GIRK K^+ channels. To achieve that, a combination of 200 µM tolbutamide and 100 nM tertiapin LQ were used and they were added after 1200 second of basal and 10 mM glucose recording. As can be seen in figure 5.9A, the response

appeared as a peak similar to that achieved by 200 μM tolbutamide alone identified in 5.4.5 and shown in figure 5.7A. The percentage effect of the combination of (tolb. & ter-LQ) on glucose stimulated Ca2+ influx (7%) was insignificant from either that achieved by tolb alone 0.5% (Mann-Whitney t test, n=3-4) or by ter-LQ alone 6% (Mann-Whitney t test, n=3-4). The combination of vehicles decreased the glucose stimulated Ca^{2+} levels but it was not statistically significant. 100 nM SRIF significantly inhibited glucose stimulated Ca^{2+} level produced by the combination of K^{+} channel blockers by 28 % and the combination of their vehicle by 22% (Fig. 5.9C&D) (Mann-Whitney t test, $P<0.0001$, n=4).

5.3.8 Effect of SRIF and glucose in Ca^{2+} free condition

To investigate the action of SRIF on extracellular Ca^{2+} influx and Ca^{2+} mobilisation from intracellular stores in MIN6 cells. In calcium free conditions (A), basal fluorescence recorded for 300 s was comparable to the baseline of Ca^{2+} containing conditions (B). As can be seen in Fig. 5.10 A, in the absence of extracellular Ca^{2+} 10 mM glucose failed to achieve the typical tri-phasic response as seen in the presence of extracellular Ca^{2+} Fig. 5.10B. In Ca^{2+} containing conditions, the signal rapidly decreased after replacement of the Ca^{2+} containing Hank's with Ca^{2+} free Hank's (Fig. 5.10B&D). As can be noticed from Fig. 5.10A&B, 100 nM SRIF did not affect the fluorescent signal in Ca^{2+} free conditions. This experiment provides evidence that changes in Ca^{2+} levels produced by SRIF depend on changes in ion influx from the extracellular fluid rather than from the intracellular stores.

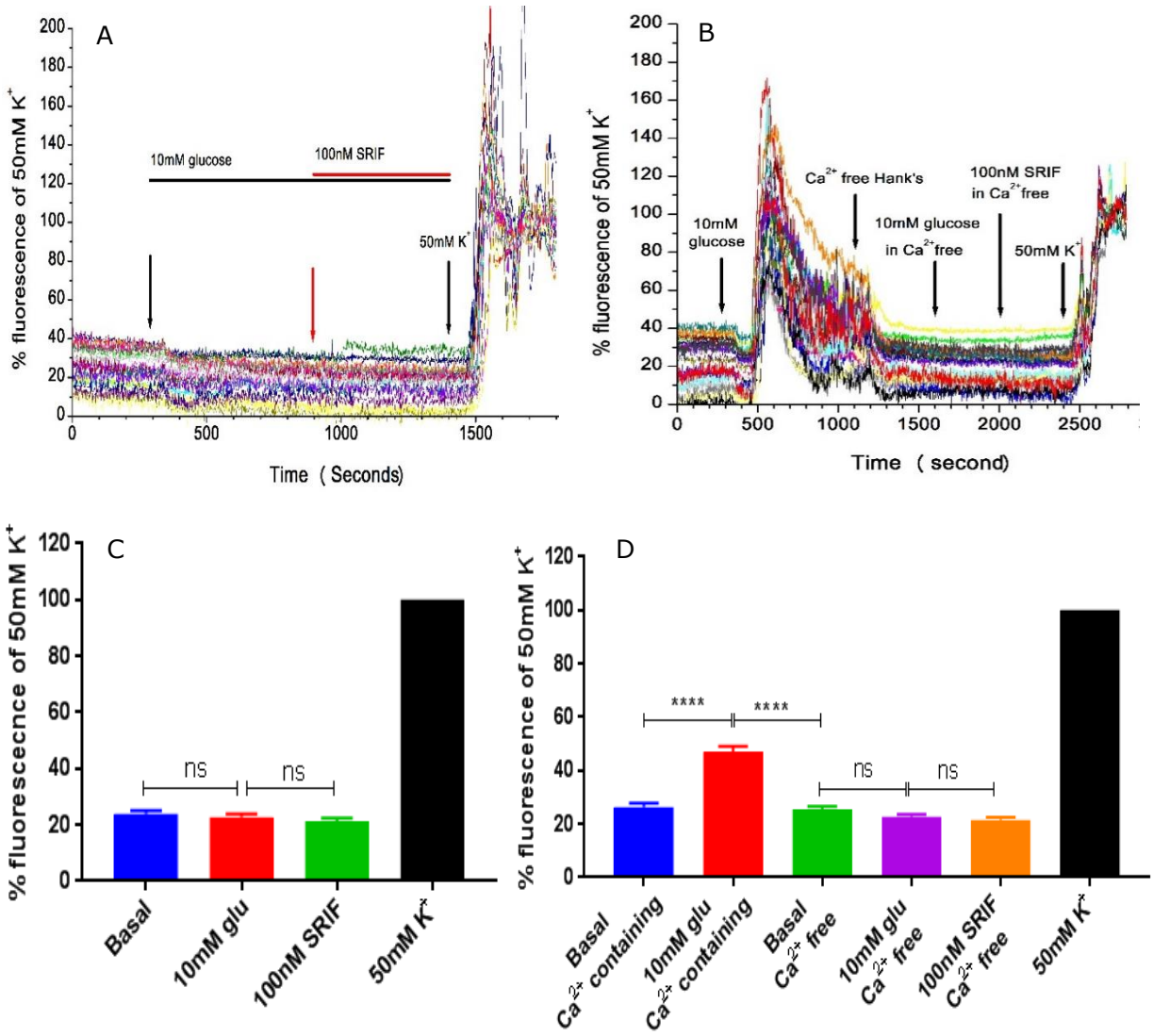

Figure 5.10: Intracellular Ca^{2+} levels as a percentage of 50 mM K^+ Fluo-4 fluorescence for glucose and SRIF prepared with Ca^{2+} free Hank's in MIN6. (A) and (C) show cells did not respond to 10 mM glucose or to 100 nM SRIF in the absence of extracellular calcium except for 50 mM K^+ which contains Ca^{2+} RM one way ANOVA corrected with Sidak's multiple comparisons test (n=3, ROIs=101). Graphs (B) and (D) show that removing of extracellular calcium lead to abolish the stimulatory effect of glucose prepared with Ca^{2+} containing Hank's RM one way ANOVA corrected with Tukey's multiple comparisons test ($p<0.0001$, n=3, ROIs=59).

5.4 Discussion

This study demonstrated the effectiveness of SRIF in controlling Ca^{2+} influx into pancreatic β-cells. The peptide inhibited Ca^{2+} influx in the presence of different substances such as 10 mM glucose, 10 mM KIC, 1 mM dbcAMP, 200 μM tolbutamide and 100 nM tertiapin LQ. MIN6 cells responded to glucose and to the mitochondrial fuel KIC as a tri-phasic response. This result is consistent with previous studies on mouse β-cells which also showed that glucose produces three phases of response (Nakagawa et al., 2015). The rapid increase in

glucose concentration initiates with a short (~200 seconds) decrease in $[Ca^{2+}]_i$ below the baseline followed by a sharp peak which ended up with a sustained plateau accompanied by signal oscillations (Roe et al., 1994a, Roe et al., 1994b, O'Neill et al., 2013). One theory to explain glucose induced Ca^{2+} reduction in mouse B-cells might be due to pumping of Ca^{2+} to the ER via the Sarcoplasmic ER Ca^{2+} ATPase (SERCA) (Roe et al., 1994a, Chow et al., 1995) because the reduction in cytoplasmic $[Ca^{2+}]_i$ was concomitant with an increase of $[Ca^{2+}]_i$ in ER (Tengholm et al., 2001, Ravier et al., 2011). Although the mechanism by which Ca^{2+} is mobilised from the cytoplasm to ER is known, however, this might happen in order to drive the Ca^{2+} toward the mitochondria. Consequently, the reduction in Ca^{2+} level in the first phase of glucose effect could be as a result of the mitochondrial uptake of some cytosolic Ca^{2+} via mitochondrial Ca^{2+} uniporter (MCU) during energy production process induced by fuels (Tarasov et al., 2012a, Tarasov et al., 2012b, Tarasov et al., 2013).

On the other hand, the 2nd phase, the rapid increase of Ca^{2+} is happening due to an increased ATP/ADP ratio which blocked K_{ATP} channels and opened the VGCCs allowing Ca^{2+} to influx from the extracellular space. Therefore, removing extracellular Ca^{2+} led to a failure of glucose to exert the tri-phasic response as can be seen in figure 5.10A. This is an indication that glucose stimulated the increase of intracellular Ca^{2+} levels initially depends on Ca^{2+} influx from the extracellular solution rather than the release of stored Ca^{2+}. It is believed that release of stored Ca^{2+} from intracellular organelles such as endoplasmic reticulum and mitochondria might play a limited role in the glucose stimulated electrical activity, since the release of Ca^{2+} from these stores is controlled either by inositol trisphosphate (IP_3) receptors or by ryanodine receptors which are responsible for calcium induced calcium release (CICR) mechanism (Santulli and Marks, 2015).

It is well established that the action of SRIF on excitable cells is via activation of different SSTRs which activate PTX-sensitive G proteins (Gαi/o) signaling cascade and leading in part to inhibition of Ca^{2+} influx. In line with this hypothesis, findings of (Yamashita et al., 1987, Tedford and Zamponi, 2006), in addition to this study are confirming the involvement of PTX-sensitive G proteins in the SRIF inhibitory action of VGCCs. These results are incompatible with those of a previous study on MIN6 cells (Smith, 2009) which also suggested that SRIF inhibits Ca^{2+} influx but via a PTX insensitive pathway.

In addition to its ability to inhibit glucose stimulated Ca^{2+} entry in MIN6 cells, SRIF also decreased Ca^{2+} levels at a resting plasma membrane potential in the absence of the sugar (Fig. 5.3). These actions of the peptide suggest activation of K^+ conductance which consequently leads to decrease Ca^{2+} levels. However, this SRIF effect was abolished by either adding a high K^+ solution or by introducing 10 mM glucose, which blocked the K^+ conductance and depolarised the membrane. These results suggest that the inhibitory action of SRIF on membrane electrical activity is surmountable. These results are in general agreement with a previous study on pituitary tumour cells conducted by (Mollard et al., 1988) using the patch clamp technique. They showed that SRIF induced K^+ conductance activated at the level of the resting potential and this action was diminished by washing out the peptide and introduction of ATP to the cells. The same study also suggested that 100 nM SRIF reduced the voltage dependent Ca^{2+} current. Furthermore, another fluorescence study on GH pituitary cells showed similar findings (Koch et al., 1988). These data are in disagreement with those of (Hsu et al., 1991) who indicated that 100 nM SRIF inhibited VGCC but without influence on K^+ currents which was measured by $^{86}Rb^+$ method in HIT pancreatic β-cells. On the other hand, (Dawson et al., 1986) suggested that even though $^{86}Rb^+$ is an acceptable isotope for studying K^+ channels, however, there are still differences between $^{86}Rb^+$ and K^+ selectivity at K^+ channels. Results of this study and many other studies emphasize that SRIF hyperpolarizes the plasma membrane and blocks Ca^{2+} influx of β-cells and other excitable cells via activation of K^+ channels. SRIF was shown to hyperpolarize the membrane potential and inhibit glucose induced electrical activity in the presence of tolbutamide (K_{ATP} channel blocker) as in figures 5.7. In support of this result, one of the most recent works on pancreatic β-cells has documented the effectiveness of SRIF in controlling glucose stimulated Ca^{2+} influx in the presence of tolbutamide (Hellman et al., 2018). The persistent action of SRIF in the presence of the K_{ATP} channel blocker indicating the involvement of another type of K^+ channels, most likely GIRK channel. Therefore, this hypothesis was examined using tertiapin-LQ a selective GIRK channel blocker and the results were compatible with prior studies on human pancreatic β-cells (Kailey et al., 2012) and murine pancreatic β-cells (Smith et al., 2001) which revealed the contribution of GIRK channel as a target of SRIF in modulation of plasma membrane

electrical activity. Interestingly, SRIF hyperpolarized the plasma membrane in the presence of a combination of tolbutamide and tertiapin-LQ. Since the K_{ATP} and GIRK channels were occupied with tolbutamide and tertiapin LQ respectively, it was expected that SRIF inhibitory effect on electrical activity could be prevented based on the assumption that SRIF is exclusively coupling to and activating of K^+ channels. Although the action of SRIF was attenuated, it still was significant, data that support the hypothesis of other channels such as VGCCs involvement in its action (Smith, 2009).

According to the study of (Landa et al., 2005), there is an interaction between Ca^{2+} and cAMP signaling pathway in MIN6 cells. Since cAMP was suggested as a possible second messenger for mediating SRIF actions (Ribalet and Eddlestone, 1995), the effects of SRIF on $[Ca^{2+}]_i$ in the presence of high cAMP levels have been examined. 1 mM dbcAMP significantly inhibited glucose stimulated Ca^{2+} elevation as in fig. 5.6.C. This action could be due to activation of SERCA induced by elevation of cAMP (1 mM dbcAMP) which leads to Ca^{2+} sequestration into ER stores (Yaekura and Yada, 1998). The inhibitory effect of SRIF in the presence of dbcAMP (15%) was less than that in the absence of the latter (23%), (Mann Whitney t test, $P<0.01$, $n=3$). The reasons were possibly because the inhibitory effect of dbcAMP preceded the action of SRIF. Since SRIF significantly inhibited Ca^{2+} influx in the presence of high cAMP level, these results suggest that the inhibitory effects of SRIF on Ca^{2+} are not mediated by suppression of cAMP levels as previously reported (Hsu et al., 1991).

Considering the molecular differences between mouse and human β-cells, an attempt to study the effect of SRIF on the human pancreatic cell line (1.1B4) has been done. However, unfortunately unlike MIN6, the 1.1B4 was poorly loaded with the Fluo-4 AM dye under the same incubation conditions, making the imaging process awkward and inadequate. Fluo-4 AM malabsorption may have occurred due to the development of multi-drug resistance (MDR) transporters (Higgins, 2007) at least in these patches of 1.1B4 cells. So that it is recommended to repeat the work with different human cell line such as EndoC-βH1 (Andersson et al., 2015).

Chapter Six:
General Discussion

6.1 Discussion

Attempts were made in previous studies to discover the mechanisms by which SRIF inhibits insulin secretion. However, only a few studies focused on the effects of SRIF on the mitochondrial metabolism and or glycolysis in pancreatic β-cells e.g. Daunt et al. (2006) who investigated the effect of SRIF on oxidative respiration of pancreatic β-cells. In this thesis, I set out to investigate further the effect of SRIF on the mitochondrial function by measuring the rate of O_2 consumption, mitochondrial membrane potential (Rh123) and ATP production. Second, I investigated the effect of SRIF on the rate of glucose uptake and glycolytic flux by measuring the rate of lactate production. Third, I investigated the functional effect of SRIF by measuring calcium influx into pancreatic β-cells MIN6.

Pancreatic β-cells are electrically excitable cells and respond to different concentrations of glucose and other stimulatory factors (Gilon et al., 2014, Rorsman, 1997). The cells require oxygen for glucose and other nutrients to be metabolised in the mitochondria to produce ATP. Measurement of oxygen consumption rate as an indicator for β-cell oxidative metabolism and subsequently, insulin secretion has been previously examined (Porterfield et al., 2000). My study showed that 10 mM glucose significantly stimulated basal oxygen consumption in MIN6 cells (10 nmol O_2 10^7 $cell^{-1}$ min^{-1}), which is comparable to that previously published (Daunt et al., 2006, Soejima et al., 1996). In MIN6 cells, the effect of glucose was found to be reversely correlated with basal OCR ($r=0.98$, $P<0.0001$, $n=32$). The mitochondrial basal OCR is adjusted to provide the cellular demand for energy. However, under certain circumstances such as excessive free fatty acid metabolism, basal oxygen consumption is increased (Cheng et al., 2012). In an attempt to find out if SRIF is able to inhibit basal respiration of β-cells in the absence of glucose, where cells depend on endogenous amino acids and/or free fatty acids metabolism. The fatty acids undergoes metabolism in peroxisomes to produce metabolites e.g. acetyl-CoA in the process of β-oxidation (Yoshikawa et al., 2001). These metabolites are then metabolized in the mitochondria to produce ATP. In this study, we found that SRIF blocked basal respiration by 43%, a finding consistent with that previously reported (Daunt et al., 2006) where SRIF reduced basal respiration by 30%. Consistent with this, I found that SRIF inhibited OCR

stimulated by the direct mitochondrial fuel KIC. However, this is in disagreement with the same above study, who found that SRIF did not change OCR stimulated by direct mitochondrial fuels such as methyl pyruvate and KIC on MIN6 cells. These results, therefore, indicate that the peptide can act on the mitochondria and more specific on TCA level. The possible explanation is SRIF inhibits NADH and FADH2 provided from TCA that is reflected on the oxidative respiration. The peptide might inhibit the effect of NADH oxidase producing less NADH from TCA to donate electrons to the ETC.

SRIF inhibited glucose stimulated OCR in MIN6 cells similar to the findings of Daunt et al., (2006) who concluded that SRIF might inhibit mitochondrial metabolism in addition to its direct action on K_{ATP} and K_{ir} channels in a receptor-dependant manner. In agreement with this notion, SRIF blocked lactate production resulted from glucose breakdown (shown in figure 4.2 of this study). The decrease in lactate levels could be due either to inhibition of glycolysis or a decrease in the conversion of pyruvate into lactate. This needs further investigation by measuring the production and output of pyruvate from β-cells because pyruvate is known to be able to enter cells and stimulate insulin release (Sener et al., 1978).

An interesting observation is that 10 mM glucose abolished the effect of the peptide as can be seen in figure 3.4. The OCR value for 10 mM glucose in the presence of 100 nM SRIF was -13 nmol O_2 10^7 $cell^{-1}$ min^{-1} compared to -11 nmol O_2 10^7 $cell^{-1}$ min^{-1} in the absence of the peptide which were statistically insignificant (Unpaired t test, n=13-31). This could happen as a result of the short duration of action (1-3 minutes) of SRIF (Appetecchia and Baldelli, 2010, Oberg, 2004) while the glucose was added after 10 minutes according to experimental design. Denaturation is another possible factor which might affect the peptide efficacy and enable glucose to exert its effect in the presence of SRIF. There are many factors that lead to peptide denaturation such as stirring for 10 minutes, oxidative damage, and temperature (32^{o}C) (Patel J, 2011). Further work should, therefore, include somatostatin analogues which are a longer duration of action and more resistant to peptidases than SRIF (Oberg, 2004, Pless et al., 1986).

As mentioned above, somatostatin inhibits glucose metabolism and lactate production suggested that SRIF might inhibit glycolysis and or glucose uptake. One of the SRIF

signaling pathways involves internalisation of SSTR (Hofland and Lamberts, 2001, Nouel et al., 1997) which may interact with glucose transporters. However, this idea was refuted by the fact that 100 nM SRIF neither affected glucose uptake nor glucokinase activity. Since SRIF did not inhibit glucose uptake or G-6-P production, its ability to inhibit lactate output may relate to effects on glycolysis. Phosphofructokinase 1 (PFK1) (Veneziale et al., 1976), phosphoglycerate dehydrogenase (Locasale et al., 2011, Possemato et al., 2011) and pyruvate kinase (Veneziale et al., 1976, Steták et al., 2007) are all possible candidates for the action of SRIF to inhibit glycolysis and lactate output. However, metabolomics studies are recommended to confirm the possible effect of SRIF on glycolytic enzymes activity. This can be achieved by probing for phosphorylation of these enzymes with specific antibodies e.g. Anti-PFKFB3 antibody, Anti-GAPDH antibody, Anti-PKM antibody, and Anti-LDHA antibody markers.

In addition, it was reported that SRIF analogue octreotide stimulated adenosine monophosphate activated protein kinase (AMPK) activity in pancreas and pituitary gland (Leontiou, 2008). This could be due to inhibition of mitochondrial metabolism by SRIF which leads to decreased ATP production and increases the AMP/ATP ratio and subsequently activates AMPK. However, the inability of SRIF to change ATP production in this study refutes the pathway above. Activation of AMPK enhances glucose uptake via stimulation of GLUT4 in skeletal muscle (Hunter et al., 2011) and stimulates glycolysis by activation of phosphofructokinase enzyme in cardiomyocytes (Marsin et al., 2000). However, the opposite has been observed in MIN6 cells, where the activation of AMPK inhibited glucose metabolism as evaluated by a decrease in cytosolic ATP, NAD(P)H, and intracellular Ca^{2+} (da Silva Xavier et al., 2000).

cAMP is a key component for insulin secretion via the activation of PKA and EPAC (Almahariq et al., 2014, Seino and Shibasaki, 2005). Moreover, many studies have shown that SRIF interferes with cAMP formation by inhibition of AC enzyme activity (Patel, 1999, Patel et al., 1994). In this study, we tried to examine the effect of cAMP firstly on β-cell metabolism and secondly in the action of SRIFs. My results provide compelling evidence that increased cAMP levels leads to a negative feedback effect on cellular metabolism to decrease OCR (figure 3.5) and subsequently decrease ATP levels. These findings extend

those studies confirming that elevation of cAMP levels in hepatocytes leads to a block of glycolysis (Panin and Tret'iakova, 1981, Pilkis et al., 1988); probably due to the ability of cAMP to inhibit glycolytic enzymes such as pyruvate kinase activity (Rodgers, 2012). Similar effects of cAMP might occur in pancreatic β-cells as there is a molecular evidence to express PK in both cell types (Blair et al., 1982, Marie et al., 1993). Furthermore, since the inhibitory effect of SRIF on OCR was reduced in the presence of dbcAMP, this suggests a possible interaction between them or a common site of action at a mitochondrial site or glycolysis. Glucagon inhibited glucose stimulated OCR in MIN6 cells which mimicked that of dbcAMP. According to the mechanism of action of glucagon, activation of adenylyl cyclase enzyme leads to increased intracellular cAMP levels subsequently enhancing insulin secretion (Kawai et al., 1995). However, an overproduction of cAMP should also inhibit OCR like that observed for dbcAMP (figure 3.5). In hepatocytes, glucagon stimulates gluconeogenesis and glycogenolysis but inhibits glycolysis during hypoglycaemia in order to raise blood glucose level (Bazotte et al., 1988, da Silva et al., 1998). This effect is either due to inhibition of Phosphofructokinase-1 (PFK-1) (Castaño et al., 1979, Veneziale et al., 1976) or by inhibition of pyruvate kinase (Pilkis et al., 1982, Pilkis and Claus, 1991). Depending on that evidence, it would be expected a similar effect of glucagon on glycolysis and OCR in pancreatic β-cells.

Many studies (Plant et al., 1991, Langer et al., 1983, Fagerholm et al., 2011, Niddam et al., 1990) demonstrated that clonidine and other α2 adrenoceptor agonists inhibit insulin secretion mainly via activation of K_{ATP} channel activity in pancreatic β-cells. A similar mechanism has been reported for the effect evoked by SRIF. As previously discussed in this study, the activation of K_{ATP} channels is achieved due to a rise in ADP against ATP, which mainly happens as a result of decreased glucose metabolism or mitochondrial failure. We found that 10 μM clonidine significantly decreased OCR stimulated by 10 mM glucose by 16% but failed to affect the basal respiration in MIN6 cells, which indeed reflects a decrease in glucose breakdown rather than direct mitochondrial inhibition. These data are consistent with the findings of (Laychock and Bilgin, 1987) who found that 10 μM clonidine suppressed glucose stimulated OCR in pancreatic β-cells by 40%. Moreover, a recent study on MIN6 cells showed that like clonidine, 100 nM epinephrine inhibited glucose stimulated

OCR by activating α_2-adrenoceptors (Kelly et al., 2018). Results of OCR inhibition by both SRIF and α_2-adrenoceptor agonists such as clonidine emphasise the relationship between inhibitory G-proteins and glucose metabolism which indirectly affect the K_{ATP} channels activity.

In line with previous research, I have found that glucose oxidation in pancreatic β-cells leads to the increase in the ATP/ADP ratio which blocks K_{ATP} channels, depolarises the plasma membrane and induces Ca^{2+} influx (Detimary et al., 1998). The inhibition of glucose metabolism by somatostatin is expected to decrease cytosolic ATP of the β-cell, however, this did not actually happen in this study. This result argues against the idea suggested that SRIF activates K_{ATP} and hyperpolarizes the membrane electrical activity by inhibition of cytosolic ATP/ADP ratio. However, some ATP measurement methods could not reflect the actual cytoplasmic ATP content because adenine nucleotides are concealed in vesicles making it difficult to detect the localised ATP (Bonora et al., 2012, Kennedy et al., 1999). ATP produced by glucose oxidation can be divided into three parts according to their cellular localisation; i.e. the cytosolic, mitochondrial matrix and sub-plasma membrane ATP (Kennedy et al., 1999). It is also demonstrated that the sub-plasma membrane [ATP] increased due to an elevation of intra-mitochondrial Ca^{2+} levels (Tarasov et al., 2012a). It is possible to suggest that SRIF activates K^+ channels by inhibiting the sub-plasma membrane ATP which is undetectable by the Luciferase methods (Kennedy et al., 1999). This can be explained as the high ATP consumption by the plasma membrane ATPases which leads to decrease [ATP] in the sub-plasma membrane domain (Ashcroft and Kakei, 1989).

Although one study reported that SRIF failed to activate K_{ATP} channels (Ribalet and Eddlestone, 1995); however, a small sample size (n=3) throws doubt on those observations. In the same study, the authors claimed that dbcAMP reversed the inhibitory effect of SRIF (n=2) which is consistent with our data. However, further confirmation of this observation could be achieved by measuring OCR when dbcAMP is added after SRIF.

100 nM SRIF has been shown to inhibit glucose oxidation, an effect suggested occurring because glucose oxidation in pancreatic β-cells is regulated by Ca^{2+} influx (Hellman et al., 1974, Sweet and Gilbert, 2006, De Marchi et al., 2014). Consequently, a metabolic effect

of SRIF may be secondary to its inhibition of Ca^{2+} influx (Nilsson et al., 1989), an action achieved by the inhibition of membrane electrical activity produced by the peptide (Smith et al., 2001). To explore this hypothesis, the inhibitory effect of SRIF was tested in the absence of extracellular Ca^{2+}. Removal of extracellular Ca^{2+} consistent with Daunt et al. (2006) showed that the removal of extracellular Ca^{2+} abolished the effect of SRIF on OCR. As a result, my study confirms that the inhibitory action of SRIF involves glucose induced Ca^{2+} influx from extracellular fluid rather than Ca^{2+} mobilisation from intracellular stores.

In the presence of a sulphonylurea (200 μM tolbutamide), I found that 100 nM SRIF still inhibited glucose induced Ca^{2+} influx, data consistent with those found by others (Seaquist et al., 1992, Abel et al., 1996). Since tolbutamide selectively blocks K_{ATP} channels (Ashcroft and Rorsman, 1989), this indicates the role of other types of K^+ channels in the SRIF action on the membrane electrophysiology of MIN6 cells such as GIRKs (Smith et al., 2001). Therefore, the effect of inhibiting GIRK by its selective inhibitor tertiapin LQ was tested with SRIF. Under these conditions, the peptide was still able to inhibit glucose induced Ca^{2+} influx. These data provide evidence for the ability of SRIF to repolarize glucose stimulated membrane depolarization via activation of both K_{ATP} and GIRK channels. However, this observation does not exclude the possible direct inhibitory effect of the peptide on VGCCs (Hsu et al., 1991, Smith, 2009).

The inhibitory actions of SRIF on hormone secretion and neuronal excitability are mediated by five G protein-coupled receptors (GPCRs) which are somatostatin receptors (SSTR1-5). All SSTRs are coupled to the pertussis toxin-sensitive $G\alpha_{i/o}$ proteins to produce their intracellular inhibitory effect (Demchyshyn et al., 1993, Carruthers et al., 1999). Although all these five receptors share common structural features and signaling pathways, however, they differ in their cellular localization and the mode of regulation (Günther et al., 2018). Activation of SSTRs leads to inhibition of two major intracellular second messengers i.e. cAMP and cytosolic Ca^{2+} which are responsible for inhibition of secretion (Patel et al., 1994, Hellman et al., 2018). A controversy in the literature regarding SSTRs signaling centrally and peripherally in both human and rodent models is still unresolved.

For example in rat pancreatic β-cells, (Roosterman et al., 1998) found that activation of SST1 but not SST2 were responsible for cell membrane hyperpolarisation and inhibition of

Ca^{2+} influx. Similar results were observed by Smith (2009) in MIN6 mouse pancreatic β-cells. On the other hand, studies on rodent islets indicate that SRIF inhibits glucose stimulated insulin secretion mainly by activation of SST5 receptors (Smith et al., 2001, Strowski et al., 2003, Strowski and Blake, 2008, Braun, 2014). In human islets, it is believed that SRIF inhibits GSIS mainly via activating SST5 and to a lesser extent by SST2 receptors (Zambre et al., 1999). These observations are in contrast with (Kailey et al., 2012) who suggested that SRIF inhibitory effect in human islets is predominantly mediated by SST2 receptors. It is known that the inhibitory effect of SRIF is mediated by Gαi signaling cascade (Ribalet and Eddlestone, 1995, Seaquist et al., 1992) which is found to be localised in the mitochondria (Lyssand and Bajjalieh, 2007). These studies support the findings suggested that mitochondrial inhibitory effect by the peptide is mediated via activation of Gαi signaling pathway.

Since the most available data on pancreatic islets are based on the experiments performed on rodent islets, more experiments must be done on human islets. Because in spite of sharing many similar characteristics, human and rodents islets are not identical and it is important to understand the human islets model rather than rodents (Rorsman and Ashcroft, 2018). Unfortunately, in this study, the human pancreatic cell line 1.1B4 did not achieve optimal results as the murine MIN6 cell line. It is recommended for future studies a further investigation of SRIF action to be conducted on human islets or different human pancreatic β-cell line such as EndoC-βH1 (Andersson et al., 2015).

6.2 Conclusion

Basal and fuels-stimulated OCR was blocked by SRIF in addition to inhibition of lactate production, suggesting that the peptide acts on mitochondria and glycolysis at the same time. However, there was no correlation found between the inhibitory effect of SRIF on the mitochondria and that on glycolysis. The inhibition of metabolism of glucose and KIC by SRIF was expected to be reflected in the production of ATP. Unexpectedly, this study found that ATP levels were unchanged in spite of the inhibition of metabolism by the peptide. As a result, it is concluded that the activation of K^+ channels by the peptide is not due to the decrease in the ATP/ADP ratio.

This may be because SRIF inhibits glucose and KIC stimulated OCR and $\Delta\Psi_{mit}$ in a lesser magnitude than that of mitochondrial complexes inhibitors (sodium azide and oligomycin) or the mitochondrial uncoupler (FCCP). These results suggest that the action of SRIF on mitochondrial complexes of ETC is unlikely and also emphasize the inhibition of the TCA cycle. A study of metabolomics is recommended to find out which key enzyme of the TCA could be affected by the peptide.

The simulated increase of cAMP levels by adding 1 mM dbcAMP leads to negative feedback effect on cellular metabolism by decreasing the OCR and Ca^{2+} influx. However, dbcAMP does not change the inhibitory effect of SRIF, therefore it is concluded that SRIF action is not mediated by cAMP in pancreatic β–cells. 100 nM glucagon shares a similar inhibitory effect of dbcAMP on OCR, this is opposite to their stimulatory action on insulin secretion. It would be interesting to know to what extent the mitochondrial inhibition will be reflected in membrane electrical activity and insulin secretion.

Similar to SRIF, 10 µM clonidine successfully suppressed the OCR stimulated by 10 mM glucose but not of basal respiration. This effect was expected because both of them are coupled to GPCRs and shared similar signaling cascade by activating G_i proteins. This also confirms the function of the GPCR system in these specific patches of MIN6 cells.

In this study, 100 nM SRIF neither affected glucose uptake nor the glucokinase activity. However, the peptide inhibited lactate production which is reflecting the glycolytic flux. Further investigation is recommended to confirm the glycolytic enzyme/s that might be affected by SRIF action. SRIF was proposed to be mediated by activation of the protein phosphatase calcineurin. This study was tested the SRIF action on OCR and LP in the presence of the protein phosphatase inhibitors CSA and OKA. In contrast to the above notion, this study could not confirm that SRIF is mediated by protein phosphatase pathway. SRIF effectively inhibits Ca^{2+} influx into MIN6 cells directly via blocking VGCCs and indirectly by activation of K^+ channels, by repolarising the plasma membrane and subsequently blocking the VGCCs. Inhibition of basal and both glucose and KIC induced Ca^{2+} influx indicating the peptide ability to modulate resting and exciting plasma membrane potential. The peptide achieved its action via a PTX sensitive pathway. From the Ca^{2+} free

experiments, it is concluded that SRIF inhibits Ca^{2+} influx from the extracellular fluid with minimum or no effect on Ca^{2+} mobilization from intracellular stores.

6.3 Future work

Many interesting ideas have been considered as future plans, and some of them have not been achieved in this study because of the lack of time. The study of metabolomics of glycolysis and TCA would be interesting because the presence of some indicators such as inhibition of lactate production and inhibition of KIC stimulated mitochondrial respiration by SRIF. Glycolytic enzymes activities can be measured by different techniques such as probe for phosphorylation with specific antibodies, as previously mentioned in the discussion section 6.1. Colorimetric assay kits can be also used to determine the effect of SRIF on the glycolytic enzymes activity which are plate based assays (Yao et al., 2018).

Glucose uptake assessed with a higher concentration of 2DG e.g. 5-10 mM instead of 1 mM could produce different results. This is because the rate of uptake is proportional to the concentration of extracellular glucose concentration (Yamamoto et al., 2015).

The measurement of mitochondrial pH gradient (ΔpH_{mit}) as a co-indicator with $\Delta\Psi_{mit}$ would be of value because the proton gradient is composed of both $\Delta\Psi_{mit}$ and the ΔpH_{mit} gradient altogether in a ratio of ~3:1 (Kim et al., 2012). Previous studies have measured the ΔpH_{mit} in isolated mitochondria (Lambert and Brand, 2004, Selivanov et al., 2008) and in intact cells (Hoek et al., 1980, Poburko et al., 2011).

It is also recommended to investigate the AMPK pathway as a potential target of SRIF action in pancreatic β-cells. Based on a previous study, anti-proliferative effects of SRIF might involve the stimulation of AMPK confirming that somatostatin analogues stimulate AMPK in rat pancreas (Leontiou, 2008). The effect of native SRIF or its analogues on the AMPK activity in pancreatic β–cells can be examined by using a functional kinase assay (Leontiou, 2008).

References

ABEL, K. B., LEHR, S. & ULLRICH, S. 1996. Adrenaline-, not somatostatin-induced hyperpolarization is accompanied by a sustained inhibition of insulin secretion in INS-1 cells. Activation of sulphonylurea K+ATP channels is not involved. *Pflugers Arch,* 432, 89-96.

AHRÉN, B. 2000. Autonomic regulation of islet hormone secretion--implications for health and disease. *Diabetologia,* 43, 393-410.

ALMAHARIQ, M., MEI, F. C. & CHENG, X. 2014. Cyclic AMP sensor EPAC proteins and energy homeostasis. *Trends Endocrinol Metab,* 25, 60-71.

AMMÄLÄ, C., ASHCROFT, F. M. & RORSMAN, P. 1993. Calcium-independent potentiation of insulin release by cyclic AMP in single beta-cells. *Nature,* 363, 356-8.

ANDERSSON, L. E., VALTAT, B., BAGGE, A., SHAROYKO, V. V., NICHOLLS, D. G., RAVASSARD, P., SCHARFMANN, R., SPÉGEL, P. & MULDER, H. 2015. Characterization of stimulus-secretion coupling in the human pancreatic EndoC-βH1 beta cell line. *PLoS One,* 10, e0120879.

ANTINOZZI, P. A., ISHIHARA, H., NEWGARD, C. B. & WOLLHEIM, C. B. 2002. Mitochondrial metabolism sets the maximal limit of fuel-stimulated insulin secretion in a model pancreatic beta cell: a survey of four fuel secretagogues. *J Biol Chem,* 277, 11746-55.

APPETECCHIA, M. & BALDELLI, R. 2010. Somatostatin analogues in the treatment of gastroenteropancreatic neuroendocrine tumours, current aspects and new perspectives. *J Exp Clin Cancer Res,* 29, 19.

ASHCROFT, F. M. 2005. ATP-sensitive potassium channelopathies: focus on insulin secretion. *J Clin Invest,* 115, 2047-58.

ASHCROFT, F. M. & KAKEI, M. 1989. ATP-sensitive K+ channels in rat pancreatic beta-cells: modulation by ATP and Mg2+ ions. *J Physiol,* 416, 349-67.

ASHCROFT, F. M. & RORSMAN, P. 1989. Electrophysiology of the pancreatic beta-cell. *Prog Biophys Mol Biol,* 54, 87-143.

ATIYA, A. W., MOLDOVAN, S., ADRIAN, T. E., COY, D., WALSH, J. & BRUNICARDI, F. C. 1997. Intraislet somatostatin inhibits insulin (via a subtype-2 somatostatin receptor) but not islet amyloid polypeptide secretion in the isolated perfused human pancreas. *J Gastrointest Surg,* 1, 251-6; discussion 256.

AUTHIER, F. & DESBUQUOIS, B. 2008. Glucagon receptors. *Cell Mol Life Sci,* 65, 1880-99.

BARACCA, A., SGARBI, G., SOLAINI, G. & LENAZ, G. 2003. Rhodamine 123 as a probe of mitochondrial membrane potential: evaluation of proton flux through F(0) during ATP synthesis. *Biochim Biophys Acta,* 1606, 137-46.

BARKER, C. J. & BERGGREN, P. O. 2012. The pancreatic beta cell as a paradigm for advances in inositide research. *Adv Biol Regul,* 52, 361-8.

BARON, A. D., WALLACE, P., BRECHTEL, G. & PRAGER, R. 1987. Somatostatin does not increase insulin-stimulated glucose uptake in humans. *Diabetes,* 36, 33-6.

BARRETT, K. E., BARMAN, S. M., BOITANO, S. & BROOKS, H. L. 2012. *Ganong's Review of Medical Physiology* New York, The McGraw-Hill Medical.

BAZOTTE, R. B., CONSTANTIN, J., HELL, N. S., IWAMOTO, E. L. & BRACHT, A. 1988. The relation between inhibition of glycolysis and stimulation of oxygen

uptake due to glucagon in livers from rats in different metabolic conditions. *Cell Biochem Funct,* 6, 225-30.

BEAVO, J. A. & BRUNTON, L. L. 2002. Cyclic nucleotide research -- still expanding after half a century. *Nat Rev Mol Cell Biol,* 3, 710-8.

BEECH, D. J., BERNHEIM, L. & HILLE, B. 1992. Pertussis toxin and voltage dependence distinguish multiple pathways modulating calcium channels of rat sympathetic neurons. *Neuron,* 8, 97-106.

BEN-SHLOMO, A. & MELMED, S. 2010. Pituitary somatostatin receptor signaling. *Trends Endocrinol Metab,* 21, 123-33.

BENDER, A. T. & BEAVO, J. A. 2006. Cyclic nucleotide phosphodiesterases: molecular regulation to clinical use. *Pharmacol Rev,* 58, 488-520.

BENUCK, M. & MARKS, N. 1976. Differences in the degradation of hypothalamic releasing factors by rat and human serum. *Life Sci,* 19, 1271-6.

BENZ, R. & MCLAUGHLIN, S. 1983. The molecular mechanism of action of the proton ionophore FCCP (carbonylcyanide p-trifluoromethoxyphenylhydrazone). *Biophys J,* 41, 381-98.

BERGGREN, P. O. & BARKER, C. J. 2008. A key role for phosphorylated inositol compounds in pancreatic beta-cell stimulus-secretion coupling. *Adv Enzyme Regul,* 48, 276-94.

BERRIDGE, M. J. & IRVINE, R. F. 1984. Inositol trisphosphate, a novel second messenger in cellular signal transduction. *Nature,* 312, 315-21.

BERRIDGE, M. J., LIPP, P. & BOOTMAN, M. D. 2000. The versatility and universality of calcium signalling. *Nat Rev Mol Cell Biol,* 1, 11-21.

BIEL, M., SCHNEIDER, A. & WAHL, C. 2002. Cardiac HCN channels: structure, function, and modulation. *Trends Cardiovasc Med,* 12, 206-12.

BLAIR, J. B., CIMBALA, M. A. & JAMES, M. E. 1982. Hepatic pyruvate kinase. Quantitative measurements of phosphorylation in vitro and in the isolated rat hepatocyte. *J Biol Chem,* 257, 7595-602.

BOEHM, B. O. 2003. The therapeutic potential of somatostatin receptor ligands in the treatment of obesity and diabetes. *Expert Opin Investig Drugs,* 12, 1501-9.

BONORA, M., PATERGNANI, S., RIMESSI, A., DE MARCHI, E., SUSKI, J. M., BONONI, A., GIORGI, C., MARCHI, S., MISSIROLI, S., POLETTI, F., WIECKOWSKI, M. R. & PINTON, P. 2012. ATP synthesis and storage. *Purinergic Signal,* 8, 343-57.

BOS, J. L. 2003. Epac: a new cAMP target and new avenues in cAMP research. *Nat Rev Mol Cell Biol,* 4, 733-8.

BRAUN, M. 2014. The somatostatin receptor in human pancreatic β-cells. *Vitam Horm,* 95, 165-93.

BRISSOVA, M., FOWLER, M. J., NICHOLSON, W. E., CHU, A., HIRSHBERG, B., HARLAN, D. M. & POWERS, A. C. 2005. Assessment of human pancreatic islet architecture and composition by laser scanning confocal microscopy. *J Histochem Cytochem,* 53, 1087-97.

BROWN, A. M., EVANS, R. D., BLACK, J. & RANSOM, B. R. 2012. Schwann cell glycogen selectively supports myelinated axon function. *Ann Neurol,* 72, 406-18.

BRUNICARDI, F. C., ATIYA, A., MOLDOVAN, S., LEE, T. C., FAGAN, S. P., KLEINMAN, R. M., ADRIAN, T. E., COY, D. H., WALSH, J. H. & FISHER, W. E. 2003. Activation of somatostatin receptor subtype 2 inhibits insulin secretion in the isolated perfused human pancreas. *Pancreas,* 27, e84-9.

BURGOYNE, R. D. & MORGAN, A. 2003. Secretory granule exocytosis. *Physiol Rev,* 83, 581-632.

CABRERA, O., BERMAN, D. M., KENYON, N. S., RICORDI, C., BERGGREN, P. O. & CAICEDO, A. 2006. The unique cytoarchitecture of human pancreatic islets has implications for islet cell function. *Proc Natl Acad Sci U S A,* 103, 2334-9.

CALHOUN, M. W., THOMAS, J. W. & GENNIS, R. B. 1994. The cytochrome oxidase superfamily of redox-driven proton pumps. *Trends Biochem Sci,* 19, 325-30.

CARO, P., KISHAN, A. U., NORBERG, E., STANLEY, I. A., CHAPUY, B., FICARRO, S. B., POLAK, K., TONDERA, D., GOUNARIDES, J., YIN, H., ZHOU, F., GREEN, M. R., CHEN, L., MONTI, S., MARTO, J. A., SHIPP, M. A. & DANIAL, N. N. 2012. Metabolic signatures uncover distinct targets in molecular subsets of diffuse large B cell lymphoma. *Cancer Cell,* 22, 547-60.

CARRUTHERS, A. M., WARNER, A. J., MICHEL, A. D., FENIUK, W. & HUMPHREY, P. P. 1999. Activation of adenylate cyclase by human recombinant sst5 receptors expressed in CHO-K1 cells and involvement of Galphas proteins. *Br J Pharmacol,* 126, 1221-9.

CASTAÑO, J. G., NIETO, A. & FELÍU, J. E. 1979. Inactivation of phosphofructokinase by glucagon in rat hepatocytes. *J Biol Chem,* 254, 5576-9.

CHABAN, Y., BOEKEMA, E. J. & DUDKINA, N. V. 2014. Structures of mitochondrial oxidative phosphorylation supercomplexes and mechanisms for their stabilisation. *Biochim Biophys Acta,* 1837, 418-26.

CHALMERS, S. & MCCARRON, J. G. 2008. The mitochondrial membrane potential and Ca2+ oscillations in smooth muscle. *J Cell Sci,* 121, 75-85.

CHAN, S. J., KEIM, P. & STEINER, D. F. 1976. Cell-free synthesis of rat preproinsulins: characterization and partial amino acid sequence determination. *Proc Natl Acad Sci U S A,* 73, 1964-8.

CHAVEZ-NORIEGA, L. E. & STEVENS, C. F. 1994. Increased transmitter release at excitatory synapses produced by direct activation of adenylate cyclase in rat hippocampal slices. *J Neurosci,* 14, 310-7.

CHENG, K., DELGHINGARO-AUGUSTO, V., NOLAN, C. J., TURNER, N., HALLAHAN, N., ANDRIKOPOULOS, S. & GUNTON, J. E. 2012. High passage MIN6 cells have impaired insulin secretion with impaired glucose and lipid oxidation. *PLoS One,* 7, e40868.

CHERRINGTON, A. D., CALDWELL, M. D., DIETZ, M. R., EXTON, J. H. & CROFFORD, O. B. 1977. The effect of somatostatin on glucose uptake and production by rat tissues in vitro. *Diabetes,* 26, 740-8.

CHOW, R. H., LUND, P. E., LÖSER, S., PANTEN, U. & GYLFE, E. 1995. Coincidence of early glucose-induced depolarization with lowering of cytoplasmic Ca2+ in mouse pancreatic beta-cells. *J Physiol,* 485 (Pt 3), 607-17.

CLAPHAM, D. E. 2007. Calcium signaling. *Cell,* 131, 1047-58.

CLARK, L. C., WOLF, R., GRANGER, D. & TAYLOR, Z. 1953. Continuous recording of blood oxygen tensions by polarography. *J Appl Physiol,* 6, 189-93.

CLEMENT, J. P., KUNJILWAR, K., GONZALEZ, G., SCHWANSTECHER, M., PANTEN, U., AGUILAR-BRYAN, L. & BRYAN, J. 1997. Association and stoichiometry of K(ATP) channel subunits. *Neuron,* 18, 827-38.

CONTI, M. 2000. Phosphodiesterases and cyclic nucleotide signaling in endocrine cells. *Mol Endocrinol,* 14, 1317-27.

COOPER, D. M. 2003. Regulation and organization of adenylyl cyclases and cAMP. *Biochem J,* 375, 517-29.

DA SILVA, A. C., KELMER-BRACHT, A. M., CONSTANTIN, J., ISHII-IWAMOTO, E. L., YAMAMOTO, N. S. & BRACHT, A. 1998. The influence of Ca2+ on the effects of glucagon on hepatic glycolysis. *Gen Pharmacol,* 30, 655-62.

DA SILVA XAVIER, G., LECLERC, I., SALT, I. P., DOIRON, B., HARDIE, D. G., KAHN, A. & RUTTER, G. A. 2000. Role of AMP-activated protein kinase in the regulation by glucose of islet beta cell gene expression. *Proc Natl Acad Sci U S A,* 97, 4023-8.

DAUNT, M., DALE, O. & SMITH, P. A. 2006. Somatostatin inhibits oxidative respiration in pancreatic beta-cells. *Endocrinology,* 147, 1527-35.

DAWSON, C. M., CROGHAN, P. C., SCOTT, A. M. & BANGHAM, J. A. 1986. Potassium and rubidium permeability and potassium conductance of the beta-cell membrane in mouse islets of Langerhans. *Q J Exp Physiol,* 71, 205-22.

DE MARCHI, U., THEVENET, J., HERMANT, A., DIOUM, E. & WIEDERKEHR, A. 2014. Calcium co-regulates oxidative metabolism and ATP synthase-dependent respiration in pancreatic beta cells. *J Biol Chem,* 289, 9182-94.

DE VOS, A., HEIMBERG, H., QUARTIER, E., HUYPENS, P., BOUWENS, L., PIPELEERS, D. & SCHUIT, F. 1995. Human and rat beta cells differ in glucose transporter but not in glucokinase gene expression. *J Clin Invest,* 96, 2489-95.

DEBERARDINIS, R. J., LUM, J. J., HATZIVASSILIOU, G. & THOMPSON, C. B. 2008. The biology of cancer: metabolic reprogramming fuels cell growth and proliferation. *Cell Metab,* 7, 11-20.

DEMCHYSHYN, L. L., SRIKANT, C. B., SUNAHARA, R. K., KENT, G., SEEMAN, P., VAN TOL, H. H., PANETTA, R., PATEL, Y. C. & NIZNIK, H. B. 1993. Cloning and expression of a human somatostatin-14-selective receptor variant (somatostatin receptor 4) located on chromosome 20. *Mol Pharmacol,* 43, 894-901.

DENTON, R. M., MCCORMACK, J. G. & EDGELL, N. J. 1980. Role of calcium ions in the regulation of intramitochondrial metabolism. Effects of Na+, Mg2+ and ruthenium red on the Ca2+-stimulated oxidation of oxoglutarate and on pyruvate dehydrogenase activity in intact rat heart mitochondria. *Biochem J,* 190, 107-17.

DETIMARY, P., GILON, P. & HENQUIN, J. C. 1998. Interplay between cytoplasmic Ca2+ and the ATP/ADP ratio: a feedback control mechanism in mouse pancreatic islets. *Biochem J,* 333 (Pt 2), 269-74.

DOU, H., WANG, C., WU, X., YAO, L., ZHANG, X., TENG, S., XU, H., LIU, B., WU, Q., ZHANG, Q., HU, M., WANG, Y., WANG, L., WU, Y., SHANG, S., KANG, X., ZHENG, L., ZHANG, J., RAOUX, M., LANG, J., LI, Q., SU, J., YU, X., CHEN, L. & ZHOU, Z. 2015. Calcium influx activates adenylyl cyclase 8 for sustained insulin secretion in rat pancreatic beta cells. *Diabetologia,* 58, 324-33.

DREWS, G., KRIPPEIT-DREWS, P. & DÜFER, M. 2010. Electrophysiology of islet cells. *Adv Exp Med Biol,* 654, 115-63.

DUCHEN, M. R., SMITH, P. A. & ASHCROFT, F. M. 1993. Substrate-dependent changes in mitochondrial function, intracellular free calcium concentration and membrane channels in pancreatic beta-cells. *Biochem J,* 294 (Pt 1), 35-42.

EIKI, J., NAGATA, Y., FUTAMURA, M., SASAKI-YAMAMOTO, K., IINO, T., NISHIMURA, T., CHIBA, M., OHYAMA, S., YOSHIDA-YOSHIMIOTO, R., FUJII, K., HOSAKA, H., GOTO-SHIMAZAKI, H., KADOTANI, A., OHE, T., LIN, S., LANGDON, R. B. & BERGER, J. P. 2011. Pharmacokinetic and

pharmacodynamic properties of the glucokinase activator MK-0941 in rodent models of type 2 diabetes and healthy dogs. *Mol Pharmacol,* 80, 1156-65.

ELIASSON, L., ABDULKADER, F., BRAUN, M., GALVANOVSKIS, J., HOPPA, M. B. & RORSMAN, P. 2008. Novel aspects of the molecular mechanisms controlling insulin secretion. *J Physiol,* 586, 3313-24.

ELIASSON, L., MA, X., RENSTRÖM, E., BARG, S., BERGGREN, P. O., GALVANOVSKIS, J., GROMADA, J., JING, X., LUNDQUIST, I., SALEHI, A., SEWING, S. & RORSMAN, P. 2003. SUR1 regulates PKA-independent cAMP-induced granule priming in mouse pancreatic B-cells. *J Gen Physiol,* 121, 181-97.

ELIASSON, L., RENSTRÖM, E., DING, W. G., PROKS, P. & RORSMAN, P. 1997. Rapid ATP-dependent priming of secretory granules precedes Ca(2+)-induced exocytosis in mouse pancreatic B-cells. *J Physiol,* 503 (Pt 2), 399-412.

ENSINCK, J. W., VOGEL, R. E., LASCHANSKY, E. C., KOERKER, D. J., PRIGEON, R. L., KAHN, S. E. & D'ALESSIO, D. A. 1997. Endogenous somatostatin-28 modulates postprandial insulin secretion. Immunoneutralization studies in baboons. *J Clin Invest,* 100, 2295-302.

ESSAYAN, D. M. 2001. Cyclic nucleotide phosphodiesterases. *J Allergy Clin Immunol,* 108, 671-80.

EVANS, G. J., WILKINSON, M. C., GRAHAM, M. E., TURNER, K. M., CHAMBERLAIN, L. H., BURGOYNE, R. D. & MORGAN, A. 2001. Phosphorylation of cysteine string protein by protein kinase A. Implications for the modulation of exocytosis. *J Biol Chem,* 276, 47877-85.

EZZAT, S., WANG, R., PINTILIE, M. & ASA, S. L. 2017. FGFR4 polymorphic alleles modulate mitochondrial respiration: A novel target for somatostatin analog action in pituitary tumors. *Oncotarget,* 8, 3481-3494.

FAGAN, S. P., AZIZZADEH, A., MOLDOVAN, S., RAY, M. K., ADRIAN, T. E., DING, X., COY, D. H. & BRUNICARDI, F. C. 1998. Insulin secretion is inhibited by subtype five somatostatin receptor in the mouse. *Surgery,* 124, 254-8; discussion 258-9.

FAGERHOLM, V., HAAPARANTA, M. & SCHEININ, M. 2011. α2-adrenoceptor regulation of blood glucose homeostasis. *Basic Clin Pharmacol Toxicol,* 108, 365-70.

FRANCIS, S. H., BLOUNT, M. A. & CORBIN, J. D. 2011. Mammalian cyclic nucleotide phosphodiesterases: molecular mechanisms and physiological functions. *Physiol Rev,* 91, 651-90.

FUJII, Y., GONOI, T., YAMADA, Y., CHIHARA, K., INAGAKI, N. & SEINO, S. 1994. Somatostatin receptor subtype SSTR2 mediates the inhibition of high-voltage-activated calcium channels by somatostatin and its analogue SMS 201-995. *FEBS Lett,* 355, 117-20.

FUJIMOTO, K., SHIBASAKI, T., YOKOI, N., KASHIMA, Y., MATSUMOTO, M., SASAKI, T., TAJIMA, N., IWANAGA, T. & SEINO, S. 2002. Piccolo, a Ca2+ sensor in pancreatic beta-cells. Involvement of cAMP-GEFII.Rim2. Piccolo complex in cAMP-dependent exocytosis. *J Biol Chem,* 277, 50497-502.

FUJITA-YOSHIGAKI, J. 1998. Divergence and convergence in regulated exocytosis: the characteristics of cAMP-dependent enzyme secretion of parotid salivary acinar cells. *Cell Signal,* 10, 371-5.

GAO, B. N. & GILMAN, A. G. 1991. Cloning and expression of a widely distributed (type IV) adenylyl cyclase. *Proc Natl Acad Sci U S A,* 88, 10178-82.

GEE, K. R., BROWN, K. A., CHEN, W. N., BISHOP-STEWART, J., GRAY, D. & JOHNSON, I. 2000. Chemical and physiological characterization of fluo-4 Ca(2+)-indicator dyes. *Cell Calcium,* 27, 97-106.

GERENCSER, A. A., MOOKERJEE, S. A., JASTROCH, M. & BRAND, M. D. 2016. Measurement of the Absolute Magnitude and Time Courses of Mitochondrial Membrane Potential in Primary and Clonal Pancreatic Beta-Cells. *PLoS One,* 11, e0159199.

GILON, P., CHAE, H. Y., RUTTER, G. A. & RAVIER, M. A. 2014. Calcium signaling in pancreatic β-cells in health and in Type 2 diabetes. *Cell Calcium,* 56, 340-61.

GILON, P., SHEPHERD, R. M. & HENQUIN, J. C. 1993. Oscillations of secretion driven by oscillations of cytoplasmic Ca2+ as evidences in single pancreatic islets. *J Biol Chem,* 268, 22265-8.

GLOYN, A. L., ELLARD, S., SHIELD, J. P., TEMPLE, I. K., MACKAY, D. J., POLAK, M., BARRETT, T. & HATTERSLEY, A. T. 2002. Complete glucokinase deficiency is not a common cause of permanent neonatal diabetes. *Diabetologia,* 45, 290.

GORUS, F. K., MALAISSE, W. J. & PIPELEERS, D. G. 1984. Differences in glucose handling by pancreatic A- and B-cells. *J Biol Chem,* 259, 1196-200.

GRIBBLE, F. M. & REIMANN, F. 2003. Sulphonylurea action revisited: the post-cloning era. *Diabetologia,* 46, 875-91.

GROMADA, J., HOLST, J. J. & RORSMAN, P. 1998. Cellular regulation of islet hormone secretion by the incretin hormone glucagon-like peptide 1. *Pflugers Arch,* 435, 583-94.

GROMADA, J., HØY, M., BUSCHARD, K., SALEHI, A. & RORSMAN, P. 2001. Somatostatin inhibits exocytosis in rat pancreatic alpha-cells by G(i2)-dependent activation of calcineurin and depriming of secretory granules. *J Physiol,* 535, 519-32.

GÜNTHER, T., TULIPANO, G., DOURNAUD, P., BOUSQUET, C., CSABA, Z., KREIENKAMP, H. J., LUPP, A., KORBONITS, M., CASTAÑO, J. P., WESTER, H. J., CULLER, M., MELMED, S. & SCHULZ, S. 2018. International Union of Basic and Clinical Pharmacology. CV. Somatostatin Receptors: Structure, Function, Ligands, and New Nomenclature. *Pharmacol Rev,* 70, 763-835.

HAJNÓCZKY, G., CSORDÁS, G., MADESH, M. & PACHER, P. 2000. The machinery of local Ca2+ signalling between sarco-endoplasmic reticulum and mitochondria. *J Physiol,* 529 Pt 1, 69-81.

HELLMAN, B., DANSK, H. & GRAPENGIESSER, E. 2018. Somatostatin promotes glucose generation of Ca. *Cell Calcium,* 74, 35-42.

HELLMAN, B., IDAHL, L. A., LERNMARK, A., SEHLIN, J. & TÄLJEDAL, I. B. 1974. The pancreatic beta-cell recognition of insulin secretagogues. Effects of calcium and sodium on glucose metabolism and insulin release. *Biochem J,* 138, 33-45.

HELMCHEN, U., SCHMIDT, W. E., SIEGEL, E. G. & CREUTZFELDT, W. 1984. Morphological and functional changes of pancreatic B cells in cyclosporin A-treated rats. *Diabetologia,* 27, 416-8.

HENQUIN, J. C. & MEISSNER, H. P. 1984. Significance of ionic fluxes and changes in membrane potential for stimulus-secretion coupling in pancreatic B-cells. *Experientia,* 40, 1043-52.

HIGGINS, C. F. 2007. Multiple molecular mechanisms for multidrug resistance transporters. *Nature,* 446, 749-57.

HIRST, J. 2010. Towards the molecular mechanism of respiratory complex I. *Biochem J,* 425, 327-39.

HOEK, J. B., NICHOLLS, D. G. & WILLIAMSON, J. R. 1980. Determination of the mitochondrial protonmotive force in isolated hepatocytes. *J Biol Chem,* 255, 1458-64.

HOFLAND, L. J. & LAMBERTS, S. W. 2001. Somatostatin receptor subtype expression in human tumors. *Ann Oncol,* 12 Suppl 2, S31-6.

HOLZ, G. G. 2004. Epac: A new cAMP-binding protein in support of glucagon-like peptide-1 receptor-mediated signal transduction in the pancreatic beta-cell. *Diabetes,* 53, 5-13.

HORSEFIELD, R., IWATA, S. & BYRNE, B. 2004. Complex II from a structural perspective. *Curr Protein Pept Sci,* 5, 107-18.

HSU, W. H., XIANG, H. D., RAJAN, A. S., KUNZE, D. L. & BOYD, A. E. 1991. Somatostatin inhibits insulin secretion by a G-protein-mediated decrease in Ca2+ entry through voltage-dependent Ca2+ channels in the beta cell. *J Biol Chem,* 266, 837-43.

HUNTER, R. W., TREEBAK, J. T., WOJTASZEWSKI, J. F. & SAKAMOTO, K. 2011. Molecular mechanism by which AMP-activated protein kinase activation promotes glycogen accumulation in muscle. *Diabetes,* 60, 766-74.

ISHIHARA, H., ASANO, T., TSUKUDA, K., KATAGIRI, H., INUKAI, K., ANAI, M., KIKUCHI, M., YAZAKI, Y., MIYAZAKI, J. I. & OKA, Y. 1993. Pancreatic beta cell line MIN6 exhibits characteristics of glucose metabolism and glucose-stimulated insulin secretion similar to those of normal islets. *Diabetologia,* 36, 1139-45.

JACOBSON, J. & DUCHEN, M. R. 2004. Interplay between mitochondria and cellular calcium signalling. *Mol Cell Biochem,* 256-257, 209-18.

JELINEK, L. J., LOK, S., ROSENBERG, G. B., SMITH, R. A., GRANT, F. J., BIGGS, S., BENSCH, P. A., KUIJPER, J. L., SHEPPARD, P. O. & SPRECHER, C. A. 1993. Expression cloning and signaling properties of the rat glucagon receptor. *Science,* 259, 1614-6.

JIANG, G. & ZHANG, B. B. 2003. Glucagon and regulation of glucose metabolism. *Am J Physiol Endocrinol Metab,* 284, E671-8.

JITRAPAKDEE, S., WUTTHISATHAPORNCHAI, A., WALLACE, J. C. & MACDONALD, M. J. 2010. Regulation of insulin secretion: role of mitochondrial signalling. *Diabetologia,* 53, 1019-32.

JONES, P. M. & PERSAUD, S. J. 1998. Protein kinases, protein phosphorylation, and the regulation of insulin secretion from pancreatic beta-cells. *Endocr Rev,* 19, 429-61.

KAILEY, B., VAN DE BUNT, M., CHELEY, S., JOHNSON, P. R., MACDONALD, P. E., GLOYN, A. L., RORSMAN, P. & BRAUN, M. 2012. SSTR2 is the functionally dominant somatostatin receptor in human pancreatic β- and α-cells. *Am J Physiol Endocrinol Metab,* 303, E1107-16.

KAKEI, M., KELLY, R. P., ASHCROFT, S. J. & ASHCROFT, F. M. 1986. The ATP-sensitivity of K+ channels in rat pancreatic B-cells is modulated by ADP. *FEBS Lett,* 208, 63-6.

KANEKO, Y. K. & ISHIKAWA, T. 2015. Diacylglycerol Signaling Pathway in Pancreatic β-Cells: An Essential Role of Diacylglycerol Kinase in the Regulation of Insulin Secretion. *Biol Pharm Bull,* 38, 669-73.

KANG, G., JOSEPH, J. W., CHEPURNY, O. G., MONACO, M., WHEELER, M. B., BOS, J. L., SCHWEDE, F., GENIESER, H. G. & HOLZ, G. G. 2003. Epac-selective

cAMP analog 8-pCPT-2'-O-Me-cAMP as a stimulus for Ca2+-induced Ca2+ release and exocytosis in pancreatic beta-cells. *J Biol Chem,* 278, 8279-85.

KASHIMA, Y., MIKI, T., SHIBASAKI, T., OZAKI, N., MIYAZAKI, M., YANO, H. & SEINO, S. 2001. Critical role of cAMP-GEFII--Rim2 complex in incretin-potentiated insulin secretion. *J Biol Chem,* 276, 46046-53.

KAUPP, U. B. & SEIFERT, R. 2002. Cyclic nucleotide-gated ion channels. *Physiol Rev,* 82, 769-824.

KAWAI, K., YOKOTA, C., OHASHI, S., WATANABE, Y. & YAMASHITA, K. 1995. Evidence that glucagon stimulates insulin secretion through its own receptor in rats. *Diabetologia,* 38, 274-6.

KAWASAKI, H., SPRINGETT, G. M., MOCHIZUKI, N., TOKI, S., NAKAYA, M., MATSUDA, M., HOUSMAN, D. E. & GRAYBIEL, A. M. 1998. A family of cAMP-binding proteins that directly activate Rap1. *Science,* 282, 2275-9.

KELLY, A. C., CAMACHO, L. E., PENDARVIS, K., DAVENPORT, H. M., STEFFENS, N. R., SMITH, K. E., WEBER, C. S., LYNCH, R. M., PAPAS, K. K. & LIMESAND, S. W. 2018. Adrenergic receptor stimulation suppresses oxidative metabolism in isolated rat islets and Min6 cells. *Mol Cell Endocrinol,* 473, 136-145.

KENNEDY, H. J., POULI, A. E., AINSCOW, E. K., JOUAVILLE, L. S., RIZZUTO, R. & RUTTER, G. A. 1999. Glucose generates sub-plasma membrane ATP microdomains in single islet beta-cells. Potential role for strategically located mitochondria. *J Biol Chem,* 274, 13281-91.

KIM, N., RIPPLE, M. O. & SPRINGETT, R. 2012. Measurement of the mitochondrial membrane potential and pH gradient from the redox poise of the hemes of the bc1 complex. *Biophys J,* 102, 1194-203.

KIM, W., FIORI, J. L., SHIN, Y. K., OKUN, E., KIM, J. S., RAPP, P. R. & EGAN, J. M. 2014. Pancreatic polypeptide inhibits somatostatin secretion. *FEBS Lett,* 588, 3233-9.

KIMBALL, S. R., SIEGFRIED, B. A. & JEFFERSON, L. S. 2004. Glucagon represses signaling through the mammalian target of rapamycin in rat liver by activating AMP-activated protein kinase. *J Biol Chem,* 279, 54103-9.

KIRKPATRICK, C. J., MELZNER, I. & GÖLLER, T. 1985. Comparative effects of trypsin, collagenase and mechanical harvesting on cell membrane lipids studied in monolayer-cultured endothelial cells and a green monkey kidney cell line. *Biochim Biophys Acta,* 846, 120-6.

KOCH, B. D., BLALOCK, J. B. & SCHONBRUNN, A. 1988. Characterization of the cyclic AMP-independent actions of somatostatin in GH cells. I. An increase in potassium conductance is responsible for both the hyperpolarization and the decrease in intracellular free calcium produced by somatostatin. *J Biol Chem,* 263, 216-25.

KUMAR, U. & GRANT, M. 2010. Somatostatin and somatostatin receptors. *Results Probl Cell Differ,* 50, 137-84.

KUMAR, U., SASI, R., SURESH, S., PATEL, A., THANGARAJU, M., METRAKOS, P., PATEL, S. C. & PATEL, Y. C. 1999. Subtype-selective expression of the five somatostatin receptors (hSSTR1-5) in human pancreatic islet cells: a quantitative double-label immunohistochemical analysis. *Diabetes,* 48, 77-85.

KUO, W. N., HODGINS, D. S. & KUO, J. F. 1973. Adenylate cyclase in islets of Langerhans. Isolation of islets and regulation of adenylate cyclase activity by various hormones and agents. *J Biol Chem,* 248, 2705-11.

LACEY, R. J., BERROW, N. S., SCARPELLO, J. H. & MORGAN, N. G. 1991. Selective stimulation of glucagon secretion by beta 2-adrenoceptors in isolated islets of Langerhans of the rat. *Br J Pharmacol,* 103, 1824-8.

LAMBERT, A. J. & BRAND, M. D. 2004. Superoxide production by NADH:ubiquinone oxidoreductase (complex I) depends on the pH gradient across the mitochondrial inner membrane. *Biochem J,* 382, 511-7.

LANDA, L. R., HARBECK, M., KAIHARA, K., CHEPURNY, O., KITIPHONGSPATTANA, K., GRAF, O., NIKOLAEV, V. O., LOHSE, M. J., HOLZ, G. G. & ROE, M. W. 2005. Interplay of Ca2+ and cAMP signaling in the insulin-secreting MIN6 beta-cell line. *J Biol Chem,* 280, 31294-302.

LANGER, J., PANTEN, U. & ZIELMANN, S. 1983. Effects of alpha-adrenoceptor antagonists on clonidine-induced inhibition of insulin secretion by isolated pancreatic islets. *Br J Pharmacol,* 79, 415-20.

LAYCHOCK, S. G. 1987. Alpha 2-adrenoceptor stimulation affects total glucose utilization in isolated islets of Langerhans. *Mol Pharmacol,* 32, 241-8.

LAYCHOCK, S. G. & BILGIN, S. 1987. Alpha 2-adrenergic inhibition of pancreatic islet glucose utilization is mediated by an inhibitory guanine nucleotide regulatory protein. *FEBS Lett,* 218, 7-10.

LEONTIOU, A. S., H. MCSHEEHY, P. GROSSMAN, AB. KORBONITS, M. 2008. Somatostatin analogues stimulate AMPK (AMP-dependent protein kinase), a metabolic enzyme with anti-proliferative effects. *Society for Endocrinology BES 2008.* Harrogate, UK.

LI, D., PENG, S. Y., ZHANG, Z. W., FENG, R. C., LI, L., LIANG, J., TAI, S. & TENG, C. B. 2013. Complete disassociation of adult pancreas into viable single cells through cold trypsin-EDTA digestion. *J Zhejiang Univ Sci B,* 14, 596-603.

LIBERTI, M. V. & LOCASALE, J. W. 2016. The Warburg Effect: How Does it Benefit Cancer Cells? *Trends Biochem Sci,* 41, 211-218.

LIN, D. C., HUANG, C. Y., TING, W. H., LO, F. S., LIN, C. L., YANG, H. W., CHANG, T. Y., LIN, C. H., TZENG, Y. W., YANG, W. S., JUANG, Y. L. & LEE, Y. J. 2019. Mutations in glucokinase and other genes detected in neonatal and type 1B diabetes patient using whole exome sequencing may lead to disease-causing changes in protein activity. *Biochim Biophys Acta Mol Basis Dis,* 1865, 428-433.

LIU, D., MARTINO, G., THANGARAJU, M., SHARMA, M., HALWANI, F., SHEN, S. H., PATEL, Y. C. & SRIKANT, C. B. 2000. Caspase-8-mediated intracellular acidification precedes mitochondrial dysfunction in somatostatin-induced apoptosis. *J Biol Chem,* 275, 9244-50.

LIU, Y., LU, D., ZHANG, Y., LI, S., LIU, X. & LIN, H. 2010. The evolution of somatostatin in vertebrates. *Gene,* 463, 21-8.

LOCASALE, J. W., GRASSIAN, A. R., MELMAN, T., LYSSIOTIS, C. A., MATTAINI, K. R., BASS, A. J., HEFFRON, G., METALLO, C. M., MURANEN, T., SHARFI, H., SASAKI, A. T., ANASTASIOU, D., MULLARKY, E., VOKES, N. I., SASAKI, M., BEROUKHIM, R., STEPHANOPOULOS, G., LIGON, A. H., MEYERSON, M., RICHARDSON, A. L., CHIN, L., WAGNER, G., ASARA, J. M., BRUGGE, J. S., CANTLEY, L. C. & VANDER HEIDEN, M. G. 2011. Phosphoglycerate dehydrogenase diverts glycolytic flux and contributes to oncogenesis. *Nat Genet,* 43, 869-74.

LYNCH, C. J., HALLE, B., FUJII, H., VARY, T. C., WALLIN, R., DAMUNI, Z. & HUTSON, S. M. 2003. Potential role of leucine metabolism in the leucine-signaling pathway involving mTOR. *Am J Physiol Endocrinol Metab,* 285, E854-63.

LYSSAND, J. S. & BAJJALIEH, S. M. 2007. The heterotrimeric [corrected] G protein subunit G alpha i is present on mitochondria. *FEBS Lett,* 581, 5765-8.

LÓPEZ-LÁZARO, M. 2008. The warburg effect: why and how do cancer cells activate glycolysis in the presence of oxygen? *Anticancer Agents Med Chem,* 8, 305-12.

MAECHLER, P., KENNEDY, E. D., POZZAN, T. & WOLLHEIM, C. B. 1997. Mitochondrial activation directly triggers the exocytosis of insulin in permeabilized pancreatic beta-cells. *EMBO J,* 16, 3833-41.

MARIE, S., DIAZ-GUERRA, M. J., MIQUEROL, L., KAHN, A. & IYNEDJIAN, P. B. 1993. The pyruvate kinase gene as a model for studies of glucose-dependent regulation of gene expression in the endocrine pancreatic beta-cell type. *J Biol Chem,* 268, 23881-90.

MARIN-VALENCIA, I., YANG, C., MASHIMO, T., CHO, S., BAEK, H., YANG, X. L., RAJAGOPALAN, K. N., MADDIE, M., VEMIREDDY, V., ZHAO, Z., CAI, L., GOOD, L., TU, B. P., HATANPAA, K. J., MICKEY, B. E., MATÉS, J. M., PASCUAL, J. M., MAHER, E. A., MALLOY, C. R., DEBERARDINIS, R. J. & BACHOO, R. M. 2012. Analysis of tumor metabolism reveals mitochondrial glucose oxidation in genetically diverse human glioblastomas in the mouse brain in vivo. *Cell Metab,* 15, 827-37.

MARSHALL, M. O., THOMAS, H. M., SEATTER, M. J., GREER, K. R., WOOD, P. J. & GOULD, G. W. 1993. Pancreatic beta-cells express a low affinity glucose transporter: functional consequences in normal and diabetic states. *Biochem Soc Trans,* 21, 164-8.

MARSIN, A. S., BERTRAND, L., RIDER, M. H., DEPREZ, J., BEAULOYE, C., VINCENT, M. F., VAN DEN BERGHE, G., CARLING, D. & HUE, L. 2000. Phosphorylation and activation of heart PFK-2 by AMPK has a role in the stimulation of glycolysis during ischaemia. *Curr Biol,* 10, 1247-55.

MARTIN, G. M., KANDASAMY, B., DIMAIO, F., YOSHIOKA, C. & SHYNG, S. L. 2017. Anti-diabetic drug binding site in a mammalian K. *Elife,* 6.

MATSCHINSKY, F. M. 1990. Glucokinase as glucose sensor and metabolic signal generator in pancreatic beta-cells and hepatocytes. *Diabetes,* 39, 647-52.

MATSCHINSKY, F. M. 2013. GKAs for diabetes therapy: why no clinically useful drug after two decades of trying? *Trends Pharmacol Sci,* 34, 90-9.

MCCLUSKEY, J. T., HAMID, M., GUO-PARKE, H., MCCLENAGHAN, N. H., GOMIS, R. & FLATT, P. R. 2011. Development and functional characterization of insulin-releasing human pancreatic beta cell lines produced by electrofusion. *J Biol Chem,* 286, 21982-92.

MEISSNER, H. P. 1976. Electrical characteristics of the beta-cells in pancreatic islets. *J Physiol (Paris),* 72, 757-67.

MEISSNER, H. P. & ATWATER, I. J. 1976. The kinetics of electrical activity of beta cells in response to a "square wave" stimulation with glucose or glibenclamide. *Horm Metab Res,* 8, 11-6.

MEISSNER, H. P. & SCHMIDT, H. 1976. The electrical activity of pancreatic beta-cells of diabetic mice. *FEBS Lett,* 67, 371-4.

MENDEZ, C. F., LEIBIGER, I. B., LEIBIGER, B., HØY, M., GROMADA, J., BERGGREN, P. O. & BERTORELLO, A. M. 2003. Rapid association of protein kinase C-epsilon with insulin granules is essential for insulin exocytosis. *J Biol Chem,* 278, 44753-7.

MIKHAILOV, M. V., CAMPBELL, J. D., DE WET, H., SHIMOMURA, K., ZADEK, B., COLLINS, R. F., SANSOM, M. S., FORD, R. C. & ASHCROFT, F. M. 2005. 3-D structural and functional characterization of the purified KATP channel complex Kir6.2-SUR1. *EMBO J,* 24, 4166-75.

MITRA, S. W., MEZEY, E., HUNYADY, B., CHAMBERLAIN, L., HAYES, E., FOOR, F., WANG, Y., SCHONBRUNN, A. & SCHAEFFER, J. M. 1999. Colocalization of

somatostatin receptor sst5 and insulin in rat pancreatic beta-cells. *Endocrinology,* 140, 3790-6.

MIYAZAKI, J., ARAKI, K., YAMATO, E., IKEGAMI, H., ASANO, T., SHIBASAKI, Y., OKA, Y. & YAMAMURA, K. 1990. Establishment of a pancreatic beta cell line that retains glucose-inducible insulin secretion: special reference to expression of glucose transporter isoforms. *Endocrinology,* 127, 126-32.

MOLDOVAN, S., ATIYA, A., ADRIAN, T. E., KLEINMAN, R. M., LLOYD, K., OLTHOFF, K., IMAGAWA, D., SHEVLIN, L., COY, D. & WALSH, J. 1995. Somatostatin inhibits B-cell secretion via a subtype-2 somatostatin receptor in the isolated perfused human pancreas. *J Surg Res,* 59, 85-90.

MOLLARD, P., VACHER, P., DUFY, B. & BARKER, J. L. 1988. Somatostatin blocks Ca2+ action potential activity in prolactin-secreting pituitary tumor cells through coordinate actions on K+ and Ca2+ conductances. *Endocrinology,* 123, 721-32.

MØLLER, N., BAGGER, J. P., SCHMITZ, O., JØRGENSEN, J. O., OVESEN, P., MØLLER, J., ALBERTI, K. G. & ORSKOV, H. 1995. Somatostatin enhances insulin-stimulated glucose uptake in the perfused human forearm. *J Clin Endocrinol Metab,* 80, 1789-93.

NAKAGAWA, Y., NAGASAWA, M., MEDINA, J. & KOJIMA, I. 2015. Glucose Evokes Rapid Ca2+ and Cyclic AMP Signals by Activating the Cell-Surface Glucose-Sensing Receptor in Pancreatic β-Cells. *PLoS One,* 10, e0144053.

NAKAZAKI, M., CRANE, A., HU, M., SEGHERS, V., ULLRICH, S., AGUILAR-BRYAN, L. & BRYAN, J. 2002. cAMP-activated protein kinase-independent potentiation of insulin secretion by cAMP is impaired in SUR1 null islets. *Diabetes,* 51, 3440-9.

NESHER, R., ANTEBY, E., YEDOVIZKY, M., WARWAR, N., KAISER, N. & CERASI, E. 2002. Beta-cell protein kinases and the dynamics of the insulin response to glucose. *Diabetes,* 51 Suppl 1, S68-73.

NEVES, S. R., RAM, P. T. & IYENGAR, R. 2002. G protein pathways. *Science,* 296, 1636-9.

NICHOLLS, D. G. & CROMPTON, M. 1980. Mitochondrial calcium transport. *FEBS Lett,* 111, 261-8.

NICHOLS, C. G. & REMEDI, M. S. 2012. The diabetic β-cell: hyperstimulated vs. hyperexcited. *Diabetes Obes Metab,* 14 Suppl 3, 129-35.

NIDDAM, R., ANGEL, I., BIDET, S. & LANGER, S. Z. 1990. Pharmacological characterization of alpha-2 adrenergic receptor subtype involved in the release of insulin from isolated rat pancreatic islets. *J Pharmacol Exp Ther,* 254, 883-7.

NIKI, I., OKAZAKI, K., SAITOH, M., NIKI, A., NIKI, H., TAMAGAWA, T., IGUCHI, A. & HIDAKA, H. 1993. Presence and possible involvement of Ca/calmodulin-dependent protein kinases in insulin release from the rat pancreatic beta cell. *Biochem Biophys Res Commun,* 191, 255-61.

NILSSON, T., ARKHAMMAR, P., RORSMAN, P. & BERGGREN, P. O. 1989. Suppression of insulin release by galanin and somatostatin is mediated by a G-protein. An effect involving repolarization and reduction in cytoplasmic free Ca2+ concentration. *J Biol Chem,* 264, 973-80.

NISHIZUKA, Y. 2003. Discovery and prospect of protein kinase C research: epilogue. *J Biochem,* 133, 155-8.

NJØLSTAD, P. R., SØVIK, O., CUESTA-MUÑOZ, A., BJØRKHAUG, L., MASSA, O., BARBETTI, F., UNDLIEN, D. E., SHIOTA, C., MAGNUSON, M. A., MOLVEN, A., MATSCHINSKY, F. M. & BELL, G. I. 2001. Neonatal diabetes mellitus due to complete glucokinase deficiency. *N Engl J Med,* 344, 1588-92.

NOUEL, D., GAUDRIAULT, G., HOULE, M., REISINE, T., VINCENT, J. P., MAZELLA, J. & BEAUDET, A. 1997. Differential internalization of somatostatin in COS-7 cells transfected with SST1 and SST2 receptor subtypes: a confocal microscopic study using novel fluorescent somatostatin derivatives. *Endocrinology,* 138, 296-306.

O'NEIL, R. G., WU, L. & MULLANI, N. 2005. Uptake of a fluorescent deoxyglucose analog (2-NBDG) in tumor cells. *Mol Imaging Biol,* 7, 388-92.

O'NEILL, C. M., LU, C., CORBIN, K. L., SHARMA, P. R., DULA, S. B., CARTER, J. D., RAMADAN, J. W., XIN, W., LEE, J. K. & NUNEMAKER, C. S. 2013. Circulating levels of IL-1B+IL-6 cause ER stress and dysfunction in islets from prediabetic male mice. *Endocrinology,* 154, 3077-88.

OBERG, K. 2004. Future aspects of somatostatin-receptor-mediated therapy. *Neuroendocrinology,* 80 Suppl 1, 57-61.

OLIAS, G., VIOLLET, C., KUSSEROW, H., EPELBAUM, J. & MEYERHOF, W. 2004. Regulation and function of somatostatin receptors. *J Neurochem,* 89, 1057-91.

ORSKOV, L., MØLLER, N., BAK, J. F., PØRKSEN, N. & SCHMITZ, O. 1996. Effects of the somatostatin analog, octreotide, on glucose metabolism and insulin sensitivity in insulin-dependent diabetes mellitus. *Metabolism,* 45, 211-7.

OZAKI, N., SHIBASAKI, T., KASHIMA, Y., MIKI, T., TAKAHASHI, K., UENO, H., SUNAGA, Y., YANO, H., MATSUURA, Y., IWANAGA, T., TAKAI, Y. & SEINO, S. 2000. cAMP-GEFII is a direct target of cAMP in regulated exocytosis. *Nat Cell Biol,* 2, 805-11.

PANIN, L. E. & TRET'IAKOVA, T. A. 1981. [Effect of cAMP of glycolysis and glycogenolysis in the liver and adrenals of white rats]. *Biull Eksp Biol Med,* 92, 37-9.

PARNELL, E., PALMER, T. M. & YARWOOD, S. J. 2015. The future of EPAC-targeted therapies: agonism versus antagonism. *Trends Pharmacol Sci,* 36, 203-214.

PATEL J, K. R., TUNGA R, RITTER N AND TUNGA B 2011. Stability Considerations for Biopharmaceuticals, Part 1: Overview of Protein and Peptide Degradation Pathways. *BioProcess™ International.*

PATEL, Y. C. 1999. Somatostatin and its receptor family. *Front Neuroendocrinol,* 20, 157-98.

PATEL, Y. C., GREENWOOD, M. T., WARSZYNSKA, A., PANETTA, R. & SRIKANT, C. B. 1994. All five cloned human somatostatin receptors (hSSTR1-5) are functionally coupled to adenylyl cyclase. *Biochem Biophys Res Commun,* 198, 605-12.

PENG, I. C., CHEN, Z., SUN, W., LI, Y. S., MARIN, T. L., HSU, P. H., SU, M. I., CUI, X., PAN, S., LYTLE, C. Y., JOHNSON, D. A., BLAESER, F., CHATILA, T. & SHYY, J. Y. 2012. Glucagon regulates ACC activity in adipocytes through the CAMKKβ/AMPK pathway. *Am J Physiol Endocrinol Metab,* 302, E1560-8.

PETROU, T., OLSEN, H. L., THRASIVOULOU, C., MASTERS, J. R., ASHMORE, J. F. & AHMED, A. 2017. Intracellular Calcium Mobilization in Response to Ion Channel Regulators via a Calcium-Induced Calcium Release Mechanism. *J Pharmacol Exp Ther,* 360, 378-387.

PFEIFFER, T., SCHUSTER, S. & BONHOEFFER, S. 2001. Cooperation and competition in the evolution of ATP-producing pathways. *Science,* 292, 504-7.

PILKIS, S. J. & CLAUS, T. H. 1991. Hepatic gluconeogenesis/glycolysis: regulation and structure/function relationships of substrate cycle enzymes. *Annu Rev Nutr,* 11, 465-515.

PILKIS, S. J., CLAUS, T. H. & EL-MAGHRABI, M. R. 1988. The role of cyclic AMP in rapid and long-term regulation of gluconeogenesis and glycolysis. *Adv Second Messenger Phosphoprotein Res,* 22, 175-91.

PILKIS, S. J., EL-MAGHRABI, M. R., MCGRANE, M., PILKIS, J. & CLAUS, T. H. 1982. Regulation by glucagon of hepatic pyruvate kinase, 6-phosphofructo 1-kinase, and fructose-1,6-bisphosphatase. *Fed Proc,* 41, 2623-8.

PINTÉR, E., HELYES, Z. & SZOLCSÁNYI, J. 2006. Inhibitory effect of somatostatin on inflammation and nociception. *Pharmacol Ther,* 112, 440-56.

PLANT, T. D., JONAS, J. C. & HENQUIN, J. C. 1991. Clonidine inhibits ATP-sensitive K+ channels in mouse pancreatic beta-cells. *Br J Pharmacol,* 104, 385-90.

PLESS, J., BAUER, W., BRINER, U., DOEPFNER, W., MARBACH, P., MAURER, R., PETCHER, T. J., REUBI, J. C. & VONDERSCHER, J. 1986. Chemistry and pharmacology of SMS 201-995, a long-acting octapeptide analogue of somatostatin. *Scand J Gastroenterol Suppl,* 119, 54-64.

POBURKO, D., SANTO-DOMINGO, J. & DEMAUREX, N. 2011. Dynamic regulation of the mitochondrial proton gradient during cytosolic calcium elevations. *J Biol Chem,* 286, 11672-84.

PORTERFIELD, D. M., CORKEY, R. F., SANGER, R. H., TORNHEIM, K., SMITH, P. J. & CORKEY, B. E. 2000. Oxygen consumption oscillates in single clonal pancreatic beta-cells (HIT). *Diabetes,* 49, 1511-6.

POSSEMATO, R., MARKS, K. M., SHAUL, Y. D., PACOLD, M. E., KIM, D., BIRSOY, K., SETHUMADHAVAN, S., WOO, H. K., JANG, H. G., JHA, A. K., CHEN, W. W., BARRETT, F. G., STRANSKY, N., TSUN, Z. Y., COWLEY, G. S., BARRETINA, J., KALAANY, N. Y., HSU, P. P., OTTINA, K., CHAN, A. M., YUAN, B., GARRAWAY, L. A., ROOT, D. E., MINO-KENUDSON, M., BRACHTEL, E. F., DRIGGERS, E. M. & SABATINI, D. M. 2011. Functional genomics reveal that the serine synthesis pathway is essential in breast cancer. *Nature,* 476, 346-50.

PRADAYROL, L., JÖRNVALL, H., MUTT, V. & RIBET, A. 1980. N-terminally extended somatostatin: the primary structure of somatostatin-28. *FEBS Lett,* 109, 55-8.

PULJUNG, M. C. 2018. Cryo-electron microscopy structures and progress toward a dynamic understanding of K. *J Gen Physiol,* 150, 653-669.

PYNE, N. J. & FURMAN, B. L. 2003. Cyclic nucleotide phosphodiesterases in pancreatic islets. *Diabetologia,* 46, 1179-89.

RAI, U., THRIMAWITHANA, T. R., VALERY, C. & YOUNG, S. A. 2015. Therapeutic uses of somatostatin and its analogues: Current view and potential applications. *Pharmacol Ther,* In press.

RATHEE, K., DHULL, V., DHULL, R. & SINGH, S. 2016. Biosensors based on electrochemical lactate detection: A comprehensive review. *Biochem Biophys Rep,* 5, 35-54.

RAVIER, M. A., DARO, D., ROMA, L. P., JONAS, J. C., CHENG-XUE, R., SCHUIT, F. C. & GILON, P. 2011. Mechanisms of control of the free Ca2+ concentration in the endoplasmic reticulum of mouse pancreatic β-cells: interplay with cell metabolism and [Ca2+]c and role of SERCA2b and SERCA3. *Diabetes,* 60, 2533-45.

RENSTRÖM, E., DING, W. G., BOKVIST, K. & RORSMAN, P. 1996. Neurotransmitter-induced inhibition of exocytosis in insulin-secreting beta cells by activation of calcineurin. *Neuron,* 17, 513-22.

RENSTRÖM, E., ELIASSON, L. & RORSMAN, P. 1997. Protein kinase A-dependent and -independent stimulation of exocytosis by cAMP in mouse pancreatic B-cells. *J Physiol,* 502 (Pt 1), 105-18.

RIBALET, B. & EDDLESTONE, G. T. 1995. Characterization of the G protein coupling of a somatostatin receptor to the K+ATP channel in insulin-secreting mammalian HIT and RIN cell lines. *J Physiol,* 485 (Pt 1), 73-86.

RODGERS, R. L. 2012. Glucagon and cyclic AMP: time to turn the page? *Curr Diabetes Rev,* 8, 362-81.

ROE, M. W., MERTZ, R. J., LANCASTER, M. E., WORLEY, J. F. & DUKES, I. D. 1994a. Thapsigargin inhibits the glucose-induced decrease of intracellular Ca2+ in mouse islets of Langerhans. *Am J Physiol,* 266, E852-62.

ROE, M. W., PHILIPSON, L. H., FRANGAKIS, C. J., KUZNETSOV, A., MERTZ, R. J., LANCASTER, M. E., SPENCER, B., WORLEY, J. F. & DUKES, I. D. 1994b. Defective glucose-dependent endoplasmic reticulum Ca2+ sequestration in diabetic mouse islets of Langerhans. *J Biol Chem,* 269, 18279-82.

ROOSTERMAN, D., GLASSMEIER, G., BAUMEISTER, H., SCHERÜBL, H. & MEYERHOF, W. 1998. A somatostatin receptor 1 selective ligand inhibits Ca2+ currents in rat insulinoma 1046-38 cells. *FEBS Lett,* 425, 137-40.

RORSMAN, P. 1997. The pancreatic beta-cell as a fuel sensor: an electrophysiologist's viewpoint. *Diabetologia,* 40, 487-95.

RORSMAN, P., AMMÄLÄ, C., BERGGREN, P. O., BOKVIST, K. & LARSSON, O. 1992. Cytoplasmic calcium transients due to single action potentials and voltage-clamp depolarizations in mouse pancreatic B-cells. *EMBO J,* 11, 2877-84.

RORSMAN, P. & ASHCROFT, F. M. 2018. Pancreatic β-Cell Electrical Activity and Insulin Secretion: Of Mice and Men. *Physiol Rev,* 98, 117-214.

ROTTENBERG, H. & MARBACH, M. 1990. The Na(+)-independent Ca2+ efflux system in mitochondria is a Ca2+/2H+ exchange system. *FEBS Lett,* 274, 65-8.

RUTECKI, P. A. 1992. Neuronal excitability: voltage-dependent currents and synaptic transmission. *J Clin Neurophysiol,* 9, 195-211.

SAITO, K., LEE, S., SHIUCHI, T., TODA, C., KAMIJO, M., INAGAKI-OHARA, K., OKAMOTO, S. & MINOKOSHI, Y. 2011. An enzymatic photometric assay for 2-deoxyglucose uptake in insulin-responsive tissues and 3T3-L1 adipocytes. *Anal Biochem,* 412, 9-17.

SANTULLI, G. & MARKS, A. R. 2015. Essential Roles of Intracellular Calcium Release Channels in Muscle, Brain, Metabolism, and Aging. *Curr Mol Pharmacol,* 8, 206-22.

SARABU, R., BIZZARRO, F. T., CORBETT, W. L., DVOROZNIAK, M. T., GENG, W., GRIPPO, J. F., HAYNES, N. E., HUTCHINGS, S., GAROFALO, L., GUERTIN, K. R., HILLIARD, D. W., KABAT, M., KESTER, R. F., KA, W., LIANG, Z., MAHANEY, P. E., MARCUS, L., MATSCHINSKY, F. M., MOORE, D., RACHA, J., RADINOV, R., REN, Y., QI, L., PIGNATELLO, M., SPENCE, C. L., STEELE, T., TENGI, J. & GRIMSBY, J. 2012. Discovery of piragliatin--first glucokinase activator studied in type 2 diabetic patients. *J Med Chem,* 55, 7021-36.

SCHUIT, F. C., DERDE, M. P. & PIPELEERS, D. G. 1989. Sensitivity of rat pancreatic A and B cells to somatostatin. *Diabetologia,* 32, 207-12.

SCHUSDZIARRA, V., HARRIS, V., CONLON, J. M., ARIMURA, A. & UNGER, R. 1978. Pancreatic and gastric somatostatin release in response to intragastric and intraduodenal nutrients and HCl in the dog. *J Clin Invest,* 62, 509-18.

SCORZIELLO, A., SAVOIA, C., SECONDO, A., BOSCIA, F., SISALLI, M. J., ESPOSITO, A., CARLUCCI, A., MOLINARO, P., LIGNITTO, L., DI RENZO, G., FELICIELLO, A. & ANNUNZIATO, L. 2013. New insights in mitochondrial calcium handling by sodium/calcium exchanger. *Adv Exp Med Biol,* 961, 203-9.

SEAQUIST, E. R., NEAL, A. R., SHOGER, K. D., WALSETH, T. F. & ROBERTSON, R. P. 1992. G-proteins and hormonal inhibition of insulin secretion from HIT-T15 cells and isolated rat islets. *Diabetes,* 41, 1390-9.

SEINO, S. & SHIBASAKI, T. 2005. PKA-dependent and PKA-independent pathways for cAMP-regulated exocytosis. *Physiol Rev,* 85, 1303-42.

SELIVANOV, V. A., ZEAK, J. A., ROCA, J., CASCANTE, M., TRUCCO, M. & VOTYAKOVA, T. V. 2008. The role of external and matrix pH in mitochondrial reactive oxygen species generation. *J Biol Chem,* 283, 29292-300.

SENER, A., KAWAZU, S., HUTTON, J. C., BOSCHERO, A. C., DEVIS, G., SOMERS, G., HERCHUELZ, A. & MALAISSE, W. J. 1978. The stimulus-secretion coupling of glucose-induced insulin release. Effect of exogenous pyruvate on islet function. *Biochem J,* 176, 217-32.

SENER, A., LEVY, J. & MALAISSE, W. J. 1976. The stimulus-secretion coupling of glucose-induced insulin release. Does glycolysis control calcium transport in the B-cell? *Biochem J,* 156, 521-5.

SENER, A. & MALAISSE, W. J. 1976. Measurement of lactic acid in nanomolar amounts. Reliability of such a method as an index of glycolysis in pancreatic islets. *Biochem Med,* 15, 34-41.

SHAPIRO, M. S. & HILLE, B. 1993. Substance P and somatostatin inhibit calcium channels in rat sympathetic neurons via different G protein pathways. *Neuron,* 10, 11-20.

SHIBASAKI, T., SUNAGA, Y., FUJIMOTO, K., KASHIMA, Y. & SEINO, S. 2004a. Interaction of ATP sensor, cAMP sensor, Ca2+ sensor, and voltage-dependent Ca2+ channel in insulin granule exocytosis. *J Biol Chem,* 279, 7956-61.

SHIBASAKI, T., SUNAGA, Y. & SEINO, S. 2004b. Integration of ATP, cAMP, and Ca2+ signals in insulin granule exocytosis. *Diabetes,* 53 Suppl 3, S59-62.

SHIOTA, C., LARSSON, O., SHELTON, K. D., SHIOTA, M., EFANOV, A. M., HOY, M., LINDNER, J., KOOPTIWUT, S., JUNTTI-BERGGREN, L., GROMADA, J., BERGGREN, P. O. & MAGNUSON, M. A. 2002. Sulfonylurea receptor type 1 knock-out mice have intact feeding-stimulated insulin secretion despite marked impairment in their response to glucose. *J Biol Chem,* 277, 37176-83.

SIMS, S. M., LUSSIER, B. T. & KRAICER, J. 1991. Somatostatin activates an inwardly rectifying K+ conductance in freshly dispersed rat somatotrophs. *J Physiol,* 441, 615-37.

SINGH, V., BRENDEL, M. D., ZACHARIAS, S., MERGLER, S., JAHR, H., WIEDENMANN, B., BRETZEL, R. G., PLÖCKINGER, U. & STROWSKI, M. Z. 2007. Characterization of somatostatin receptor subtype-specific regulation of insulin and glucagon secretion: an in vitro study on isolated human pancreatic islets. *J Clin Endocrinol Metab,* 92, 673-80.

SLIWIŃSKA-MOSSOŃ, M., VESELÝ, M. & MILNEROWICZ, H. 2014. The clinical significance of somatostatin in pancreatic diseases. *Ann Endocrinol (Paris),* 75, 232-40.

SMITH, P. A. 2009. N-type Ca(2+) -channels in murine pancreatic beta-cells are inhibited by an exclusive coupling with somatostatin receptor subtype 1. *Endocrinology,* 150, 741-8.

SMITH, P. A., RORSMAN, P. & ASHCROFT, F. M. 1989. Modulation of dihydropyridine-sensitive Ca2+ channels by glucose metabolism in mouse pancreatic beta-cells. *Nature,* 342, 550-3.

SMITH, P. A., SELLERS, L. A. & HUMPHREY, P. P. 2001. Somatostatin activates two types of inwardly rectifying K+ channels in MIN-6 cells. *J Physiol,* 532, 127-42.

SOEJIMA, A., INOUE, K., TAKAI, D., KANEKO, M., ISHIHARA, H., OKA, Y. & HAYASHI, J. I. 1996. Mitochondrial DNA is required for regulation of glucose-stimulated insulin secretion in a mouse pancreatic beta cell line, MIN6. *J Biol Chem,* 271, 26194-9.

SONG, W. J., MONDAL, P., LI, Y., LEE, S. E. & HUSSAIN, M. A. 2013. Pancreatic β-cell response to increased metabolic demand and to pharmacologic secretagogues requires EPAC2A. *Diabetes,* 62, 2796-807.

SPRINGETT, G. M., KAWASAKI, H. & SPRIGGS, D. R. 2004. Non-kinase second-messenger signaling: new pathways with new promise. *Bioessays,* 26, 730-8.

STANLEY, C. A. 2016. Perspective on the Genetics and Diagnosis of Congenital Hyperinsulinism Disorders. *J Clin Endocrinol Metab,* 101, 815-26.

STETÁK, A., VERESS, R., OVÁDI, J., CSERMELY, P., KÉRI, G. & ULLRICH, A. 2007. Nuclear translocation of the tumor marker pyruvate kinase M2 induces programmed cell death. *Cancer Res,* 67, 1602-8.

STRAUB, S. G. & SHARP, G. W. 2012. Evolving insights regarding mechanisms for the inhibition of insulin release by norepinephrine and heterotrimeric G proteins. *Am J Physiol Cell Physiol,* 302, C1687-98.

STRIGGOW, F. & EHRLICH, B. E. 1996. Ligand-gated calcium channels inside and out. *Curr Opin Cell Biol,* 8, 490-5.

STROWSKI, M. Z. & BLAKE, A. D. 2008. Function and expression of somatostatin receptors of the endocrine pancreas. *Mol Cell Endocrinol,* 286, 169-79.

STROWSKI, M. Z., KOHLER, M., CHEN, H. Y., TRUMBAUER, M. E., LI, Z., SZALKOWSKI, D., GOPAL-TRUTER, S., FISHER, J. K., SCHAEFFER, J. M., BLAKE, A. D., ZHANG, B. B. & WILKINSON, H. A. 2003. Somatostatin receptor subtype 5 regulates insulin secretion and glucose homeostasis. *Mol Endocrinol,* 17, 93-106.

SU, Y., LAM, T. K., HE, W., POCAI, A., BRYAN, J., AGUILAR-BRYAN, L. & GUTIÉRREZ-JUÁREZ, R. 2012. Hypothalamic leucine metabolism regulates liver glucose production. *Diabetes,* 61, 85-93.

SUNAHARA, R. K., DESSAUER, C. W. & GILMAN, A. G. 1996. Complexity and diversity of mammalian adenylyl cyclases. *Annu Rev Pharmacol Toxicol,* 36, 461-80.

SVOBODA, M., TASTENOY, M., VERTONGEN, P. & ROBBERECHT, P. 1994. Relative quantitative analysis of glucagon receptor mRNA in rat tissues. *Mol Cell Endocrinol,* 105, 131-7.

SWEET, I. R. & GILBERT, M. 2006. Contribution of calcium influx in mediating glucose-stimulated oxygen consumption in pancreatic islets. *Diabetes,* 55, 3509-19.

SYMERSKY, J., OSOWSKI, D., WALTERS, D. E. & MUELLER, D. M. 2012. Oligomycin frames a common drug-binding site in the ATP synthase. *Proc Natl Acad Sci U S A,* 109, 13961-5.

TAKAHASHI, N., KADOWAKI, T., YAZAKI, Y., ELLIS-DAVIES, G. C., MIYASHITA, Y. & KASAI, H. 1999. Post-priming actions of ATP on Ca2+-dependent exocytosis in pancreatic beta cells. *Proc Natl Acad Sci U S A,* 96, 760-5.

TAL, M., LIANG, Y., NAJAFI, H., LODISH, H. F. & MATSCHINSKY, F. M. 1992. Expression and function of GLUT-1 and GLUT-2 glucose transporter

isoforms in cells of cultured rat pancreatic islets. *J Biol Chem,* 267, 17241-7.

TANG, W. J. & GILMAN, A. G. 1991. Type-specific regulation of adenylyl cyclase by G protein beta gamma subunits. *Science,* 254, 1500-3.

TARASOV, A., DUSONCHET, J. & ASHCROFT, F. 2004. Metabolic regulation of the pancreatic beta-cell ATP-sensitive K+ channel: a pas de deux. *Diabetes,* 53 Suppl 3, S113-22.

TARASOV, A. I., GRIFFITHS, E. J. & RUTTER, G. A. 2012a. Regulation of ATP production by mitochondrial Ca(2+). *Cell Calcium,* 52, 28-35.

TARASOV, A. I., SEMPLICI, F., LI, D., RIZZUTO, R., RAVIER, M. A., GILON, P. & RUTTER, G. A. 2013. Frequency-dependent mitochondrial Ca(2+) accumulation regulates ATP synthesis in pancreatic β cells. *Pflugers Arch,* 465, 543-54.

TARASOV, A. I., SEMPLICI, F., RAVIER, M. A., BELLOMO, E. A., PULLEN, T. J., GILON, P., SEKLER, I., RIZZUTO, R. & RUTTER, G. A. 2012b. The mitochondrial Ca2+ uniporter MCU is essential for glucose-induced ATP increases in pancreatic β-cells. *PLoS One,* 7, e39722.

TAUSSIG, R., TANG, W. J., HEPLER, J. R. & GILMAN, A. G. 1994. Distinct patterns of bidirectional regulation of mammalian adenylyl cyclases. *J Biol Chem,* 269, 6093-100.

TEDFORD, H. W. & ZAMPONI, G. W. 2006. Direct G protein modulation of Cav2 calcium channels. *Pharmacol Rev,* 58, 837-62.

TENGHOLM, A., HELLMAN, B. & GYLFE, E. 2001. The endoplasmic reticulum is a glucose-modulated high-affinity sink for Ca2+ in mouse pancreatic beta-cells. *J Physiol,* 530, 533-40.

TERRITO, P. R., MOOTHA, V. K., FRENCH, S. A. & BALABAN, R. S. 2000. Ca(2+) activation of heart mitochondrial oxidative phosphorylation: role of the F(0)/F(1)-ATPase. *Am J Physiol Cell Physiol,* 278, C423-35.

TESLAA, T. & TEITELL, M. A. 2014. Techniques to monitor glycolysis. *Methods Enzymol,* 542, 91-114.

THOMPSON, J. L. & SHUTTLEWORTH, T. J. 2015. Anchoring protein AKAP79-mediated PKA phosphorylation of STIM1 determines selective activation of the ARC channel, a store-independent Orai channel. *J Physiol,* 593, 559-72.

THORENS, B. 2015. GLUT2, glucose sensing and glucose homeostasis. *Diabetologia,* 58, 221-32.

THORENS, B., SARKAR, H. K., KABACK, H. R. & LODISH, H. F. 1988. Cloning and functional expression in bacteria of a novel glucose transporter present in liver, intestine, kidney, and beta-pancreatic islet cells. *Cell,* 55, 281-90.

TIAN, Y. & LAYCHOCK, S. G. 2001. Protein kinase C and calcium regulation of adenylyl cyclase in isolated rat pancreatic islets. *Diabetes,* 50, 2505-13.

TIRONE, T. A., NORMAN, M. A., MOLDOVAN, S., DEMAYO, F. J., WANG, X. P. & BRUNICARDI, F. C. 2003. Pancreatic somatostatin inhibits insulin secretion via SSTR-5 in the isolated perfused mouse pancreas model. *Pancreas,* 26, e67-73.

TRAN, Q., LEE, H., PARK, J. & KIM, S. H. 2016. Targeting Cancer Metabolism - Revisiting the Warburg Effects. *Toxicol Res,* 32, 177-93.

TRUBE, G., RORSMAN, P. & OHNO-SHOSAKU, T. 1986. Opposite effects of tolbutamide and diazoxide on the ATP-dependent K+ channel in mouse pancreatic beta-cells. *Pflugers Arch,* 407, 493-9.

TUCKER, S. J., GRIBBLE, F. M., ZHAO, C., TRAPP, S. & ASHCROFT, F. M. 1997. Truncation of Kir6.2 produces ATP-sensitive K+ channels in the absence of the sulphonylurea receptor. *Nature,* 387, 179-83.

ULLRICH, S., PRENTKI, M. & WOLLHEIM, C. B. 1990. Somatostatin inhibition of Ca2(+)-induced insulin secretion in permeabilized HIT-T15 cells. *Biochem J,* 270, 273-6.

ULLRICH, S. & WOLLHEIM, C. B. 1985. Expression of both alpha 1- and alpha 2-adrenoceptors in an insulin-secreting cell line. Parallel studies of cytosolic free Ca2+ and insulin release. *Mol Pharmacol,* 28, 100-6.

UNWIN, R. D., CRAVEN, R. A., HARNDEN, P., HANRAHAN, S., TOTTY, N., KNOWLES, M., EARDLEY, I., SELBY, P. J. & BANKS, R. E. 2003. Proteomic changes in renal cancer and co-ordinate demonstration of both the glycolytic and mitochondrial aspects of the Warburg effect. *Proteomics,* 3, 1620-32.

VALDEOLMILLOS, M., SANTOS, R. M., CONTRERAS, D., SORIA, B. & ROSARIO, L. M. 1989. Glucose-induced oscillations of intracellular Ca2+ concentration resembling bursting electrical activity in single mouse islets of Langerhans. *FEBS Lett,* 259, 19-23.

VALLEY, M. P., KARASSINA, N., AOYAMA, N., CARLSON, C., CALI, J. J. & VIDUGIRIENE, J. 2016. A bioluminescent assay for measuring glucose uptake. *Anal Biochem,* 505, 43-50.

VALSECCHI, F., RAMOS-ESPIRITU, L. S., BUCK, J., LEVIN, L. R. & MANFREDI, G. 2013. cAMP and mitochondria. *Physiology (Bethesda),* 28, 199-209.

VAN DE BUNT, M. & GLOYN, A. L. 2012. A tale of two glucose transporters: how GLUT2 re-emerged as a contender for glucose transport into the human beta cell. *Diabetologia,* 55, 2312-5.

VAN OP DEN BOSCH, J., ADRIAENSEN, D., VAN NASSAUW, L. & TIMMERMANS, J. P. 2009. The role(s) of somatostatin, structurally related peptides and somatostatin receptors in the gastrointestinal tract: a review. *Regul Pept,* 156, 1-8.

VAN SCHRAVENDIJK, C. F., FORIERS, A., HOOGHE-PETERS, E. L., ROGIERS, V., DE MEYTS, P., SODOYEZ, J. C. & PIPELEERS, D. G. 1985. Pancreatic hormone receptors on islet cells. *Endocrinology,* 117, 841-8.

VANDER HEIDEN, M. G., CANTLEY, L. C. & THOMPSON, C. B. 2009. Understanding the Warburg effect: the metabolic requirements of cell proliferation. *Science,* 324, 1029-33.

VASU, S., MCCLENAGHAN, N. H., MCCLUSKEY, J. T. & FLATT, P. R. 2013. Cellular responses of novel human pancreatic β-cell line, 1.1B4 to hyperglycemia. *Islets,* 5, 170-7.

VENEZIALE, C. M., DEERING, N. G. & THOMPSON, H. J. 1976. Gluconeogenesis in isolated rat hepatic parenchymal cells. IX. Differential effects of glucagon and epinephrine on phosphofructokinase and pyruvate kinase. *Mayo Clin Proc,* 51, 624-31.

WANG, Y., LI, G., GOODE, J., PAZ, J. C., OUYANG, K., SCREATON, R., FISCHER, W. H., CHEN, J., TABAS, I. & MONTMINY, M. 2012. Inositol-1,4,5-trisphosphate receptor regulates hepatic gluconeogenesis in fasting and diabetes. *Nature,* 485, 128-32.

WINZELL, M. S. & AHRÉN, B. 2007. G-protein-coupled receptors and islet function-implications for treatment of type 2 diabetes. *Pharmacol Ther,* 116, 437-48.

XU, Y. & XIE, X. 2009. Glucagon receptor mediates calcium signaling by coupling to G alpha q/11 and G alpha i/o in HEK293 cells. *J Recept Signal Transduct Res,* 29, 318-25.

YABE, D. & SEINO, Y. 2011. Two incretin hormones GLP-1 and GIP: comparison of their actions in insulin secretion and β cell preservation. *Prog Biophys Mol Biol,* 107, 248-56.

YAEKURA, K. & YADA, T. 1998. [Ca2+]i-reducing action of cAMP in rat pancreatic beta-cells: involvement of thapsigargin-sensitive stores. *Am J Physiol,* 274, C513-21.

YAMADA, M., INANOBE, A. & KURACHI, Y. 1998. G protein regulation of potassium ion channels. *Pharmacol Rev,* 50, 723-60.

YAMAMOTO, N., UEDA-WAKAGI, M., SATO, T., KAWASAKI, K., SAWADA, K., KAWABATA, K., AKAGAWA, M. & ASHIDA, H. 2015. Measurement of Glucose Uptake in Cultured Cells. *Curr Protoc Pharmacol,* 71, 12.14.1-26.

YAMASHITA, N., KOJIMA, I., SHIBUYA, N. & OGATA, E. 1987. Pertussis toxin inhibits somatostatin-induced K+ conductance in human pituitary tumor cells. *Am J Physiol,* 253, E28-32.

YAMAZAKI, H., ZAWALICH, K. C. & ZAWALICH, W. S. 2010. Physiologic implications of phosphoinositides and phospholipase C in the regulation of insulin secretion. *J Nutr Sci Vitaminol (Tokyo),* 56, 1-8.

YANG, S. K., PARKINGTON, H. C., BLAKE, A. D., KEATING, D. J. & CHEN, C. 2005. Somatostatin increases voltage-gated K+ currents in GH3 cells through activation of multiple somatostatin receptors. *Endocrinology,* 146, 4975-84.

YANKOVSKAYA, V., HORSEFIELD, R., TÖRNROTH, S., LUNA-CHAVEZ, C., MIYOSHI, H., LÉGER, C., BYRNE, B., CECCHINI, G. & IWATA, S. 2003. Architecture of succinate dehydrogenase and reactive oxygen species generation. *Science,* 299, 700-4.

YAO, J., LIU, J. & ZHAO, W. 2018. By blocking hexokinase-2 phosphorylation, limonin suppresses tumor glycolysis and induces cell apoptosis in hepatocellular carcinoma. *Onco Targets Ther,* 11, 3793-3803.

YOSHIKAWA, H., TAJIRI, Y., SAKO, Y., HASHIMOTO, T., UMEDA, F. & NAWATA, H. 2001. Effects of free fatty acids on beta-cell functions: a possible involvement of peroxisome proliferator-activated receptors alpha or pancreatic/duodenal homeobox. *Metabolism,* 50, 613-8.

YOSHIOKA, K., TAKAHASHI, H., HOMMA, T., SAITO, M., OH, K. B., NEMOTO, Y. & MATSUOKA, H. 1996. A novel fluorescent derivative of glucose applicable to the assessment of glucose uptake activity of Escherichia coli. *Biochim Biophys Acta,* 1289, 5-9.

YOSHITOMI, H., FUJII, Y., MIYAZAKI, M., NAKAJIMA, N., INAGAKI, N. & SEINO, S. 1997. Involvement of MAP kinase and c-fos signaling in the inhibition of cell growth by somatostatin. *Am J Physiol,* 272, E769-74.

ZAMBRE, Y., LING, Z., CHEN, M. C., HOU, X., WOON, C. W., CULLER, M., TAYLOR, J. E., COY, D. H., VAN SCHRAVENDIJK, C., SCHUIT, F., PIPELEERS, D. G. & EIZIRIK, D. L. 1999. Inhibition of human pancreatic islet insulin release by receptor-selective somatostatin analogs directed to somatostatin receptor subtype 5. *Biochem Pharmacol,* 57, 1159-64.